6-2002

Protein-Protein Interactions and Muscle cell Signaling Via Syntrophin

Shilpa A. Oak
University of Tennessee Health Science Center

Protein-Protein Interactions and Muscle cell Signaling Via Syntrophin

Abstract

Absence of dystrophin results in Duchenne muscular dystrophy (DMD), a lethal neuromuscular d isorder that afflicts 1 in 3500 live male births. In the sarcolemma, dystrophin is associated with a complex of proteins and glycoproteins, known as the dystrophin glycoprotein complex. The DGC constituents are dystrophin, a-dys troglycan, b-dystroglycan, syntrophin, a-sarcoglycan, b-sarcoglycan, g-sarcoglycan, d-sarcoglycan, and sarcospan. Not al l of these are single protein species. The syntrophins consists of a group of three homologous proteins composed of acidic (a) and basic (b) components. Syntrophins are known to self-associate to form oligomers.

In this dissertation, syntrophin's oligomerization and its interactions with the cell signaling components *in vitro* in skeletal muscle were investigated.

Mouse a1-syntrophin sequences, produced as chimeric fusion proteins in bacteria, als o oligomerize and in a micromolar Ca^{2+}-dependent manner. Oligomerization was localized to the N-terminal pleckstrin homology domain (PH1) or adjacent sequences; the second, C-terminal PH2 domain did not show oligomerization. PH1 was found to se lf-associate and calmodulin or Ca^{2+} chelating agents such as EGTA could effectively prevent this oligomerization. A single calmodulin bound per syntrophin to cause inhibition of the precipitation. Calmodulin inhibited syntrophin oligomerization in the presence or absence of Ca^{2+}. Ca^{2+}-binding to syntrophin is responsible for the inhibition by EGTA of syntrophin oligomerization.

Syntrophins have been proposed to serve as adapter proteins. Blot overlay experiment s demonstrate that a-, b-dystroglycan, and syntrophins all bind Grb2, the growth factor receptor bound adapter protein. Mouse a1-syntrophin chimeric fusion proteins bind Grb2 in a Ca^{2+}-independent manner. This binding was localized to two proline rich sequences near the N terminal PH1 domain. This domain is interrupted by a PDZ domain inserted nearly in middle of the PH1 domain dividing it into two parts: the N ter minal PH1 and C terminal PH1b subdomains. One proline rich sequence is Cterminal of PH1b while the other is adjacent to and overlapping with the N terminal of PH1b. Grb2 contains two SH3 domains and both contribute to binding. Intact, bacterial expressed Grb2 bound syntrophin with an apparent KD of 563 ± 15 nM. Grb2-C-SH3 domain bound syntrophin with slightly higher affinity than Grb2-N-SH3 domain. Crk-L, an SH2/SH3 protein of similar domain structure but different specificity does not bind these s yntrophin sequences.

Dystrophin glycoprotein complex has been proposed to be involved in signal transduction. We have shown that laminin binding to a–dystroglycan causes syntrophin to recruit Rac1. Laminin-Sepha rose precipitates Rac1, and to a lesser extent Rho-A and Ras, from the rabbit skeletal muscle membranes in a pull-down assay. The presence of heparin, which inhibits the interaction between laminin and a–dystroglycan preven ts recruitment of Rac1. A syntrophin antibody blocks recruitment of Rac1 suggesting that the signaling pathway requires syntrophin. Sos1 is also present in the recruited complex. Jun N terminal kinase 2 is phosphorylated and activated only when laminin is attached to the dystrophin glycoprotein complex. Thus, dystrophin glycoprotein complex recruits Rac1 via syntrophin through a Grb2-Sos complex leading to activation of Jun N terminal kinase 2 only when it is attached to laminin. We postulate this signals the muscle cell to grow.

Document Type

Dissertation

Protein-Protein Interactions and Muscle Cell Signaling via Syntrophin

A Dissertation

Presented for

The Graduate Studies Council

The University of Tennessee

Health Science Center

In Partial Fulfillment

Of the Requirements for the Degree

Doctor of Philosophy

From The University of Tennessee

By

Shilpa A. Oak

June 2002

.

Dedication

This dissertation is dedicated to my husband

Himanshu

And to my parents

Anil and Anjali Oak

Acknowledgements

I would like to thank my mentor Dr. Harry Jarrett, for his guidance in and outside the lab. I would also like to thank the other committee members Dr. Tayebeh Pourmotabbed, Dr. Walter Lang, and Dr. Tulio Bertorini for their critical comments and assistance. I would specially like to thank Dr. Susan Senogles for providing some reagents as well as for her intellectual support for the work on studies of interaction of syntrophin with Gβγ. I profoundly appreciate the camaraderie I shared with my lab mates Dr. Luis Jurado, Dr. Priya Chockalingam, Dr. Yanwen Zhou, Robert Moxley Stuart Wallace, Darlene Robinson, and Pallavi Patel and thank them for their help. I also thank my parents Anil and Anjali Oak and my sisters for motivating me towards my goals. I also thank my parents-in law for their support. I thank my husband and lab mate Himanshu for his support and for being a constant source of inspiration.

Abstract

Absence of dystrophin results in Duchenne muscular dystrophy (DMD), a lethal neuromuscular disorder that afflicts 1 in 3500 live male births. In the sarcolemma, dystrophin is associated with a complex of proteins and glycoproteins, known as the dystrophin glycoprotein complex. The DGC constituents are dystrophin, α–dystroglycan, β–dystroglycan, syntrophin, α–sarcoglycan, β–sarcoglycan, γ–sarcoglycan, δ-sarcoglycan, and sarcospan. Not all of these are single protein species. The syntrophins consists of a group of three homologous proteins composed of acidic (α) and basic (β) components. Syntrophins are known to self-associate to form oligomers.

In this dissertation, syntrophin's oligomerization and its interactions with the cell signaling components *in vitro* in skeletal muscle were investigated.

Mouse α1-syntrophin sequences, produced as chimeric fusion proteins in bacteria, also oligomerize and in a micromolar Ca^{2+}-dependent manner. Oligomerization was localized to the N-terminal pleckstrin homology domain (PH1) or adjacent sequences; the second, C-terminal PH2 domain did not show oligomerization. PH1 was found to self-associate and calmodulin or Ca^{2+} chelating agents such as EGTA could effectively prevent this oligomerization. A single calmodulin bound per syntrophin to cause inhibition of the precipitation. Calmodulin inhibited syntrophin oligomerization in the presence or absence of Ca^{2+}. Ca^{2+}-binding to syntrophin is responsible for the inhibition by EGTA of syntrophin oligomerization.

Syntrophins have been proposed to serve as adapter proteins. Blot overlay experiments demonstrate that α-, β-dystroglycan, and syntrophins all bind Grb2, the

growth factor receptor bound adapter protein. Mouse α1-syntrophin chimeric fusion proteins bind Grb2 in a Ca^{2+}-independent manner. This binding was localized to two proline rich sequences near the N terminal PH1 domain. This domain is interrupted by a PDZ domain inserted nearly in middle of the PH1 domain dividing it into two parts: the N terminal PH1 and C terminal PH1b subdomains. One proline rich sequence is C-terminal of PH1b while the other is adjacent to and overlapping with the N terminal of PH1b. Grb2 contains two SH3 domains and both contribute to binding. Intact, bacterial expressed Grb2 bound syntrophin with an apparent K_D of 563 ± 15 nM. Grb2-C-SH3 domain bound syntrophin with slightly higher affinity than Grb2-N-SH3 domain. Crk-L, an SH2/SH3 protein of similar domain structure but different specificity does not bind these syntrophin sequences.

Dystrophin glycoprotein complex has been proposed to be involved in signal transduction. We have shown that laminin binding to α–dystroglycan causes syntrophin to recruit Rac1. Laminin-Sepharose precipitates Rac1, and to a lesser extent Rho-A and Ras, from the rabbit skeletal muscle membranes in a pull-down assay. The presence of heparin, which inhibits the interaction between laminin and α–dystroglycan prevents recruitment of Rac1. A syntrophin antibody blocks recruitment of Rac1 suggesting that the signaling pathway requires syntrophin. Sos1 is also present in the recruited complex. Jun N terminal kinase 2 is phosphorylated and activated only when laminin is attached to the dystrophin glycoprotein complex. Thus, dystrophin glycoprotein complex recruits Rac1 via syntrophin through a Grb2-Sos complex leading to activation of Jun N terminal kinase 2 only when it is attached to laminin. We postulate this signals the muscle cell to grow.

Table Of Contents

List of Figures

List Of Abbreviations

Acetylcholine receptor	AchR
Becker muscular dystrophy	BMD
5-bromo-4-chloro-3-indolyphosphate	BCIP
bovine serum albumin	BSA
Congenital muscular dystrophy	CMD
Duchenne muscular dystrophy	DMD
Dystrophin glycoprotein comlex	DGC
Dystrophin associated proteins	DAPs
Dystrophin associated glycoprotein	DAG
Focal adhesion kinase	FAK
Heterotrimeric GTPase β- and γ- subunit complex	$G_{\beta\gamma}$
Guanine nucleotide exchange factor	GEF
Growth factor receptor bound 2	Grb2
Glutathione-S-transferase	GST
c-jun N terminal kinase	JNK
Kilodaltons	kDa
Mitogen activated protein	MAP
Maltose binding protein	MBP
4-morpholinepropanesulfonic acid	MOPS
Nitroblue tetrazolium	NBT
Nitrilotriacetic acid	NTA

p21-activated kinase	PAK1
Pleckstrin homology	PH
Phosphatidylinositol 4,5-bisphosphate	Ptdlns4,5P_2
Stress activated protein kinase 3	SAPK3
Sodium dodecylsulfate- polyacrylamide gel electrophoresis	SDS-PAGE
Src homology 3	SH3
Son of sevenless	Sos

Chapter 1. Introduction

This dissertation deals with the proteins involved in muscular dystrophies. In this chapter, I will review briefly this group of diseases and the proteins, which are found to be malfunctioning.

Muscular dystrophies

Different pathological conditions can afflict muscle. While myopathy refers to any pathological change, a dystrophy is characterized by a progressive course with continued regeneration and fibrosis. Regeneration serves to replenish the part of the muscle, which dies. Fibrosis is an undesired side effect due to the activation of connective tissue cells producing an interstitial type of extracellular matrix rich in interstitial collagen. Many myopathies are caused by defects in the link between the muscle cell interior and the surrounding basement membrane (1,2). In muscular dystrophies a primary defect causes muscle necrosis, regeneration and a progressive degeneration of the muscle tissue.

Muscular dystrophies are a group of almost 40 neuromuscular disorders. Various muscular dystrophies that are caused by the defect in the basal lamina, dystrophin, dystroglycans and sarcoglycans will be discussed in this section. Each defect gives rise to a different phenotype. Since components of the dystrophin glycoprotein complex (see below) are involved in Duchenne muscular dystrophy-like disorders, a number of related neuromuscular diseases are now collectively called as dystrophinopathies (3,4).

Duchenne muscular dystrophy (DMD)

This is the most common of the different muscular dystrophies. Even as recently as 15 years ago, the genetic basis of this disease was unknown. The fact that essentially all of the patients were males showed that the disease is X-linked. Linkage analysis of random cloned genomic DNA fragments and analysis of rare female DMD patients eventually led to localization of the gene for this disorder to chromosome Xp21 (5). Further studies to purify dystrophin, showed that dystrophin is a cytoskeletal protein closely associated with other peripheral and integral membrane proteins and glycoproteins (6,7), the complex is now called the dystrophin glycoprotein complex. In 1986, the DMD gene was identified (8) and its complementary DNA (cDNA) was sequenced within a year (9) and the DMD gene product, dystrophin, identified (10). DMD is a compound lesion due to disruption of the dystrophin glycoprotein complex, caused by the loss of dystrophin. The subsarcolemmal undercoat of DMD muscle is deficient in dystrophin. DMD is a devastating neuromuscular disorder with an occurrence of 1 in 3500 live male births (3,11). Progressive muscle weakness, elevated serum creatine kinase activity, as well as an abnormal variation in muscle fiber diameter, the presence of necrotic and regenerative muscle fibers and an increase of endomysial fat and connective tissue is present before the age of 5 years (11). A loss of unassisted ambulation usually occurs before the age of 13 years and progressive weakening of the heart and other essential muscle groups lead to lethal cardiac or respiratory failure (11). The two animal models *mdx* mouse and *grmd* dog are both related to DMD (none produce dystrophin). Dystrophin deficient skeletal muscle

biopsied from patients affected with DMD exhibited 80 to 90% reduction in all dystrophin-associated proteins.

Becker muscular dystrophy (BMD)

BMD is typically the milder of the two. In BMD, the dystrophin rod is shorter than normal in most cases (resulting from internal deletions within the DMD gene) or longer in others (resulting from duplication of the DMD gene). The shorter dystrophin has intact actin-, dystroglycan- and syntrophin-binding domains. So even severely truncated (12) or elongated dystrophins may connect the dystroglycan complex to the actin filaments.

In BMD muscle fibers, the dystrophin axis is present even though the amount of dystrophin is decreased and utrophin, a dystrophin related protein, expression is upregulated (13). Thus, the dystrophin-axis is reduced but still partially preserved. This could be responsible for the milder symptoms of BMD as compared to DMD.

Dystrophin glycoprotein complex (DGC)

Dystrophin is a long, slender protein and is found almost exclusively in the cell periphery on the cytoplasmic face of the sarcolemma in normal muscle (14), exhibits properties typical for membrane cytoskeletal components (7,15,16). The 427 kDa form of dystrophin is found in skeletal, cardiac, and smooth muscle tissue and is also present in neurons and glia cells of the central nervous system. Confocal microscopy has shown dystrophin to lie in an array of thick bands that localize at the sites of attachment of the sarcomeres to the muscle plasma membrane (17,18). Dystrophin binds to F-actin at the N-terminal region. The C-terminal domain of dystrophin binds DGC glycoproteins.

Dystrophin forms an intricate part of the muscle cytoskeleton and may function to link the normal contractile apparatus to the sarcolemma. Following the discovery of dystrophin (8,9), the protein missing in Duchenne muscular dystrophy, a number of proteins forming a complex tightly associated with dystrophin (dystrophin associated proteins, DAPs) has been revealed (6,19) in the digitonin solubilized sarcolemmal fraction. Dystrophin along with its associated proteins and glycoproteins, also called the DGC, is present in the skeletal and cardiac muscle sarcolemma at regular intervals. The membrane organization of the DGC in the sarcolemma is shown in Figure 1.1. This complex of proteins at the sarcolemma of skeletal and cardiac muscle is critical for the integrity of the cell membrane (20). Dystrophin is associated with the 156 kDa dystrophin associated glycoprotein (α-DG) by way of the 50 kDa (α-sarcoglycan), 43 kDa (β-dystroglycan), and 35 kDa (γ-sarcoglycan) transmembrane glycoprotein complex and this suggests that the dystrophin serves as a special link between the actin cytoskeleton and components external to the sarcolemmal membrane (20). This complex can be subdivided into three subcomplexes according to their localization namely, the dystroglycan complex, sacrcoglycan complex and a complex conatining syntrophin, dystrophin and dystrobrevin.

The dystroglycan subcomplex consists of

α-dystroglycan (156 DAG)

β-dystroglycan (43 DAG)

These are translated from a single mRNA as a 97 kDa protein which is then processed into two peptides (21) which are closely associated (22). They are ubiquitously expressed in various tissues. The high mass is a result of extensive

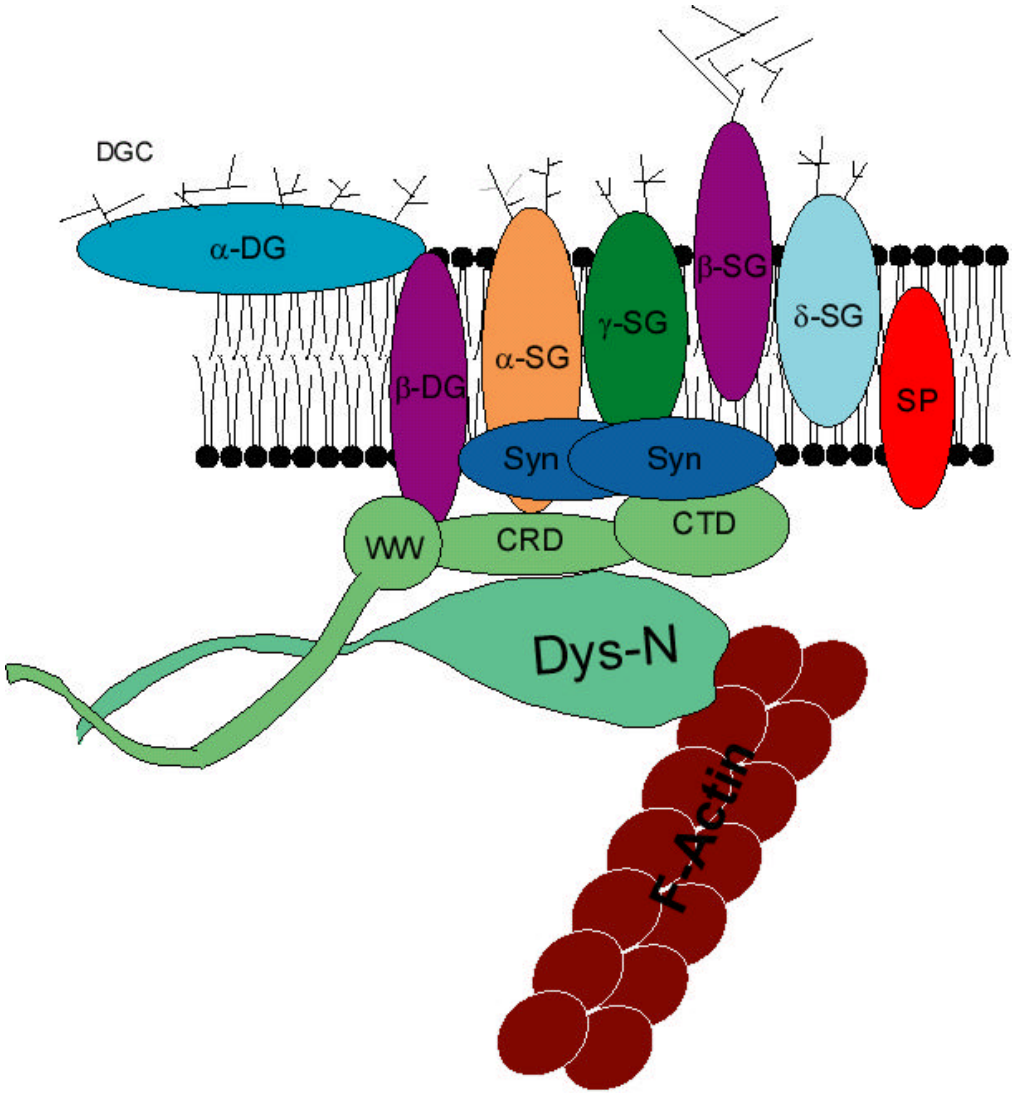

Figure 1.1 The membrane organization of the dystrophin glycoprotein complex. Dystrophin (Dys) is associated with α-dystroglycan (α-DG) by way of the 50 kDa (α-SG), 43 kDa (β-DG), and 35 kDa (γ-SG) transmembrane glycoprotein complex. β-Sarcoglycan (β-SG), δ-sarcoglycan (δ-SG) and sarcospan are parts of the sarcoglycan complex. Syn indiacates syntrophin while CTD stands for C-terminal domain, CRD for cysteine rich domain and WW for WW domain of dystrophin.

glycosylation. The sarcoglycan subcomplex consists of four transmembrane glycoproteins namely α–, β–, γ–, δ–sarcoglycan, and sarcospan. ε–Sarcoglycan is a fifth sarcoglycan, which is highly homologous to α-sarcoglycan. α- and ε-sarcoglycan however do not exist together in a complex. The sarcoglycan complex is expressed specifically in skeletal and cardiac muscles (23,24).

A subsarcolemmal complex comprising:

Dystrophin (427 kDa)

Syntrophins (59 kDa)

Dystrobrevins (87 kDa)

Syntrophins and dystrobrevin are intracellular proteins that are associated with the C-terminal domain of dystrophin.

The dystroglycan subcomplex interacts with the basal lamina

α-Dystroglycan, an extracellular protein, binds to laminin probably via its sugar chains (25). This interaction is Ca^{2+} dependent (25) and heparin and Ca^{2+} chelators such as ethylene diamine tetraacetic acid (EDTA) inhibit it (25). α-Dystroglycan seems to be essential in cell surface matrix organization (26,27). α-Dystroglycan also binds to β-dystroglycan (22). β-Dystroglycan, in turn binds to the cysteine-rich domain and the first half of the C-terminal domain of dystrophin, which are collectively called the dystroglycan-binding domain (D-domain). β-Dystroglycan appears to play a fundamental role, among the DAPs, in connecting the intracellular cytoskeleton to the extracellular basal lamina (28), a function that does not appear to be limited to the skeletal and cardiac muscles. The dystroglycan knockout mice do not survive embryonic life (29).

Basal lamina is composed of a network including collagen fibers, laminin, entactin, and heparan sulfate proteoglycans. The basal lamina covers each muscle fiber in close contact with the sarcolemma forming a thick sheet and serves to protect the muscle fibers from mechanical damage. Laminin-2, the muscle specific isoform of laminin which is also called as merosin, when missing leads to severe form of congenital muscular dystrophy (30) or the milder dystrophy of the dy/dy mice (31). However merosin is also present in peripheral nervous system and brain. It also binds $\alpha 7\beta 1$ integrin at the sarcolemma of skeletal muscle (27) and mutations of the $\alpha 7$ subunit also causes muscular dystrophy (32). Congenital muscular dystrophy (CMD) is a collective name of muscular dystrophies probably due to defects in various genes. Merosin negative muscular dystrophy is caused by the absence of the $\alpha 2$ subunit of laminin also called merosin. There is an increased expression of the $\alpha 1$ subunit of laminin in skeletal muscle basal lamina (33). Defects of dystrophin, the dystroglycan complex and the sarcoglycan complex are not present. However, because of absence of laminin the mechanical link between the extracellular matrix and the cytoskeleton may be interrupted leading to weakening of the muscle and the DGC may not be fully functional. The defect of merosin is primarily responsible for the muscle necrosis observed.

The sarcoglycan subcomplex

Sarcoglycans are associated with the DAPs by a lateral association with the dystroglycan complex. Except for β– and ε–sarcoglycan, all sarcoglycans are specifically expressed in striated muscles. Sarcoglycans can be copurified as a

subcomplex, however, only β-, γ-, and δ- sarcoglycans can be chemically cross-linked to each other (22,34). All five sarcoglycans have cysteine residues in the extracellular domain, although, only β-, γ-, and δ- sarcoglycans appear to form disulfide bonds (34). The extracellular portion of sarcoglycans has been shown to interact with the dystroglycans and each other in *in vitro* experiments (22). Recent investigations have shown that the association between β-, and δ- sarcoglycans, and, to a lesser extent, γ-sarcoglycan is very strong. Among the sarcoglycan complex, α-sarcoglycan appears to be loosely associated with the other components. From these observations, the authors concluded that β-, γ-, and δ- sarcoglycans form a distinct subcomplex, whereas α-sarcoglycan appears to function as a separate unit (34).

Except for ε–sarcoglycan, deficiencies of other sarcoglycans have been implicated in etiology of several of the limb girdle muscular dystrophies (35). Severe childhood autosomal recessive muscular dystrophy (SCARMD) is pathologically and symptomatically very similar to that of DMD (36). Originally, it was defined as α–sarcoglycan deficiency (37), in which dystrophin and the dystroglycan complex are present at normal levels. However, it was later found that this is not a genetically homogeneous disease, but a group of muscular dystrophies with similar phenotypes caused by damage to different genes (38). Thus, in SCARMD, all components of the sarcoglycan complex are absent. The hamster with autosomal recessive muscular dystrophy has been reported to have defect of the entire sarcoglycan complex and is considered an animal model of SCARMD (39). However, the phenotypes of SCARMD and hamster dystrophy are different. In addition, skeletal muscle is involved predominantly in SCARMD while in hamster dystrophy cardiac muscle is predominantly

involved.

Sarcospan is the most recently characterized component of the DAPs (40). It is a member of a tetraspan super family of proteins, which are known to mediate transmembrane protein interactions. It also interacts with sarcoglycans driving their assembly to the sarcolemma and thereby stabilizing the complex (40).

Syntrophin

The 58 kDa cytoplasmic peripheral membrane protein was originally identified in the *Torpedo* electric organ, and shown to localize to the post synaptic neuromuscular junction in mammals (41). This 58 kDa component is called syntrophin (syntrophos from Greek, meaning companion). Syntrophin also copurifies with dystrophin. Syntrophins associated with dystrophin from rabbit skeletal muscle are biochemically heterogeneous group of three 58 kDa intracellular membrane associated proteins. Syntrophins appear as a triplet by one dimensional SDS-PAGE while when separated by two-dimensional electrophoresis it appears as two clusters of 58 kDa proteins with different isoelectric points (pI), one which is slightly acidic (α, pI=6.4) and the other which is quite basic (β, pI=9) (42). Human acidic α1-syntrophin and the basic β2 syntrophin have been cloned and characterized (43). The deduced amino acid sequence of the three syntrophins namely α1, β1, and β2 show overall sequence similarity (α1-syntrophin sequence is 54 and 50% identical to β1 and β2 syntrophin) and that they are nearly identical to their homologues in mouse, suggesting a strong functional conservation among the individual isoforms. Human α1-syntrophin is most predominantly expressed in striated muscles and in brain while the β syntrophins are more ubiquitously expressed (43,44).

Syntrophin binding to the DGC components

α–Syntrophin has been shown to bind to all three syntrophins (45,46), α–sarcoglycan (46,47), and γ–sarcoglycan (46). Syntrophin also has been shown to bind dystrophin (48) and this is discussed later.

Domain structure of syntrophin

All syntrophins contain two pleckstrin homology domains (PH domain), an N-terminal PH1 domain and a PH2 domain. This domain structure is shown in Figure 1.2. The PH1 domain is interrupted by a PDZ domain, a homologous domain found in post synaptic density 95 kDa protein, neuronal nitric oxide synthetase, and other membrane proteins. The PDZ domain was named for the first three proteins in which this ~90 amino acid motif was identified: the Postsynaptic density protein (PSD-95), the Drosophila disks-large protein (Dlg), and the Zona Occludens 1 (ZO-1) protein. Syntrophins also have a unique domain at the C-terminus, called the SU domain. Different interactions of syntrophin with other proteins have been localized and are discussed below.

PH domain

Pleckstrin homology domains derive their name from pleckstrin, the major protein kinase C substrate of platelets. PH domains are a family of compact protein modules defined by a sequence of roughly 100 amino acids. Many enzymes, which have important regulatory functions, contain PH domains, and the mutant forms of several

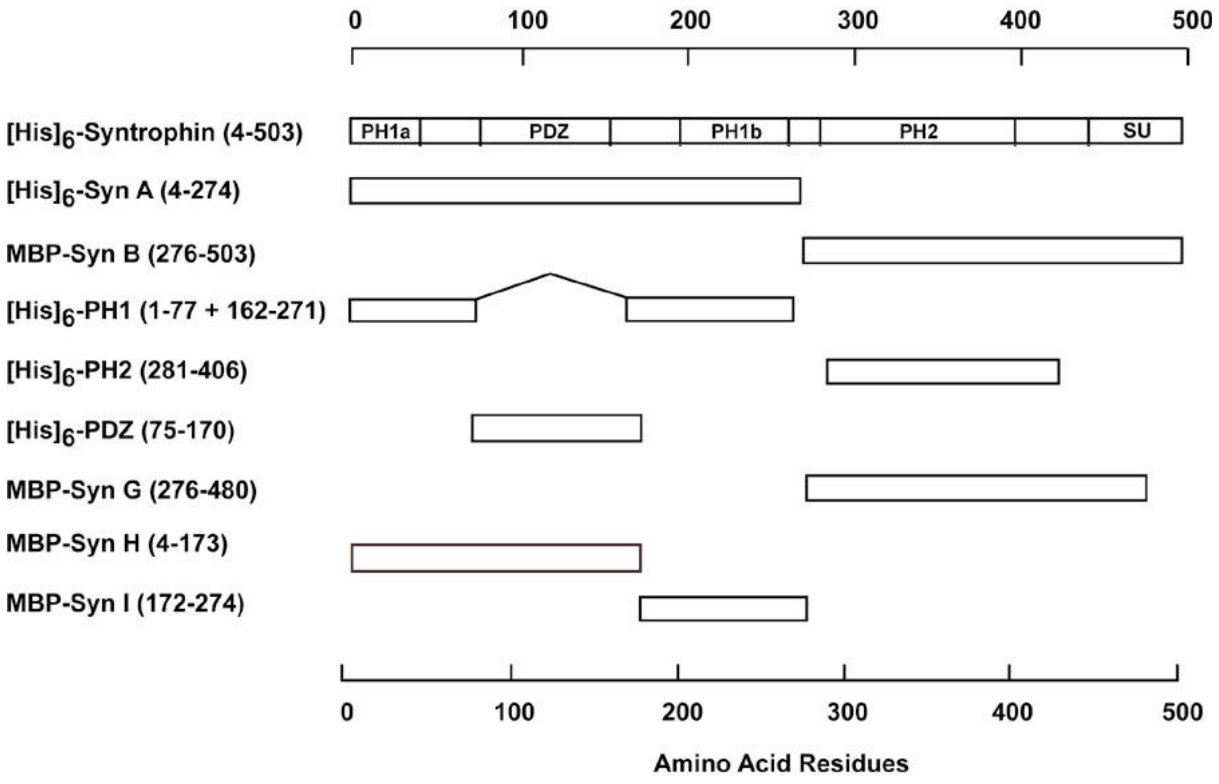

Figure 1.2 Domain structure of syntrophin.

Numbers in the parentheses represent the syntrophin amino acid sequences present in each fusion protein.

such proteins are implicated in oncogenesis and developmental disorders. PH domains frequently possess two biological activities: they bind phosphatidylinositol 4,5-bisphosphate and the heterotrimeric GTPase protein $\beta\gamma$ subunits (49-51). The PH domain of $\alpha 1$-syntrophin binds phosphatidylinositol 4,5-bisphosphate (PtdIns4,5P_2) (52). The half-maximal binding occurred at 1.9 μM PtdIns4,5P_2. The binding is specific for PtdIns4,5P_2 and does not occur with six other tested lipids including the similar phosphatidylinositol-4-phosphate. The binding is localized to the N terminal PH1 domain; the second C-terminal PH2 domain does not bind lipids. Key residues in PtdIns4,5P_2 binding to a PH domain are conserved in α–syntrophin's PH1 domain and absent in PH2 domains (52).

Syntrophins also bind calmodulin (53). This binding has been localized to two sites, one at the N-terminal region of the PH1 domain and the other at the N-terminal of the PDZ domain (54). Whether this N-terminal calmodulin binding is Ca^{2+} dependent (54) or independent (48) is controversial (55).

Syntrophin has also been shown to bind Ca^{2+} (48) at two sites residing in the amino-terminal 274 residues, and Ca^{2+} binding affects calmodulin binding at high concentrations of syntrophin (48).

PDZ domain

PDZ domains are known to play a role in protein-protein interactions. Syntrophin's PDZ domain has been shown to bind neuronal nitric oxide synthetase (56). Neuronal nitric oxide synthetase (nNOS) is concentrated at synaptic junctions in brain and at motor endplates in skeletal muscle. nNOS contains a PDZ motif of ~100 amino

acids and mediates association with syntrophin through the PDZ domains on each protein (57,58). nNOS and α1-syntrophin share similar distribution in skeletal muscle fast fibers (56). Thus syntrophin acts as a modular adapter protein linking a signaling enzyme, nNOS, to the sarcolemmal dystrophin complex.

Stress activated protein kinase-3 (SAPK3), a member of mitogen activated protein kinase family is abundantly expressed in skeletal muscles (59). It also binds through its C-terminal sequence –KETXL to the PDZ domain of α1-syntrophin (59). SAPK3 phosphorylates α1-syntrophin at Serine residues 193 and 201 *in vitro*. SAPK3 and α1-syntrophin colocalize at the neuromuscular junction in skeletal muscle.

Sodium channels SkM1 and SkM2 from extracts of skeletal and cardiac muscle, respectively, copurify with syntrophin and dystrophin. Peptides corresponding to the C-terminal 10 amino acids of SkM1 and SkM2 are sufficient to bind detergent-solubilized muscle syntrophins and inhibit the binding of native sodium channels to syntrophin PDZ domain fusion proteins. They bind specifically to PDZ domains from α1-, β1-, and β2-syntrophin. These peptides also inhibit binding of the syntrophin PDZ domain to the PDZ domain of neuronal nitric oxide synthase, an interaction that is not mediated by C-terminal sequences. Brain sodium channels, which lack the (S/T)XV consensus sequence, also copurify with syntrophin and dystrophin, an interaction that does not appear to be mediated by the PDZ domain of syntrophin. Thus, syntrophins link sodium channels to the actin cytoskeleton and the extracellular matrix via dystrophin and the DAPs (60).

SU domain

A domain unique to syntrophins, the SU domain has been shown to bind Ca^{2+}-calmodulin with an apparent affinity of 18 nM (48) and the SU domain, in addition to other sequences in the C-terminal of the protein, binds to dystrophin. This binding does not require Ca^{2+}. Ca^{2+}-calmodulin binding inhibits the syntrophin-dystrophin interaction (48).

Function of the DGC

Progress in identifying and characterizing DGC proteins was accompanied by investigations on their role in maintaining muscle cell integrity. Studies on isolated DGC have shown that α–dystroglycan is an extracellular, matrix binding-protein (20) and is attached to the transmembrane proteins of the DGC. Later it was also shown that α–dystroglycan showed direct binding to the extracellular matrix protein, laminin (61). This binding was Ca^{2+} dependent and the entire DGC could be purified by using laminin-Sepharose affinity chromatography (25). Homology studies showed that dystrophin's N terminal domain bears a strong resemblance to the actin-binding domain of chicken α–actinin (62). The binding of actin by dystrophin and the interaction of α–dystroglycan with laminin led to the hypothesis that one of the DGC functions is to link the extracellular matrix to the actin cytoskeleton (25). A loss of dystrophin and the accompanying loss of other DGC proteins, such as α–dystroglycan (19) would result in a loss of this link, making the tissue susceptible to degradation. Disruption of this link has been proposed to cause DMD/BMD and SCARMD (63).

Signal transduction

The DGC is important in maintaining muscle cell integrity. Madhavan, et al. originally proposed in 1992 that the DGC was a signal transduction complex (53). Ca^{2+} - calmodulin binding and phosphorylation-dephosphorylation have been shown to operate on DGC proteins, and suggest that these signal transduction mechanisms may be important to the etiology of muscular dystrophies.

Dystrophic tissue has been shown to have increased levels of Ca^{2+} and calmodulin, the major intracellular mediator of Ca^{2+} signal in eukaryotes (64). The increased Ca^{2+} concentration was suggested to be responsible for increased muscle protein degradation by increased Ca^{2+} activated proteases (65).

Protein phosphorylation-dephosphorylation is an important form of signal transduction that occurs in all cells (66). Dystrophin is phosphorylated by an endogenous protein kinase (67). DGC is also phosphorylated *in vivo* (68,69) and in sarcolemmal preparations (70). A protein phosphatase has also been shown to dephosphorylate dystrophin (67) and is probably calcineurin, the type 2b protein phosphatase (71).

Indeed, the numerous signal transduction proteins now known to have association with the DGC makes it almost certain that this complex is involved somehow in cell signaling. Binding of syntrophin to nNOS (56), SAPK3 (59), muscle and nerve voltage gated Na^{+} channels (60) may participate in signal transduction mechanisms. Grb2 has also been shown to recruit focal adhesion kinase, FAK^{125}, to the DGC (72,73). Phosphorylated tyrosines on FAK^{125} act as docking sites for molecules

such as Grb2 that participate in multiple signal transduction pathways.

Various other types of muscular dystrophies such as Fukuyama type muscular dystrophy, Emery-Dreifuss muscular dystrophy along with congenital muscular dystrophy (CMD), severe childhood autosomal recessive muscular dystrophy, and limb girdle muscular dystrophy have been discussed in detail by Bertorini et al. (4).

Summary

In this dissertation, different *in vitro* interactions of syntrophin are studied. Oligomerization of syntrophin has been characterized and discussed in Chapter 2. Syntrophin binding to Grb2 has been identified, characterized and discussed in Chapter 3. Chapter 4 describes the signal transduction pathway going via syntrophin when the DGC is attached to laminin leading to phosphorylation and activation of the Jun N terminal kinase 2. Several discoveries were made during the course of these studies that contribute towards a more complete characterization of the DGC. An understanding of the DGC function is required in order to effectively develop treatments for patients afflicted with muscular dystrophy.

Chapter 2. The Oligomerization Of Mouse α1-Syntrophin And Self-Association Of Its Pleckstrin Homology Domain 1 Containing Sequences[i]

Introduction

Syntrophin, a peripheral membrane protein, was first identified in the postsynaptic membrane of *Torpedo* (74). Syntrophins were found to be associated with the dystrophin glycoprotein complex (75) whose defects cause Duchenne, Becker, various limb girdle, and other muscular dystrophies (30). Syntrophins are a multigene family of homologous proteins, namely α1, β1 and β2. α1-Syntrophin is predominantly expressed in striated muscles and brain, whereas β syntrophins are ubiquitous in mammalian tissues (43). All syntrophins are known to contain two pleckstrin homology (PH) domains, an N-terminal PH1 domain and a PH2 domain. This domain structure is shown diagrammatically in Figure 2.1. The PH1 domain is interrupted by an inserted PDZ domain, a homologous domain found in the postsynaptic density 95 kDa protein, neuronal nitric oxide synthetase, and other membrane proteins (57,58). Syntrophins also have a unique domain at the C-terminus, the syntrophin unique (SU) domain. Recently, the PH1 domain of α1-syntrophin has been reported to bind[ii]

---

[i] Reproduced with permission from Biochemistry, Oak, S. A., and Jarrett, H. W. (2000) 39(30), 8870-7. Copyright [2000] American Chemical Society.

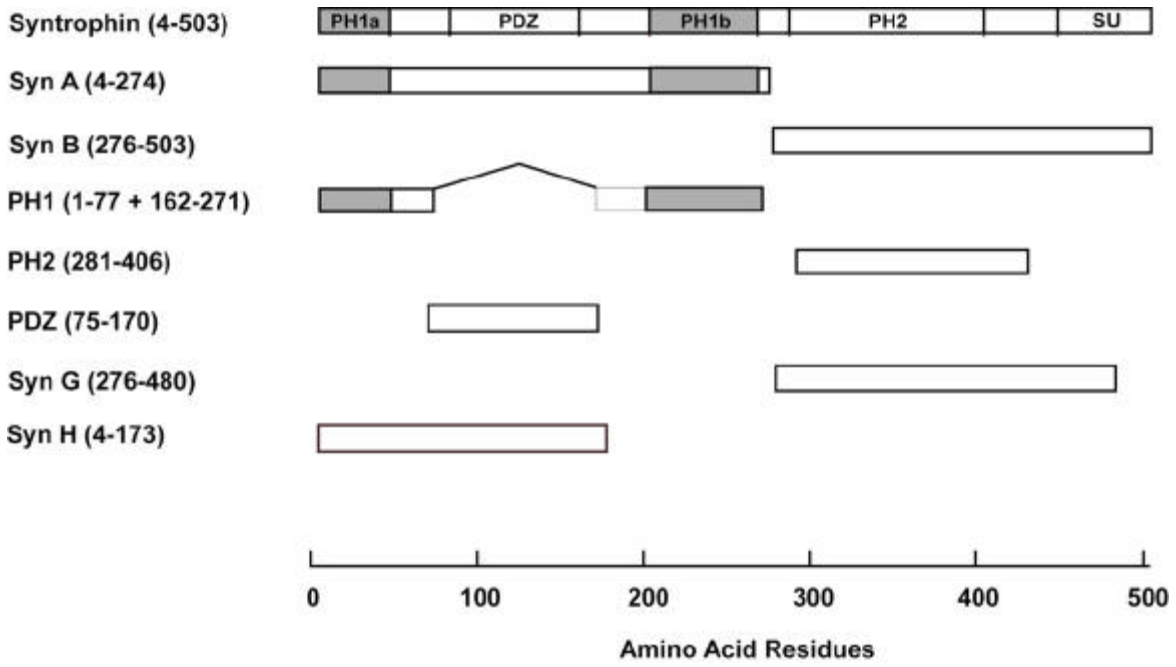

Figure 2.1 Diagrammatic representation of fusion proteins containing α1-syntrophin sequences.

The shaded portion shows the location of PH1 domain. Numbers in the parentheses represent the syntrophin amino acid sequences present in each fusion protein.

phosphatidylinositol 4,5-bisphosphate (Ptdlns4,5P_2) (52). Syntrophins also bind calmodulin (53). The SU domain of syntrophin has also been shown to bind Ca^{2+}-calmodulin (48), a ubiquitous calcium binding protein. The N-terminal of the PH1 domain and the N-terminal of the PDZ domain have been reported (54) to also bind calmodulin. Whether this N-terminal calmodulin binding is Ca^{2+}-dependent (54) or -independent (48) is controversial (55). α1-Syntrophin has also been shown to bind calcium (48). Thus, Ca^{2+}, calmodulin, and Ptdlns4,5P_2 may affect the activities of syntrophins. Syntrophins may also play a role as an adapter that links different cellular proteins to the dystrophin glycoprotein complex (76). PH domains are also known to bind heterotrimeric G protein, $G_{\beta\gamma}$ and syntrophin's PDZ domain binds voltage gated Na^+-channels in muscles and nerves (60) and the MAP kinase, SAPK3 (59). The SU domain binds Ca^{2+}-calmodulin and the SU domain plus other sequences in the C-terminal of the protein bind to dystrophin, the protein product of the Duchenne muscular dystrophy gene. Ca^{2+}-calmodulin binding inhibits the syntrophin-dystrophin interaction (48). α1-Syntrophins are known to self-associate and associate with other syntrophins (43,45,46,48). This oligomerization is currently only poorly characterized. Oligomerization of syntrophins is also likely to be physiologically relevant since the dystrophin glycoprotein complex contains one copy of most constituents but two syntrophins, suggesting self-association to at least a dimer *in vivo* (20). In this part of the dissertation, we have studied oligomerization of the mouse α1-syntrophin. We show here that the PH1 domain of α1-syntrophin is involved in the oligomerization of syntrophin *in vitro* and that Ca^{2+} regulates it.

Experimental procedures

Materials

Endoproteinase Xa (from bovine plasma) was from New England Biolabs. T7 monoclonal antibody for $[His]_6$-Tag fusion proteins was from Novagen. Goat anti-rabbit IgG (H+L)-alkaline phosphatase conjugate and goat anti-mouse IgG (H+L)-alkaline phosphatase conjugate were from BioRad. Ni^{2+}-NTA-agarose was from Qiagen. Cyanogen bromide pre-activated Sepharose was from Sigma. All other chemicals were of the highest purity available commercially.

Fusion proteins

The syntrophin fusion proteins $[His]_6$-Syn, $[His]_6$-Syn A, maltose binding protein (MBP) fusions MBP-Syn B, and MBP-Syn H were prepared as described previously (48). pET32 plasmid constructs for PH1, PH2, and the PDZ domain were the generous gift from Drs. Steven Gee and Stan Froehner, (Department of Physiology, University of North Carolina, Chapel Hill). pET32 plasmids encoding $[His]_6$-thioredoxin-PH1, -PH2, and -PDZ were used to express proteins referred to here as: $[His]_6$-PH1, -PH2, and –PDZ (60). The His-Tag fusion proteins were purified by using Ni^{2+}-NTA-agarose from Qiagen as described earlier (48). The MBP fusion proteins were purified using amylose affinity chromatography as described previously (77). The purity of the proteins was determined by 12% SDS-polyacrylamide gel electrophoresis using the method of Laemmli (78). The major bands of the fusion proteins were of expected size and

relatively high purity. The Bradford assay (79) was used to determine the protein concentrations with bovine serum albumin as the standard.

Ultracentrifuge oligomerization assay

All proteins were centrifuged at 100,000 rpm (BeckmanTLA-100 rotor) before dialysis in order to remove any insoluble protein. 50 μl of fusion protein was dialyzed in buffer A (50 mM Tris, pH 7.5, 100 mM KCl) containing 100 μM Ca^{2+} or 100 μM EGTA overnight at 4^0. The next day 10 μl of the dialyzed sample was saved as the total 'T'. To this 10 μl of 2X Laemmli buffer was added. 20 μl of the remaining sample was subjected to centrifugation at 100,000 rpm (Beckman TL-100 Ultracentrifuge, TLA - 100 rotor, 440,000 g_{max}) for 15 min at 4^0 in polycarbonate tubes (7 x 20 mm; Beckman). Then 10 μ l of the supernatant (S) was taken and 10 μl of 2X Laemmli buffer (1X is 62.5 mM Tris/HCl, pH 6.8, 0.001% bromophenol blue, 6.25% glycerol, 2% sodium dodecylsulfate, and 0.7 M 2-mercaptoehanol) was added to it. After removing the remaining supernatant, the pellet (P) was dissolved in 40 μl of 1X Laemmli buffer with vigorous vortexing and using a bath type sonicator. The samples were heated for 5 min at 95^0, applied to a 12% SDS-PAGE gel (78), and stained with Coomassie brilliant blue. The amount of protein in the total, supernatant and pellet was compared using Alpha Innotech Camera System (The Alpha Innotech Corp.) and AlphaImager 2000 3.3b software. The amount of the protein in ‘T’ was treated as 100% and the percentage of the protein in ’S’ and ‘P’ was calculated accordingly.

Solid phase binding assays

1.6 mg of Syn (0.8 mg/ml) and 1.8 mg of PH1 (1.5 mg/ml) were coupled to 1 g of cyanogen bromide-activated Sepharose (Sigma) using procedures recommended by the manufacturer (Pharmacia). The support was then washed with the coupling buffer (0.1 M $NaHCO_3$, pH 8.3, 0.5 M NaCl) and blocked for 2 hours with 0.1 M Tris-HCl, pH 8, 0.5 M NaCl. The amount of the protein coupled (0.2 mg/g of Sepharose for syntrophin and 1.67 mg/g of Sepharose for PH1) was determined by the difference in the ultraviolet absorption of the added protein and that recovered from coupling in the wash fractions. For negative controls, CNBr-activated Sepharose to which no protein was coupled was used.

200 μl of a 50% slurry of Syn-Sepharose containing 3 μg Syn was equilibrated with buffer A containing 100 μM Ca^{2+} and then incubated with different fusion proteins (25 μg) for 1 hour at room temperature and for 30 minutes on ice with gentle mixing in a final volume of 200 μl. For control, Sepharose without any protein coupled to it was used. After the incubation, Syn-Sepharose was washed three times with 0.5 ml of BSA/TTBS (1 mg/ml BSA in 20 mM Tris-HCl, pH 7.5, 0.5 M NaCl and 0.05%Tween-20). The protein was eluted using 60 μl of 2x Laemmli buffer. Samples were heated for 5 min at 95^0. The samples were then centrifuged for 5 min at room temperature to remove the resin, applied to electrophoresis on a 12% SDS-PAGE gel (78), and electroblotted onto nitrocellulose paper (80). The paper was then blocked with 10 mg/ml BSA in TTBS. After washing extensively with 1 mg/ml BSA/TTBS, the blot was incubated with affinity purified anti-MBP (1:1000 dilution) for MBP fusion proteins or T7 monoclonal antibody

(Novagen, 1:10,000 dilution) for His-Tag fusion proteins. Goat anti-rabbit IgG (H+L)-alkaline phosphatase conjugate and goat anti-mouse IgG (H+L)-alkaline phosphatase conjugate (both 1:1000 dilution, BioRad) were used, respectively, following the primary antibodies. The blot was developed using 1:100 dilution each of 30 mg/ml NBT (in 70% dimethylformamide) and 15 mg/ml BCIP (in 100% dimethylformamide) in buffer AP (0.1M $NaHCO_3$, 1mM $MgCl_2$, pH 9.8). A similar experiment was carried out using PH1-Sepharose.

His tag digestion

50 μl of the Syn A was digested with 1 μl of endoproteinase Xa (1 mg/ml) by dialyzing for 12 hours at 4^0 in digestion buffer (50 mM Tris, pH 7.5, 100 mM NaCl, 2 mM $CaCl_2$ and 1 mM NaN_3). Cleavage of the fused sequences was confirmed on 12% SDS-PAGE. The ultracentrifugation experiment was performed using the digested protein and compared with the undigested protein.

Size exclusion chromatography

Syn A (0.8 mg/ml) was dialyzed in MC (10 mM Mops, pH 7.0, 90 mM KCl, 1 mM $CaCl_2$) or ME buffer (10 mM Mops, pH 7.0, 90 mM KCl, 1 mM EGTA) for 12 hr at 4^0. 300 μl of the dialyzed protein was loaded on a Sepharose 4B column (1.4 cm x 42.5 cm). 80 ml of mobile phase (MC or ME buffer) was passed through the column at a flow rate of 0.33 ml/min and 1.5 ml fractions were collected. Three equivalents of calmodulin were added to Syn A in the experiments involving calmodulin. A microtiter plate (Dynatech Immulon 1) was coated by incubation of 100 μl/well of each fraction for 4 hr

at 4^0. The plate was then blocked by replacing the fractions with 300 μl/well of 30 mg/ml BSA in AC7.5 buffer (50 mM Tris-Cl, pH 7.5, 100 mM KCl, 3 mM $MgCl_2$, 1 mM $CaCl_2$). All subsequent operations were at room temperature and 100 μl/well. After washing extensively with AC7.5T/BSA (buffer AC7.5, 0.1 % Tween-20, 1 mg/ml BSA), the plate was incubated with T7 monoclonal antibody (Novagen, 1:10,000 dilution). Goat anti-mouse IgG (H+L)-alkaline phosphatase conjugate (both 1:1000 dilution, BioRad) was used following the primary antibody. The plate was then washed once with 1 mg/ml AC7.5T/BSA followed by two immediate washes of diethanolamine buffer (10 mM diethanolamine, 0.5 mM $MgCl_2$). The plate was then developed by incubation with 100 μ l/well of 1 mg/ml *p*-nitrophenylphosphate in diethanolamine buffer. The absorption at 405 nm was determined.

Results

Mouse α1-syntrophin sequences expressed as fusion proteins are diagrammatically represented in Figure 2.1. The regions of mouse α1-syntrophin's amino acid sequence in each construct are given in parenthesis. The boundaries of the PH1 domain are not well defined. Our PH1 construct contains some additional sequences as shown in Figure 2.1. PH1 domain sequences are shaded in the fusion proteins containing them as these are involved in oligomerization (see below). Syn, Syn A, PH1, PH2 and PDZ were produced as His-Tag fusion proteins while Syn B and Syn H were produced as maltose binding fusion proteins. Each fusion protein was expressed and affinity purified using Ni^{2+}-NTA-agarose for His-Tag fusion proteins and amylose-agarose for maltose binding fusion proteins.

Figure 2.2 shows the purity of the proteins used for the experiments. The purified proteins are mostly full length but some show partial proteolysis. This partial proteolysis has been investigated and discussed previously (48,77). All the proteins were boiled for 5 min in the presence of SDS and 2-mercaptoethanol. This was necessary to observe predominantly the monomer molecular weight of PDZ domain protein which otherwise migrates as a dimer (52). The experiments were repeated with different preparations of each protein and were reproducible with all of the preparations tested.

Syntrophins self associate (43,45,46,48) and the larger oligomers can be collected by centrifugation. Oligomerization and precipitation in the centrifuge for Syn A in different Ca^{2+} concentrations or in EGTA is shown in Figure 2.3. Though approximately 20% of the protein precipitated in the presence of EGTA, the majority of the protein precipitated at Ca^{2+} concentrations at or above micromolar. This difference is statistically significant. Figure 2.4 summarizes the precipitation observed for all the proteins tested namely Syn, Syn A, Syn B, Syn H, PH1, PH2 and PDZ in presence of 100 μM Ca^{2+} and 100 μM EGTA. $[His]_6$-green fluorescent protein GFP (81) and MBP-LacZα (22) were used as controls for His-Tag and maltose binding fusion proteins, respectively, and as expected, neither shows appreciable aggregation. Figure 2.4 shows that Syn, Syn A, Syn H, and PH1 aggregate in Ca^{2+} while other proteins, namely Syn B, PH2, and PDZ, which did not show any significant precipitation are shown in Figure 2.5. Thus fusion proteins containing the PH1 domain precipitate in a Ca^{2+}-dependent manner. Though Syn H shows less precipitation as compared to other PH1 domain containing fusion proteins, it should be noted (see Figure 2.1) that Syn H has only the N-terminal portion of the PH1 domain (PH1a) and lacks C-terminal sequences

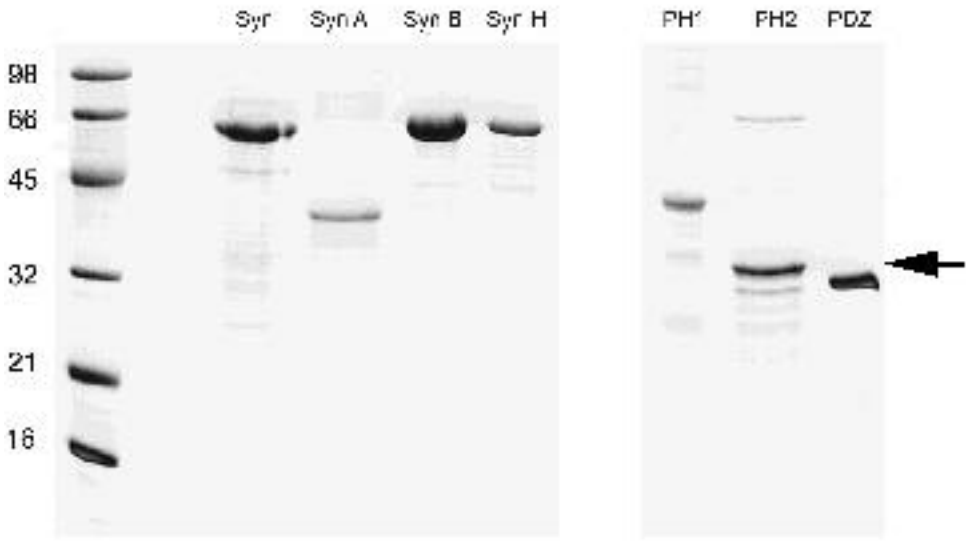

Figure 2.2 Purity of the fusion proteins used.

Two micrograms of each fusion protein with the tag intact was applied to 12% sodium dodecylsulfate-polyacrylamide gel electrophoresis and stained with Coomassie brilliant blue. The molecular weight of the markers, in kilodaltons, is shown to the left. The arrow to the right shows the position of full length PH2.

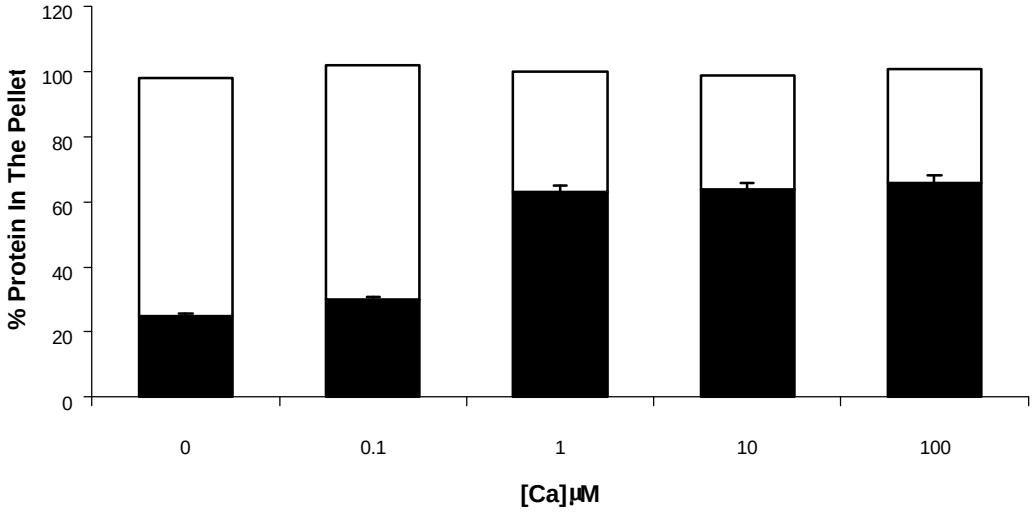

Figure 2.3 Syn A precipitates in a Ca^{2+} dependent manner and the Ca^{2+} chelating reagent, EGTA inhibits it.

The ultracentrifuge oligomerization assay was performed as described in Materials and Methods. Full bar length represents total protein. Open bars (white), percent protein in the supernatant, closed bars (black), percent protein in the pellet. The standard error of the mean (of duplicates) is given as error bars in each graph. The amount of Ca^{2+} given here is the calculated, free concentration after adding Ca^{2+} to 0.1 mM EGTA in the buffer.

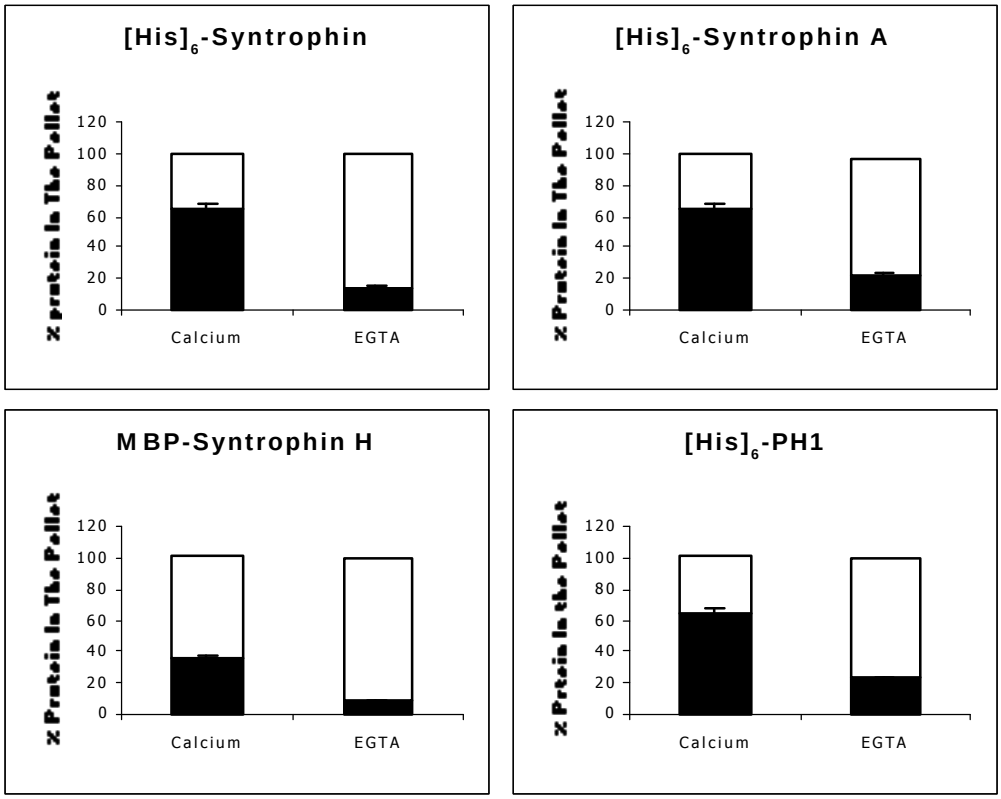

Figure 2.4 Extent of precipitation of Syn, Syn A, Syn H, Syn B, PH2, PDZ, and PH1 in the presence or absence of Ca^{2+}.

Extent of precipitation of Syn, Syn A, Syn H, and PH1 in a Ca^{2+} dependent manner.

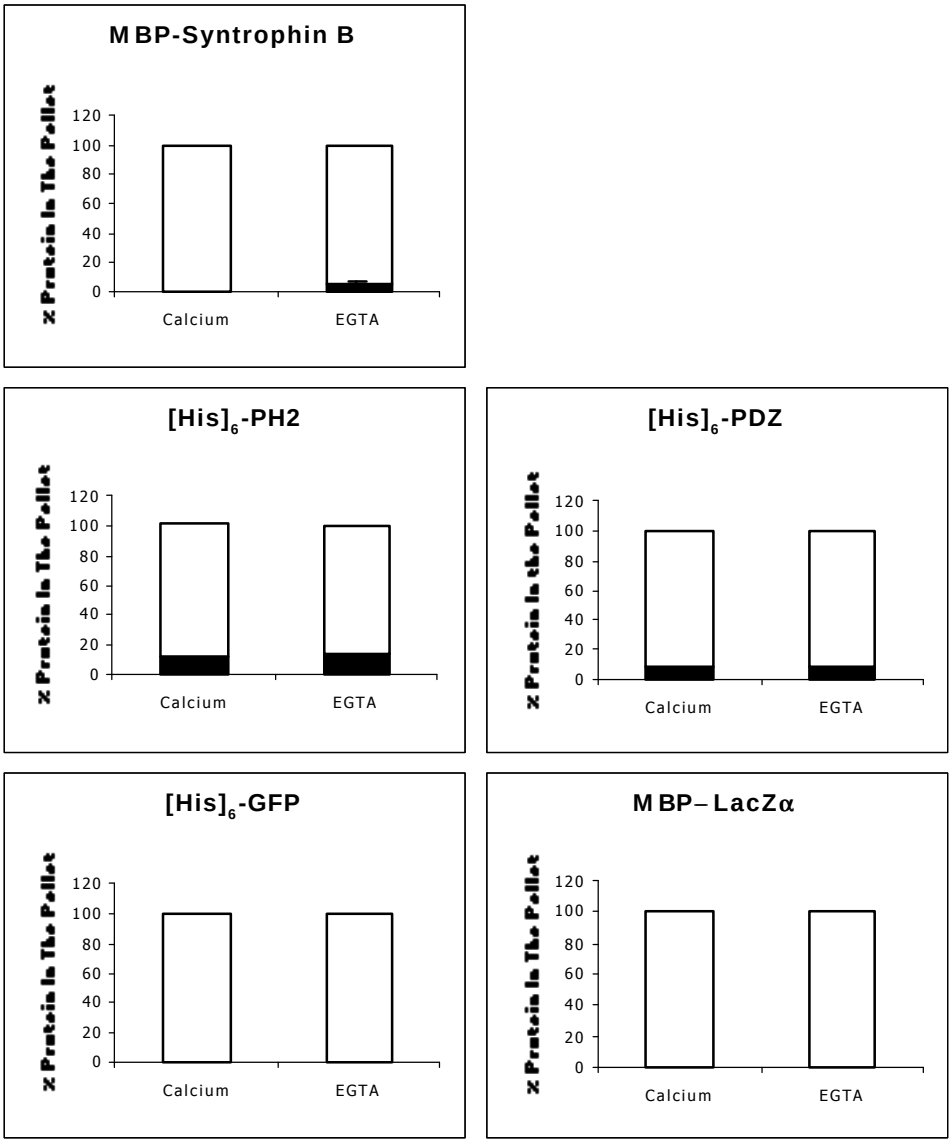

Figure 2.5 Extent of precipitation of Syn B, PH2, PDZ, GFP, and Laczα in a Ca^{2+} dependent manner.

Syn B, PH2, PDZ, and the controls used for His-Tag and MBP fusion proteins, GFP and MBP-LacZα do not show significant precipitation. The labels are as defined in Figure 2.3. The standard error of the mean (of duplicates) is given as error bars in each graph.

(PH1b). To show that these results were not artifacts caused by prolonged dialysis or centrifugation, freshly dialyzed protein was centrifuged to remove any aggregate and this was briefly incubated with Syn-Sepharose. Figure 2.6 confirms the localization of the syntrophin-syntrophin interaction as shown previously in Figure 2.4. Syn, Syn A, Syn H, PH1 show binding to Syn-Sepharose while Syn B and PDZ did not show any binding. CNBr-activated Sepharose-4B without any protein coupled to it was used as a negative control. Other fusion proteins such as PH2 also did not show any binding (data not shown).

The syntrophin-syntrophin interaction is further localized in Figure 2.7. Syn, Syn A, Syn H, and PH1 show binding to PH1-Sepharose while PH2 did not show any binding. None of the fusion proteins bound significantly to the control Sepharose (lacking PH1). The combined results of Figure 2.6 and 2.7 show that the sequences present in the PH1 fusion protein are necessary and sufficient for syntrophin-syntrophin interaction. These also demonstrate that PH2 and PDZ domains do not play an obvious role in syntrophin-syntrophin interactions.

Ca^{2+}-calmodulin has been shown to bind the N-terminal sequences of the PH1 domain (54), which are also involved in oligomerization. The effect of calmodulin on the syntrophin-syntrophin interaction was also tested. PH1 was incubated with PH1-Sepharose in the presence or absence of calmodulin in the presence of 100 μM Ca^{2+} or 100 μM EGTA. Inhibition of the PH1-PH1 interaction by calmodulin is shown in Figure 2.8. While Ca^{2+} enhances the PH1-PH1 interaction, calmodulin inhibits it in Ca^{2+} or EGTA. Figure 2.9 shows the precipitation of Syn A at different concentrations of calmodulin in the presence of 100 μM Ca^{2+} or 100 μM EGTA. In Ca^{2+}, calmodulin

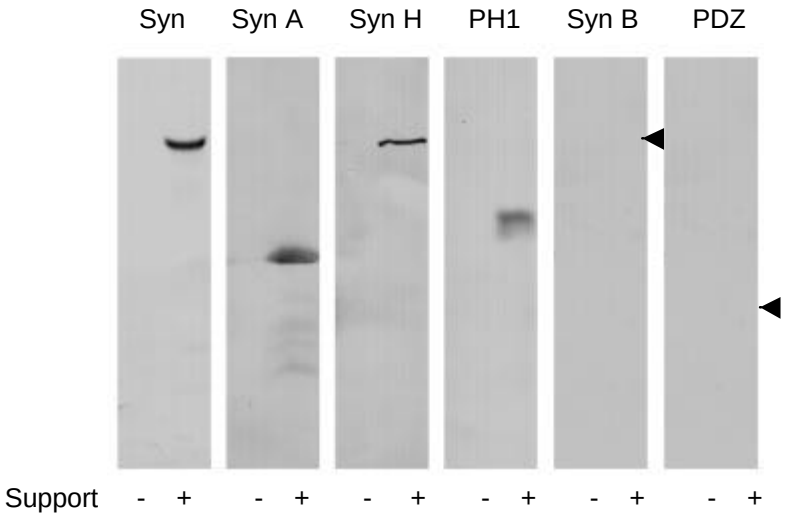

Figure 2.6 Localization of the region involved in the oligomerization of syntrophin. Syn, Syn A, Syn H, PH1 show binding to Syn-Sepharose. (-) represents control-Sepharose (no protein coupled), (+) represents Syn-Sepharose. To the right are two arrows; the upper shows the molecular weight of Syn B, the lower shows the molecular weight of PDZ which do not show binding to Syn-Sepharose.

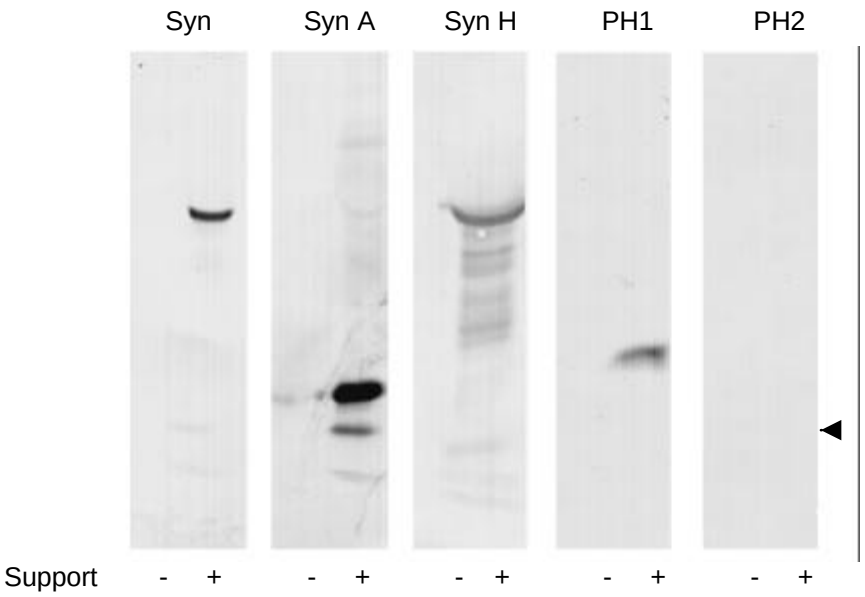

Figure 2.7 Syntrophin's self-association is localized to the PH1 domain containing sequences.

Syn, Syn A, Syn H, PH1 show binding to PH1-Sepharose. (-) represents control-Sepharose, (+) represents PH1-Sepharose. The arrow to the right shows molecular weight of PH2, which do not bind to PH1-Sepharose.

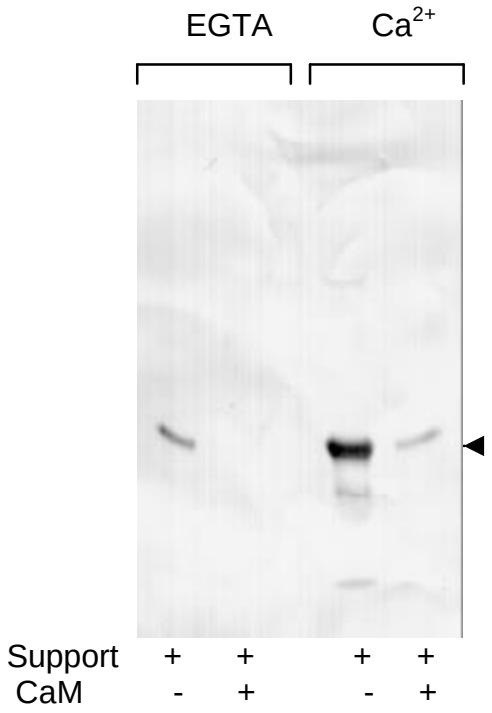

Figure 2.8 Calmodulin inhibits syntrophin self-association in the presence or absence of Ca^{2+}.

Calmodulin inhibits syntrophin self-association in the presence or absence of Ca^{2+}. PH1-Sepharose was incubated with the PH1 fusion protein in the presence (+) and absence (-) of calmodulin in the presence of 100 μM Ca^{2+} or 100 μM EGTA.

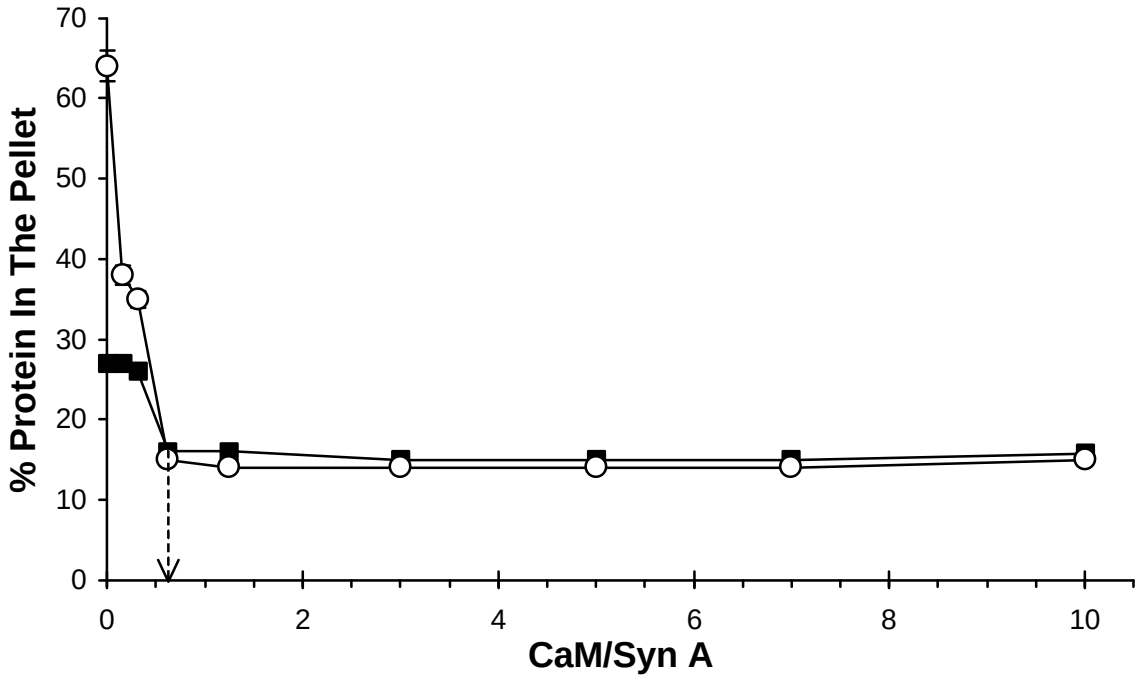

Figure 2.9 Precipitation Syn A at different concentrations of calmodulin in the presence of Ca^{2+} or EGTA.

Precipitation of Syn A (using the ultracentrifuge oligomerization assay) at different concentrations of calmodulin in the presence of 100 μM Ca^{2+} (open circles) or 100 μM EGTA (closed squares). The standard error of the mean is given as error bars. The dotted line shows that the breakpoint in the titration occurs near one calmodulin per syntrophin.

reduces the precipitation of Syn A from 64% to 14% in a dose-dependent manner. In addition, Figure 2.9 shows that calmodulin also inhibits precipitation of Syn A in EGTA over a similar concentration range. For both curves, a sharp break occurs at 0.65 mol calmodulin / mol syntrophin suggesting that a single calmodulin binds to cause inhibition of the precipitation.

Nickel has been reported to induce oligomerization of proteins containing the $[His]_6$-Tag and removal of this affinity tag by treatment with endoproteinase Xa abolished the ability of the proteins to form oligomers (82). Since Syn, Syn A, and PH1 are all His-Tag fusion proteins, to show that the observed precipitation was not due to the affinity tag, these fused sequences were digested using endoproteinase Xa to test whether they contributed to the precipitation. The experiment was performed with the digested protein and compared with the undigested protein. Both the digested and undigested proteins precipitated to a similar extent in a Ca^{2+} dependent manner (data not shown). That PH2, PDZ, and GFP (also His-Tag fusion proteins, see Figure 2.4) do not precipitate confirms that precipitation is not due to His-Tag sequences.

Syntrophin oligomerizes in Ca^{2+} and, to a lesser extent, in EGTA; to determine the size of Syn in presence of Ca^{2+} or EGTA, His-Tag Syn A was subjected to size exclusion chromatography on Sepharose 4B. Figure 2.10a (lower panel) shows that in the presence of Ca^{2+}, Syn A forms oligomers of several different sizes but 17% of the protein is larger than a 20 mer (>670kDa). When calmodulin was added to Syn A (upper panel) in the presence of Ca^{2+}, it effectively inhibited oligomerization of Syn A resulting in protein that was predominantly present as monomeric to octameric forms. When a similar experiment was repeated in the presence of EGTA, protein was

Figure 2.10 Size exclusion chromatography of Syn A in presence of Ca^{2+} and in EGTA. The column was run as described in the methods. The dashed lines show the position of molecular weight standards thyroglobulin, (TH); β-galactosidase, (BG); and carbonic anhydrase, (CA) on the chromatogram for reference. The numbers in the parentheses indicate molecular weight of the standards. The arrows indicate the size of different oligomers of Syn A on the chromatogram also for reference.

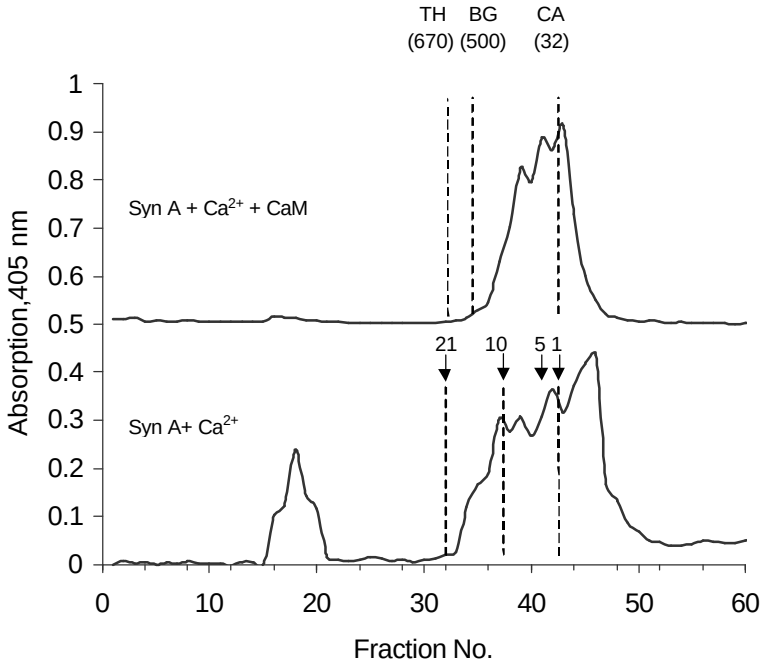

a) Size exclusion chromatography of Syn A in presence of Ca^{2+}.

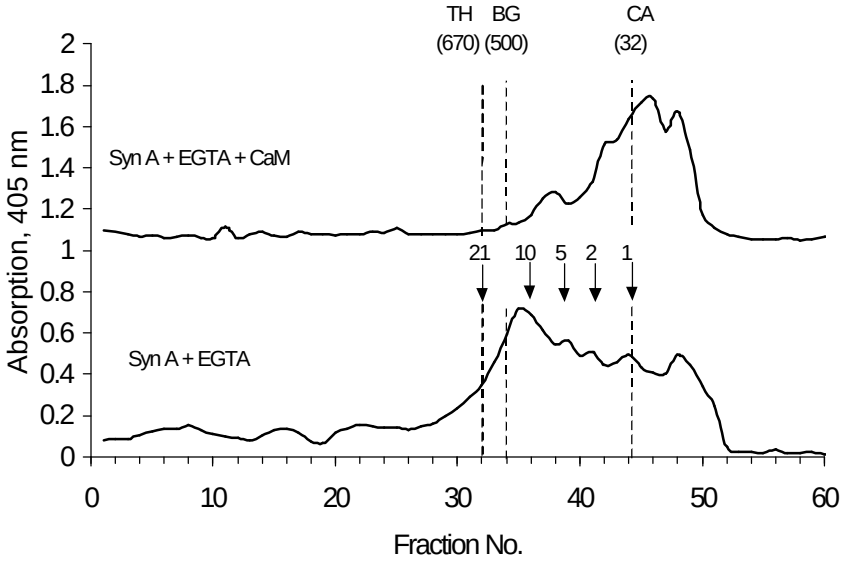

b) Size exclusion chromatography of Syn A in presence of EGTA.

predominantly present as monomeric to decameric forms even in the absence of calmodulin as shown in Figure 2.10b. The small peak at fraction number 16, which represents protein larger than a 20 mer, could account for the small amount of protein which precipitates in the ultracentrifugation experiments described earlier. When calmodulin was added to Syn A in the presence of EGTA, it prevented oligomerization and most of the protein was present at sizes consistent with a monomer.

The PH1 domain of syntrophin has been reported to bind Ptdlns4,5P_2 (52). Other experiments showed that the presence of Ptdlns4,5P_2 did not have any effect on oligomerization of Syn (data not shown) suggesting that lipid binding does not alter syntrophin's oligomeric state.

Discussion

α-Syntrophins were known to self-associate and associate with other syntrophins (43,45,46,48). A consistent level of aggregation of the syntrophins in the immunoprecipitation experiments was observed by Ahn et.al (43). *In vitro* translated α1-syntrophin has been shown to bind to all the three components of the syntrophin triplet in the overlay experiment by Yang et.al (45). The binding of α1-syntrophin with both β1 and β2 syntrophins has been previously seen in the overlay experiments by Madhavan et.al (46). Peters et al. (44) have shown that pairs of different syntrophins occur *in vivo*. This oligomerization was poorly characterized. Recently, it has been shown that the PH1 domain of mouse α1- syntrophin binds Ptdlns4,5P_2 (52). Syntrophin's PDZ domain is known to form a dimer (52) and thus was thought to play a role in the oligomerization of syntrophin. The syntrophin sequence has a leucine approximately every seventh

residue at its N-terminus from amino acid 107 to 137 similar to the leucine zipper motif (where leucine is present at exactly every seventh residue). Leucine zippers are known to mediate protein-protein interaction raising the possibility that this leucine zipper could function as an oligomerization motif of syntrophin. But in none of the experiments was $[His]_6$-PDZ, which contains the leucine-rich sequence, found to bind syntrophin or aggregate in the ultracentrifugation experiments. It may however account for the PDZ dimerization reported by others (52).

Here, we have shown that the PH1 domain containing sequence of α1-syntrophin is required for the oligomerization of syntrophin, which occurs in a Ca^{2+} dependent manner (Figure 2.4 and 2.6), and that micromolar concentrations of Ca^{2+} increase oligomerization (Figure 2.3). Conversely, Ca^{2+} chelating agents such as EGTA inhibit oligomerization (Figure 2.3). Since syntrophin alone, in the absence of calmodulin, responds to Ca^{2+}, Ca^{2+} must bind directly to syntrophin to cause this effect. Since Ca^{2+} affects even constructs as small as PH1, Ca^{2+}-binding must occur somewhere within these sequences. The PH domain of Dbl has been shown to bind Ca^{2+} with a K_d of 10 μM (83). It is curious to note that Ca^{2+} also regulates the oligomerization of other proteins such as actin (84) and tubulin (85).

Oligomerization does not occur with fusion proteins lacking the PH1 domain (Figure 2.5). Fusion proteins containing an intact PH1 domain precipitate to a larger extent than does Syn H which lacks C-terminal sequences (PH1b) of the PH1 domain (Figure 2.4). This may suggest that oligomerization is primarily a property of the N-terminal sequences of the PH1 domain (PH1a) or adjacent sequences. Interestingly, fusion proteins containing the PH2 domain do not seem to play a role in the

oligomerization of syntrophin (Figure 2.4 and 2.7). Non-PH1 domain sequences do not oligomerize (Figure 2.3 and 2.6).

We have also shown that the PH1 domain containing sequence alone is capable of self-association (Figure 2.7). Calmodulin inhibits the PH1-PH1 interaction (Figure 2.8) and inhibition does not require Ca^{2+} (Figure 2.8 and 2.9). This agrees with the observation by Iwata et.al. (54) that calmodulin binds to N-terminal sequences of PH1 domain. However, Iwata et.al. (54) found that calmodulin binding to this region was Ca^{2+}-dependent, while we had previously found it to be Ca^{2+}-independent. These results confirm that calmodulin binding to this region is Ca^{2+}-independent. Figure 2.9 shows that calmodulin inhibits oligomerization in the presence or absence of Ca^{2+}. Thus, Ca^{2+}-calmodulin or apocalmodulin (Ca^{2+}-free) can prevent self-association of the PH1 domain containing sequences and hence oligomerization of syntrophin. A single calmodulin apparently binds per syntrophin to inhibit syntrophin self-association (Figure 2.9).

We have also shown that when syntrophin oligomerizes in the presence of Ca^{2+} much of the protein is larger than a 20-mer (>670 kDa). It also forms several species of syntrophin oligomers such as 5-mer, 10-mer etc. The presence of calmodulin effectively prevents this oligomerization, converting the protein from 20-mer and larger to predominantly the monomer and hence shifting the peaks to the right on the chromatogram (Figure 2.10a). The peaks actually shift in both directions. When calmodulin is added to Syn A, Syn A can no longer form large aggregates and hence shifting the peak to the right on the chromatogram but because calmodulin binds to it, the molecular weights of the complexes increase, shifting the peaks slightly to the left on the chromatogram.

In the presence of EGTA, protein is predominantly present as monomeric to decameric forms (Figure 2.10b). When calmodulin is added to Syn A in presence of EGTA, it prevents oligomerization converting the protein to predominantly a monomer. The oligomerization of syntrophin is complex and a model depicting this oligomerization process is presented in Figure 2.11. This model suggests that the oligomerization of syntrophin, denoted by $(syn^*)_{p,}$ where P represents polymeric forms of syntrophin occurs by binding of Ca^{2+}-syntrophin (denoted by an asterisk), and this process is regulated by Ca^{2+} (Figure 2.3, 2.4, and 2.6) and calmodulin (Figure 2.8 and 2.9). Calmodulin inhibits the oligomerization in a Ca^{2+}-independent manner (Figure 2.9). Syn in this model is not meant to strictly refer to monomeric syntrophin but to include this and simple oligomers. The somewhat larger oligomers (Figure 2.10b) (up to decamer) which occur in the absence of Ca^{2+} are shown as $(Syn)_O$. In our previous report (48), another form of syntrophin is shown, indicated as Syn^X, which occurs at high concentrations in absence of Ca^{2+} that does not bind dansyl-calmodulin. This form is not shown in this scheme because it was not investigated in the experiments presented and is currently less well-defined but may represent a predominance of $(Syn)_O$ at high protein concentrations.

From these *in vitro* results, the state of syntrophin *in vivo* may be inferred. Calmodulin is present in many tissues as high as micromolar and is probably in sufficient concentration to inhibit or limit the oligomerization of syntrophin. In the resting muscle, Ca^{2+} would be submicromolar in concentration and this would also limit aggregation. The calmodulin bound would be the Ca^{2+}-free, apocalmodulin conformer (55). As intracellular Ca^{2+} increases, preceding and during muscle contraction, this Ca^{2+}

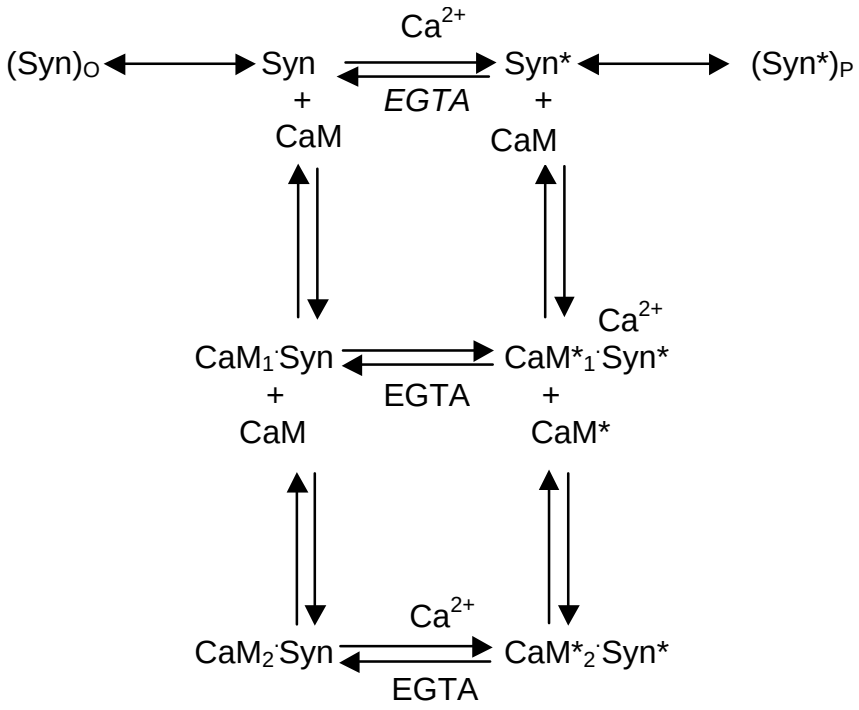

Figure 2.11 A model depicting oligomerization of syntrophin.

In this model calcium bound forms of syntrophin and calmodulin (CaM) are denoted with an asterisk (*). The polymeric forms of Ca^{2+}-syntrophin are denoted as $(Syn^*)_p$. The smaller oligomeric forms of syntrophin in the absence of Ca^{2+} are shown as $(Syn)_O$. $CaM_1{\cdot}Syn$ and $CaM_2{\cdot}Syn$ represent calmodulin binding to one or both of the two sites known (54) at the N-terminus of syntrophin.

could bind to syntrophin and favor syntrophin aggregation. Additionally, as Ca^{2+} binds calmodulin, calmodulin would be able to bind to other, more numerous cell proteins, which bind only the Ca^{2+}-calmodulin conformer. Thus, Ca^{2+}-calmodulin could be bound elsewhere, allowing syntrophin's oligomerization. Thus, one can envision syntrophin as monomeric in the resting cell and oligomeric in the contracting muscle. The oligomeric state of syntrophin may be important to maintaining the clusters of ion channels at the neuromuscular junction during contraction. Alternatively, syntrophins may respond to Ca^{2+} during contraction in a way that makes the protein complexes which contain it more resistant to the contractile forces. Indeed, it is now apparent that the dystrophin-actin (77), syntrophin-dystrophin (46), and syntrophin-syntrophin interactions all are responsive to Ca^{2+} and calmodulin suggesting that during muscle contraction, the protein-protein interactions within the dystrophin glycoprotein complex are altered and probably rearrange.

Phosphotidyl inositol-4,5 bisphosphate binds the PH1 domain (52) but it does not influence oligomerization. This would not be predicted from other PH domains, particularly of both dynamin isoforms, that require oligomerization for high affinity phosphoinositide binding (86). Since Ptdlns4,5P_2 did not affect oligomerization, it is clear that it does not regulate this syntrophin activity. What role(s) it plays remains to be elucidated. Binding this lipid probably serves the role of localizing syntrophin to the membrane surface. Syntrophins bind Na^{+}-channels (60), NO-synthetase (57,58), dystrophin, α- and γ- sarcolglycans (46), SAPK3 (59) and to themselves. This self-association could bring together cellular signaling components and ion channels. Calmodulin can thus inhibit syntrophin oligomerization in a Ca^{2+}-independent manner

(this report) and inhibit syntrophin's interaction with dystrophin in a Ca^{2+}-dependent manner (48). Furthermore, since Ca^{2+} promotes aggregation of syntrophin even in the absence of calmodulin, it must be able to bind to syntrophin itself and alter its chemical and physical properties. This agrees with our previous observation of Ca^{2+} binding by syntrophin.

Chapter 3. Mouse α1-Syntrophin Binding To Grb2: Further Evidence Of A Role For Syntrophin In Cell Signaling[ii]

Introduction

Syntrophins are a group of peripheral membrane proteins first identified in *Torpedo* postsynaptic membranes (74). Syntrophins have been found to be closely associated with dystrophin (75), the protein product of the Duchenne muscular dystrophy gene locus (75,87). In skeletal muscle, dystrophin and syntrophins are found in a complex with other proteins and glycoproteins, the dystrophin glycoprotein complex or DGC[1] (6,20) whose defects cause Duchenne, Becker, various limb girdle, and other muscular dystrophies. Syntrophins are a multigene family of homologous proteins. Three syntrophin isoforms, α1, β1, and β2, are products of different genes (58,88-90). The α1-syntrophin is primarily expressed in striated muscles and brain, while the β-syntrophins are ubiquitous in mammalian tissues (43). Each of the syntrophins contains two pleckstrin homology (PH) domains, an N-terminal PH1 domain and a PH2 domain (see Figure 3.1). The PH1 domain of α1-syntrophin has been reported to bind phosphatidylinositol 4,5-bisphosphate (PtdIns4,5P_2) (52). Recently, this domain has also been shown to be involved in the oligomerization of syntrophin *in vitro* in a Ca^{2+}-dependent manner. in which this ~90 amino acid motif was identified: the Postsynaptic

---

[ii] Reproduced with permission from Biochemistry, Oak, S. A., Russo, K., Petrucci, T. C., and Jarrett, H. W. (2001) 40(37), 11270-8. Copyright [2001] American Chemical Society.

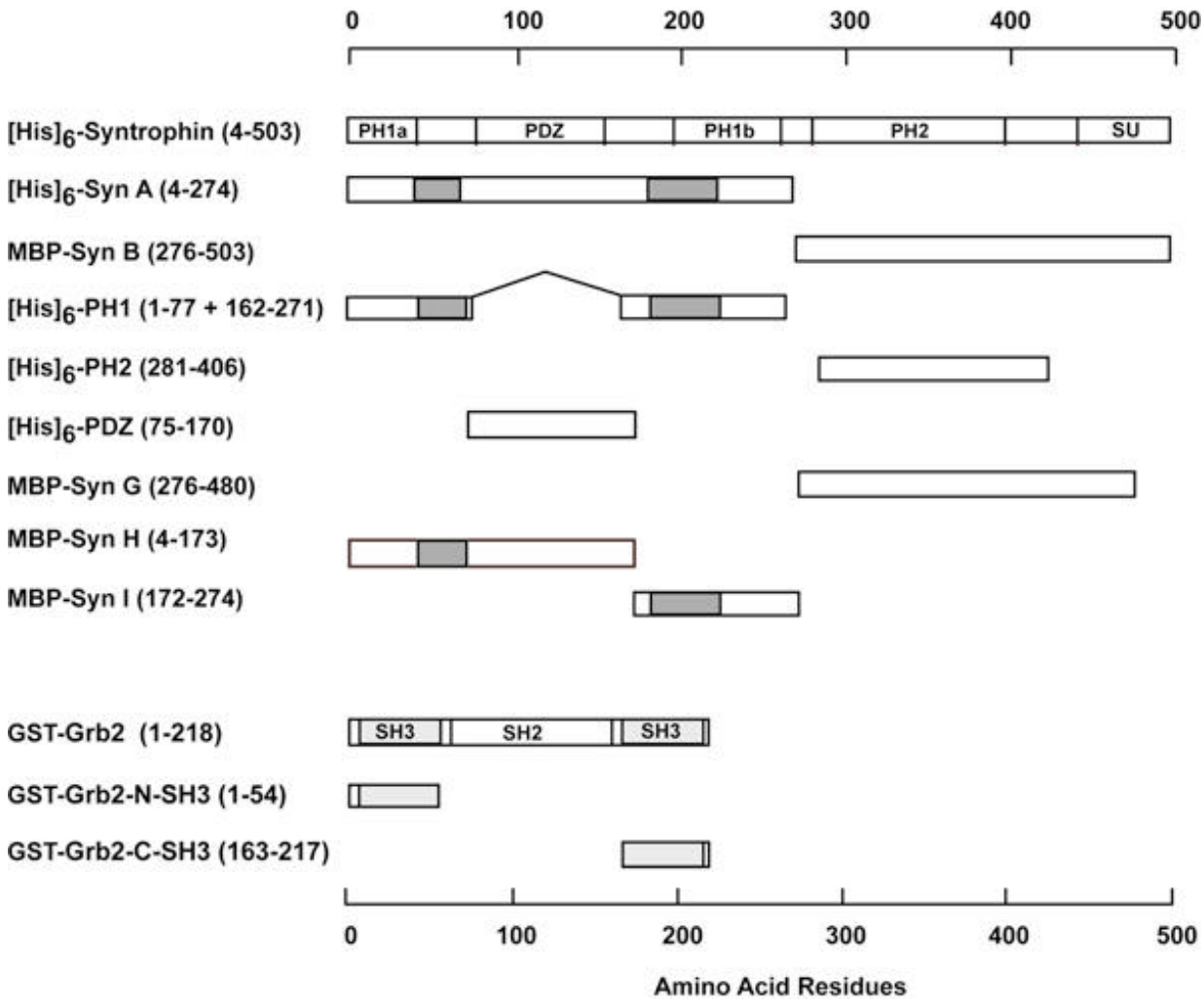

Figure 3.1 Diagrammatic representation of fusion proteins containing α1-syntrophin and Grb2 sequences.

The darkly shaded portion shows the location of proline rich motifs in syntrophin. The lighter shading highlight the SH3 domains of Grb2. Numbers in parentheses represent the amino acid sequences present in each fusion protein.

density protein (PSD-95), the Drosophila disks-large protein (Dlg), and the Zona Occludens 1 (ZO-1) protein. Calmodulin inhibits oligomerization in a Ca^{2+}-independent manner (91). The amino terminal PH domain is interrupted by an inserted PDZ domain. The PDZ domain is found in membrane proteins and was named for the first three proteins Syntrophin's PDZ domain has been shown to bind neuronal nitric oxide synthetase (57,58), muscle and nerve voltage gated Na^{+} channels (60), and the MAP kinase, SAPK3 (59). Syntrophins also bind calmodulin (53). A domain unique to syntrophins, the SU domain has been shown to bind Ca^{2+}-calmodulin (48) and the SU domain in addition to other sequences in the C-terminal of the protein binds to dystrophin. Ca^{2+}-calmodulin binding inhibits the syntrophin-dystrophin interaction (48). The N-terminal of the PH1 domain and the N-terminal of the PDZ domain have been reported to bind calmodulin (54) in a Ca^{2+}-independent manner (48,91). Thus, syntrophins act as adapters, in between the dystrophin complex of proteins and components of the cell signaling apparatus.

Grb2 (growth factor receptor bound 2), the human homologue of the nematode *Caenorhabditis elegans* protein Sem-5, is an adapter protein consisting of one *src* homology (SH) 2 domain flanked by two SH3 domains. The N-terminal SH3 domain stretches from amino acids 5 to 55, the SH2 domain from 60 to 158 and the C-terminal SH3 domain from 164 to 214. This structure suggests that Grb2 is capable of binding phosphotyrosine proteins through its SH2 domains, while its SH3 domains interacts with proteins possessing PXXP motifs. While investigating the known interaction (45, 72) between Grb2 and β-dystroglycan, we discovered that syntrophin was also a Grb2-binding protein. The N-terminus of syntrophin contains two proline-rich regions that

could interact with the SH3 domains of signaling proteins, namely:

PADGPGPEPEPAQLNGAAEPGAAPPQLPEAL (α-syntrophin 44-75)

WASPPASPLQRQPSSPGPQPRNLSEAKHVSLKMAYVSRRCTPTDPEPRY (181 to 229)

These are located in the intervening sequences between the PH1a and PDZ domain sequences and between the PDZ and PH1b domains and overlapping the N-terminus of the latter.

In this chapter, we have characterized the interaction of the mouse α1-syntrophin with the adapter protein, Grb2.

Experimental procedures

Materials

Antibodies against recombinant Grb2 (anti-Grb2), GST (anti-GST) and α-syntrophin were produced in rabbit and purified by affinity chromatography. Mouse monoclonal Grb2 antibody was from Transduction Laboratories. Crk-L rabbit polyclonal antibody was from Santa Cruz Biotechnology. S-protein alkaline phosphatase conjugate was from Novagen. Goat anti-rabbit IgG (H+L)-alkaline phosphatase conjugate, goat anti-mouse IgG (H+L)-alkaline phosphatase conjugate and goat anti-rabbit IgG (H+L)-horseradish peroxidase conjugate were from BioRad. Ni^{2+}-NTA-agarose was from Qiagen. Cyanogen bromide pre-activated Sepharose was from Sigma. All other chemicals were of the highest purity available commercially.

Dystrophin glycoprotein complex (DGC) was partially purified from digitonin solubilized rabbit skeletal muscle using the procedure of Ervasti, et al. (7) up through

the succinylated wheat germ agglutinin (sWGA) chromatography. Aliquots were stored frozen at –85°. DGC was further fractionated by electrophoresis on 4-15% gradient sodium dodecylsulfate polyacrylamide gels and blotted to nitrocellulose as previously described (46). The gel blots were then overlaid with Grb2 as described under *Overlay Experiments* below. Gel blots were also stained with specific antibodies for α-syntrophin, α- and β-dystroglycan, and α-sarcoglycan to confirm the identity of bands interacting with Grb2.

Fusion proteins

The syntrophin fusion proteins $[His]_6$-Syn, $[His]_6$-Syn A, maltose binding protein (MBP) fusions MBP-Syn B, MBP-Syn H, and MBP-Syn I were prepared as described previously (48). pET32 plasmid constructs for PH1, PH2, and the PDZ domain were the generous gift from Drs. Steven Gee and Stan Froehner, (Department of Physiology, University of North Carolina, Chapel Hill). pET32 plasmids encoding $[His]_6$-thioredoxin-PH1, -PH2, and –PDZ were used to express proteins referred to as $[His]_6$-PH1, -PH2, and -PDZ (60). The His-Tag fusion proteins were purified by using Ni^{2+}-NTA-agarose from Qiagen as described earlier (48). The MBP fusion proteins were purified using the batch method described previously by Jarrett and Foster on amylose resin (77). GST-Grb2, GST-Grb2-N-SH3 (amino acids 1-54), and GST-Grb2-C-SH3 (amino acids 163-217) domains, (kindly provided by Dr. O. Segatto, Instituto Regina Elena, Roma, Italy), GST-βC1 (rabbit β–dystroglycan coding amino acids 787-895) (92) were all expressed in *E. coli* BL21 strain and purified by affinity chromatography on glutathione-agarose beads (Amersham Pharmacia Biotech) as described elsewhere (92,93). The purity of

the proteins was determined by 12% SDS-polyacrylamide gel electrophoresis using the method of Laemmli (78). The major bands of the fusion proteins were of expected size and relatively high purity (data not shown). The Bradford assay (79) was used to determine the protein concentrations using bovine serum albumin as the standard.

Overlay experiments

The fusion proteins Syn, Syn A, Syn B, Syn H, PH1, MBP-LacZα, and $[His]_6$-green fluorescent protein (GFP) were applied to electrophoresis on a 12% SDS-PAGE gel, and electroblotted onto nitrocellulose paper. The paper was then blocked with 10 mg/ml BSA in TTBS (20 mM Tris-HCl, pH 7.5, 0.5 M NaCl and 0.2%Tween-20). After washing extensively with 1 mM $CaCl_2$ in BSA/TTBS (1 mg/ml BSA in TTBS), the blot was overlaid with 0.1 mg/ml GST-Grb2 for 2h in the presence of 1 mM Ca^{2+}. The blot was then washed extensively with Ca^{2+}/BSA/TTBS, and incubated with affinity purified anti-GST (1:5000 dilution). Goat anti-rabbit IgG (H+L)-alkaline phosphatase conjugate (1:1000 dilution, BioRad) was used, following the primary antibody. The blot was developed using 1:100 dilution each of 30 mg/ml NBT (in 70% dimethylformamide) and 15 mg/ml BCIP (in 100% dimethylformamide) into buffer AP (0.1M $NaHCO_3$, 1mM $MgCl_2$, pH 9.8). Alternatively, after primary antibody and washing as above, blots were probed with 1:3000 diluted goat anti-rabbit IgG (H+L)-horseradish peroxidase conjugate, washed as above, and developed for chemiluminescence by incubating the blot in a mixture of 15 ml of solution A (90 mM Coumaric acid and 250 mM Luminol, 1 M Tris HCl, pH 8.5) and 15 ml solution B (7.2 µl H_2O_2 in 1 M Tris HCl, pH 8.5) in the dark room and then exposing it to Kodak Scientific Imaging film. MBP-LacZα and $(His)_6$-GFP were

used as controls for maltose and His-Tag fusion proteins, respectively. A similar experiment was performed to test binding of Grb2 to syntrophin from partially purified dystrophin glycoprotein complex. Bovine serum albumin was used as a control for this experiment.

Immunoprecipitation

Samples in phosphate buffered saline (0.13 M NaCl, 2.68 mM KCl, 5.37 mM Na_2HPO_4, 1.76 mM KH_2PO_4, pH 7.4) containing 1% Triton X-100 were prepared by incubation with protein A-Sepharose at 4^0 for 1h. The supernatants were incubated with 100 µl of fresh protein A-Sepharose with anti-syntrophin or anti-MBP polyclonal antibodies at room temperature for 1h and then on ice for 30 min. The beads were washed three times with phosphate buffered saline containing 1% Triton X-100. The bound proteins were eluted by boiling in SDS-PAGE sample buffer and separated on a 4-15% gradient sodium dodecylsulfate polyacrylamide gel (BioRad) and blotted to nitrocellulose membrane as described previously (80). The blots were then analyzed by using different antibodies and were developed using the enhanced chemiluminescence method.

Solid phase binding assays

0.9 mg of GST-Grb2 (0.9 mg/ml) was coupled to 1 g of cyanogen bromide-activated Sepharose (Sigma) using procedures recommended by the manufacturer (Pharmacia). The support was then washed with the coupling buffer (0.1 M $NaHCO_3$, pH 8.3, 0.5 M NaCl) and blocked for 2h with 0.1 M Tris-HCl, pH 8, 0.5 M NaCl. The amount

of the protein coupled (0.115 mg Grb2/ml 50% slurry Sepharose) was determined by the difference in the ultraviolet absorption of the added protein and that recovered from coupling in the wash fractions. For negative controls, CNBr-activated Sepharose was used to which either no protein or glutathione-S-transferase (GST) was coupled.

200 μl of a 50% slurry of Grb2-Sepharose containing 23 μg Grb2 was equilibrated with buffer A (50 mM Tris, pH 7.5, 100 mM KCl) containing 0.1 mM EGTA and then incubated with different fusion proteins (25 μg) or rabbit skeletal muscle extract prepared in a manner similar to the immunoprecipitation experiment. Incubation was for 1h at room temperature and for 30 min on ice with gentle mixing in a final volume of 200 μl. For control, Sepharose without any protein coupled to it or Sepharose with glutathione–S-transferase coupled to it was used. After the incubation, Grb2-Sepharose was washed three times with 0.5 ml of 1 mg/ml BSA/TTBS. The protein was eluted using 60 μl of 2x Laemmli sample buffer (78). Samples were heated for 5 min at 95^0. The samples were then centrifuged for 5 min at room temperature to remove the resin, applied to electrophoresis on a 12% SDS-PAGE gel (78), and electroblotted onto nitrocellulose paper (80). The paper was then blocked with 10 mg/ml BSA in TTBS. After washing extensively with 1 mg/ml BSA/TTBS, the blot was incubated with affinity purified anti-MBP (1:1000 dilution) for MBP fusion proteins or T7 monoclonal antibody (Novagen, 1:10,000 dilution) for His-Tag fusion proteins. Goat anti-rabbit IgG (H+L)-alkaline phosphatase conjugate and goat anti-mouse IgG (H+L)-alkaline phosphatase conjugate (both 1:1000 dilution) were used for the rabbit and mouse primary antibodies, respectively. For fusion proteins containing S-Tag, namely PH1, PH2 and PDZ, S-protein alkaline phosphatase conjugate (1:5000, Novagen) was used.

Surface plasmon resonance

SPR assays were performed using a BIAcore instrument (BIAcore X) equipped with a two flow cell sensor chip, using purified Grb2 or Grb2-C-SH3 or Grb2-N-SH3 domain GST fusion proteins. Proteins were immobilized by covalent coupling to CM-5 sensor chips (research grade) (BIAcoreAB) after activation of the carboxymethylated dextran surface by a mixture of 0.05 M N-hydroxysuccinimide and 0.2 M N-ethyl-N'-3-(dimethylaminopropyl) carbodiimide hydrochloride. The reaction was performed by injecting 45 μg/ml of Grb2 in 10 mM acetate buffer, pH 4.8 at a flow rate of 10 μl/min at 25^{o} for 7 min. Residual activated groups were blocked with 1 M ethanolamine-HCl, pH 8.5. Immobilization resulted in about 4000 resonance units (RU) Grb2 protein. Binding assays were performed in HBS (10 mM HEPES, 0.15 M NaCl, 3 mM EDTA, 0.5% surfactant P20, pH7.4) with a flow rate of 2, 5, 10, 15, 20 μl/min. The soluble ligand (Syn) was applied in the range of concentration of 15.5 nM – 82.7 μM. At the end of the sample plug, HBS buffer was allowed to flow past the sensor surface to allow dissociation. The sensor surface was regenerated for the next Syn sample using a 30–120 sec pulse of regenerating buffer (50 mM NaOH) at a flow rate of 20 μl/min. Non specific binding on the sensor surfaces and mass-transport problems were avoided by flowing the same solution past the two sensor surfaces in sequence and using different flow rates. The response was monitored as a function of time (sensogram) at 25^{o}. The integrity of immobilized proteins was tested with anti-Grb2 antibody.

The data evaluation was carried out using a BIAevaluation software version 3.0, following the manufacturer's instructions. The kinetics constants were calculated by

non-linear regression of data using the pseudo first order rate equation as described in detail by Herzog et al. (94).

Solid phase immunoassay

To measure the binding of GST-Grb2 to Syn A, a microtiter assay was used. A microtiter plate (Dynatech Immulon 1) was coated by incubation of 100 µl/well of 0.05 mg/ml His-Tag Syn or –Syn A for 4h at 4^0. The plate was then blocked by replacing the fusion proteins with 300 µl/well of 30 mg/ml BSA in AC7.5 buffer (50 mM Tris-Cl, pH 7.5, 100 mM KCl, 3 mM $MgCl_2$, 1 mM $CaCl_2$). All subsequent operations were at room temperature and 100 µl/well. After washing the plate three times (5 min per wash) with AC7.5T/BSA (buffer AC7.5, 0.1 % Tween-20, 1 mg/ml BSA), serial dilutions of each of GST-Grb2, GST-Grb2-C-SH3, GST-Grb2-N-SH3, or GST were added. The plate was incubated for 2h. The plate was washed three times as described above and then incubated with anti-GST antibody for 1h. The plate was washed three more times as described and incubated with goat anti-rabbit IgG (H+L)-alkaline phosphatase conjugate (1:1000 dilution, BioRad) for 1h. The plate was then washed once with 1 mg/ml AC7.5T/BSA followed by two immediate washes of diethanolamine/Mg (10 mM diethanolamine, 0.5 mM $MgCl_2$). The plate was developed by incubation with 100 µl/well of 1 mg/ml *p*-nitrophenylphosphate in diethanolamine/Mg. The absorption at 405 nm was determined versus time. The concentration giving half maximal response was calculated and is denoted here as Kd.

For the experiments performed in EGTA, $CaCl_2$ was replaced by EGTA in all the buffers up to the stage at which the anti-GST antibody was added. After that stage, the

experiment was continued as specified above using the $CaCl_2$ containing AC7.5T/BSA.

Results

The schematic representation of mouse α1-syntrophin and Grb2 sequences expressed as fusion proteins is shown in Figure 3.1. The regions of mouse α1-syntrophin's amino acid sequence in each construct are given in parenthesis. The boundaries of the PH1 domain are not well defined; our PH1 construct contains some additional sequences as shown in Figure 3.1. Syn, Syn A, PH1, PH2 and PDZ were produced as His-Tag fusion proteins while Syn B, Syn H and Syn I were produced as maltose binding fusion proteins. Glutathione S-transferase (GST) fusions of Grb2 and selected regions of it were also produced. Each fusion protein was affinity purified.

Gel blots of partially purified dystrophin glycoprotein complex bind Grb2 as shown in Figure 3.2. Coomassie blue staining of the purified dystrophin glycoprotein complex is shown in the figure. Clearly, the dystrophin glycoprotein complex is only partially purified and other proteins are present but it is sufficient to determine Grb2 binding. In the Coomassie stain, the syntrophins appear as two bands but the upper, more intense band is itself a doublet of the two β-syntrophins. The lower, less intense band is α-syntrophin. The three asterisks show the position, in descending order, of the α-dystroglycan, the syntrophins, and β-dystroglycan; all bind Grb2. Specific staining with α-syntrophin, β-dystroglycan and α-dystroglycan antibodies confirm these identities. The DGC was also probed with dystrophin antibody (NCL-DYS2) from Novacastra (data not shown). The DGC was also overlaid with GST alone and did not show any binding (data not shown). β-Dystroglycan (lowermost asterisk) had been previously shown to

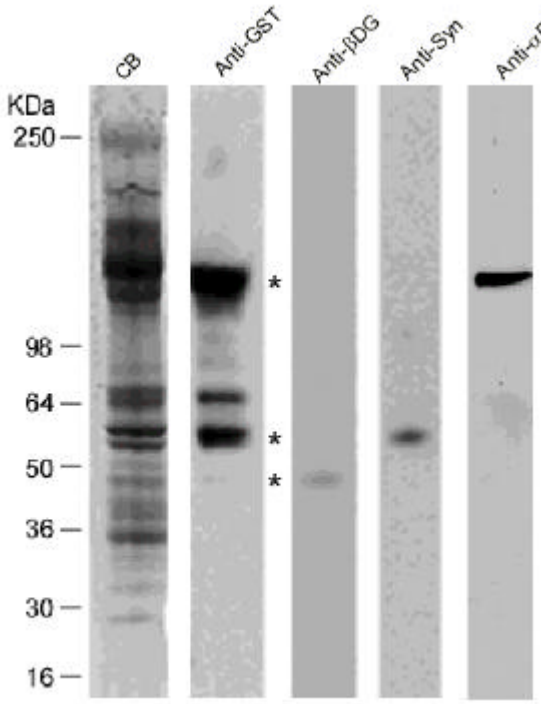

Figure 3.2 Grb2 binds syntrophin in the partially purified dystrophin glycoprotein complex (DGC) from rabbit skeletal muscle.

Partially purified DGC was applied to electrophoresis on a 4-15% gradient sodium dodecylsulfate- polyacrylamide gel and electroblotted onto nitrocellulose paper. The blot was then overlaid with 0.1 mg/ml GST-Grb2 for 2 hr in the presence of 1 mM $CaCl_{2.}$ The binding was detected with anti-GST antibody. Three asterisks (*) show the positions of α-dystroglycan, the syntrophins and β-dystroglycan in the descending order. Anti-βDG, Anti-Syn, Anti-αDG show the bands detected by the β-dystroglycan , α-syntrophin and α-dystroglycan antibodies, respectively. To the left are shown molecular weight markers.

bind Grb2 (95), but this is actually the least intense of the staining observed. α-Sarcoglycan showed binding to Grb2 in some of the dystrophin glycoprotein complex preparations we tested (data not shown) though it did not bind Grb2 well in this particular preparation. Close inspection of its sequence demonstrated that the only PXXP motifs present are PYNP from amino acid 83 to 86 and PEGP, from amino acid 128 to 131, regions of the protein believed to be on the exterior face of the sarcolemma (96) and are of questionable relevance to *in vivo* binding. α-Dystroglycan (uppermost asterisk) shows the strongest binding to Grb2. Though its sequence contains PXXP motifs such as PSEP from amino acid 29 to 32, PTLP from amino acid 302 to 305, PTSP, from amino acid 340 to 343, PIQP from amino acid 382 to 385, PATP from amino acid 432 to 435 and PRTP from amino acid 451 to 454, this protein is believed to be on the exterior face of the sarcolemma and therefore, is also of questionable relevance to *in vivo* intracellular binding. Therefore, the remainder of this chapter will focus on this newly discovered (Figure 3.2) interaction with α-syntrophin (middle asterisk), an intracellular peripheral membrane protein.

In other experiments, the partially purified dystrophin glycoprotein complex was probed with other antibodies. The uppermost band seen in the Coomassie stained gel in Figure 3.2 is dystrophin and is detected with a dystrophin antibody (NCL-Dys2 from Novacastra). It co-migrates with the 250 kDa marker in this gel system although its true molecular weight is much larger. Dystrophin did not bind Grb2 in any of our experiments and neither did the other (β, δ, and γ) sarcoglycans. There is a band at about 70 kDa which does bind Grb2 (Figure 3.2, lane 2) which is near the molecular weight of one of the shortened dystrophin (DP71) forms but it did not bind dystrophin C-terminal antibody

and so it is not this protein (data not shown). We made no other attempts to identify it.

To confirm the observed interaction of syntrophin with Grb2, GST-Grb2-Sepharose was incubated with rabbit skeletal muscle extract. GST-Sepharose was used as a control. Although a small amount of syntrophin is present in the flow through, most of the syntrophin binds to Grb2 (top arrow, Anti-Syn) can be seen in Figure 3.3. β-dystroglycan has been shown to bind Grb2 by Yang et al.(95) and is used as a positive control (middle arrow, Anti-βDG). Anti-CrkL was used as unrelated antibody which served as a negative control. Grb2 did not show any binding to CrkL and all of the CrkL was present in the flow through.

To investigate if a complex of syntrophin and Grb2 is present in skeletal muscle and if this interaction is specific, syntrophin was immunoprecipitated (“S” in Figure 3.4) from rabbit skeletal muscle extract and results were analyzed by immunoblotting. For comparison, the irrelevant anti-MBP antibody was also used (“M” in Figure 3.4). The gel blot of the bound proteins was probed with two antibodies against SH3 domain proteins: the mouse monoclonal anti-Grb2 -antibody (Trasduction Laboratories) and anti-Crk-L antibody (Santa Cruz). It can be seen from Figure 3.4 that Grb2 binds syntrophin (Figure 3.4, anti-Grb2) while Crk does not (Figure 3.4, antiCrkL). The antibody light chain band in the immunoblot (Figure 3.4, anti-CrkL, lane S) is near the expected size for Crk but migrates faster on the gel than expected for Crk and faster than the Crk band detected in the muscle extract used (Figure 3.4 anti-CrkL, lane Cr). Similar results were also obtained using an anti-Grb2 polyclonal antibody (data not shown), Grb2 bound syntrophin while Crk did not although the muscle extract contained both proteins(data not shown). Thus, Grb2 binds but not Crk. Syntrophin contains a PQLP

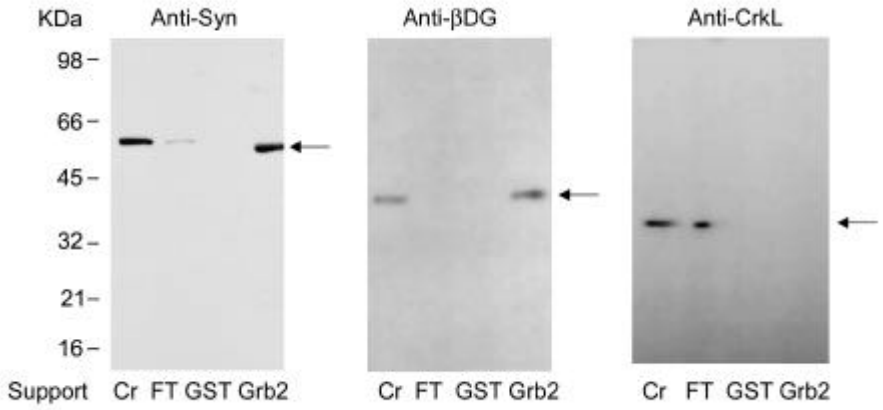

Figure 3.3 Grb2 binds syntrophin and β-dystroglycan from rabbit skeletal muscle membrane.

GST-Grb2-Sepharose or GST-Sepharose was incubated with the rabbit skeletal muscle extract containing 1% Triton X-100 as described in the experimental procedures. Cr represents crude extract, FT is the fraction not bound by the Grb2-Sepharose, GST represents GST-Sepharose that was used as negative control, and Grb2 represents the GST-Grb2-Sepharose bound fraction. The top arrow shows the band detected by α-syntrophin antibody (anti-Syn), the middle arrow shows the band detected by β-dystroglycan antibody (anti-βDG), and the bottom arrow shows the band detected by the CrkL antibody (anti-CrkL). Molecular weight markers are shown to the left.

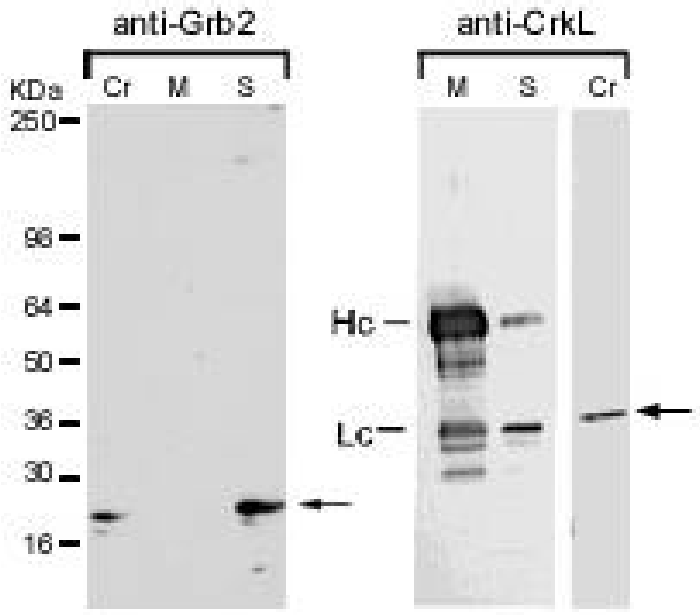

Figure 3.4 Immunoprecipitation of Grb2 from rabbit skeletal muscle extract.

Rabbit skeletal muscle extract containing 1% Triton X-100 was incubated with Protein A Sepharose and α-syntrophin antibody (S) or anti-MBP antibody (M), a negative control. After extensive washing, bound proteins were eluted with SDS-PAGE sample buffer. Samples, after electrophoresis and electroblotting, were probed with antibodies for Grb2 (mouse monoclonal, anti-Grb2) and Crk (rabbit polyclonal, anti-CrkL). The positions of Grb2 (lower arrow) and Crk (higher arrow) are indicated. Heavy and light chains of IgG are indicated in the middle as Hc and Lc, respectively. The crude extract (Cr) was also applied to the same gel.

sequence (69-72), which is similar to a motif known to bind Crk (97). Thus, this experiment was designed to test if a reasonable alternative SH3 domain protein bound instead of Grb2. Apparently though, Grb2 binds while Crk does not. The reverse experiment using mouse monoclonal anti-Grb2 and anti-Crk-L antibody was also performed to immunoprecipitate syntrophin from rabbit skeletal muscle extract and showed also that Grb2 but not Crk binds syntrophin (data not shown). This was also confirmed using muscle extract and syntrophin –Sepharose; Grb2 bound while Crk-L did not (data not shown).

Figure 3.5 summarizes the Grb2 interaction observed for all the syntrophin fusion proteins tested, namely Syn, Syn A, Syn B, Syn H, Syn I, PH1, PH2, and PDZ. A typical experiment is shown in Figure 3.5. Syn, Syn A, Syn B, PH1, and PDZ were briefly incubated with Grb2-Sepharose in the presence of 1 mM EGTA, since Syn, Syn A, and PH1 have been shown to oligomerize in the presence of Ca^{2+} (91). Syn, Syn A, and PH1 showed binding to Grb2-Sepharose while Syn B and PDZ did not bind (Figure 3.5). CNBr-activated Sepharose-4B without any protein coupled to it was used as a negative control. This assay also demonstrated that Syn H and Syn I also bound Grb2 in other experiments (data not shown).

To confirm the region involved in this interaction, an overlay experiment was carried out where gel blots of syntrophin fusion proteins were overlaid with Grb2 in the presence of 1 mM Ca^{2+}. Figure 3.6 confirms the localization of the Grb2-syntrophin interaction. $[His]_6$-green fluorescent protein (GFP) and MBP-LacZα were used as controls for His-Tag and maltose binding fusion proteins, respectively, and as expected neither shows any binding to Grb2. Syn, Syn A, Syn H, Syn I, and PH1 all bind Grb2

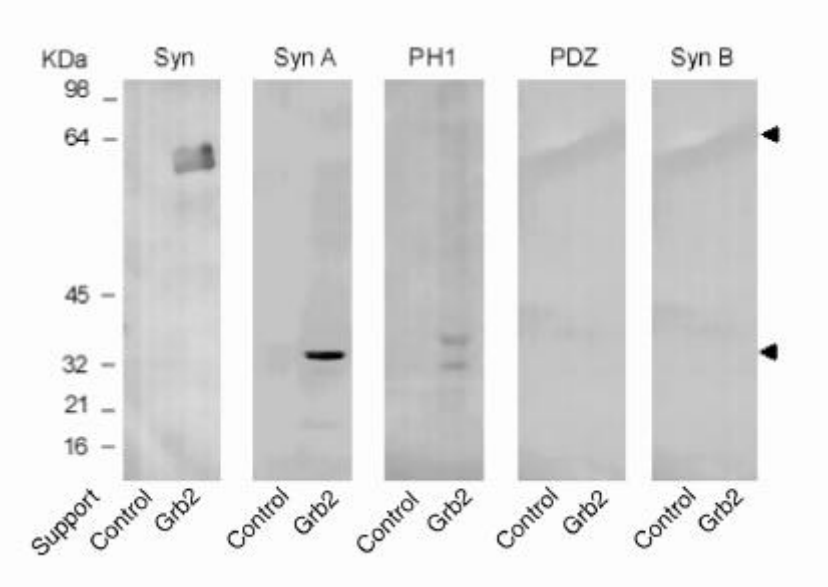

Figure 3.5 Syntrophin's Grb2 binding region is localized to the proline-rich motifs adjacent to and overlapping the PH1 domain.

Syntrophin's Grb2 binding region is localized to the proline-rich motifs adjacent to and overlapping the PH1 domain. Grb2-Sepharose was incubated with the Syn fusion protein in the presence of 1 mM EGTA. GST represents GST-Sepharose, Grb2 represents Grb2-Sepharose. To the right are two arrows, the upper arrow shows molecular weight of Syn B, and the lower arrow shows molecular weight of PDZ which do not bind to Grb2-Sepharose. To the left are shown molecular weight markers.

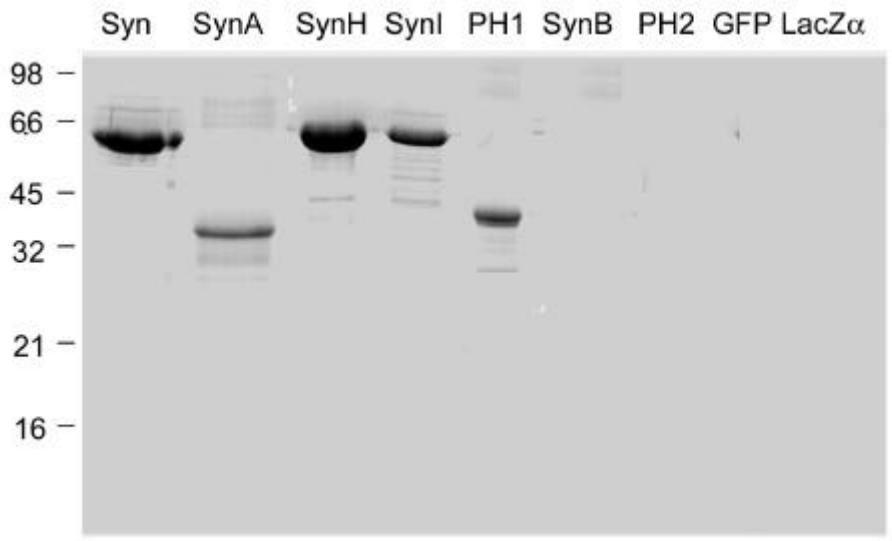

Figure 3.6 Localization of syntrophin's Grb2 binding region to the polyproline sequences.

A gel blot overlay experiment was performed as described in the experimental procedures in the presence of 1 mM $CaCl_2$. Syn fusion proteins were separated by electrophoresis, blotted to nitrocellulose, and overlaid with GST-Grb2 and the binding was detected with anti-GST antibody. $[His]_6$-green fluorescent protein (GFP) and MBP-LacZα were used as controls for His-Tag and maltose binding fusion proteins, respectively. To the left are shown molecular weight markers.

while Syn B, PH2, and PDZ don't. Notice that the two proline-rich regions are separately expressed in Syn H and Syn I (see Figure 3.1) and that both bind full-length Grb2 (Figure 3.6). Binding occurs to the same proteins in the absence (Figure 3.5) or presence (Figure 3.6) of Ca^{2+}.

The binding affinity of Syn for Grb2 was determined by surface plasmon resonance. This experiment unlike all the others in this dissertation was not performed by Shilpa oak. Sensograms for the binding are shown in Figure 3.7. Similar experiments were also done for Syn/Grb2-C-SH3 and Syn/Grb2-N-SH3 interactions (data not shown). The initial part of each curve corresponds to signal of the buffer flowing on sensor surface. The rising part of the curve (association) results from syntrophin binding to the Grb2 on the surface of the sensor chip. Finally, buffer alone flows over the chip and the decreasing signal results as bound syntrophin dissociates. Control experiments demonstrate that the syntrophin association occurs only when the chip surface contains Grb2 (data not shown). Increasing concentrations of Syn ranging from 15.5 nM-82.7 μM were allowed to flow over the sensor surface. The observed association rate constant, k_{on} (7.89×10^3 M^{-1} s^{-1}), and the dissociation rate constant, k_{off} (4.44×10^{-3} s^{-1}), was calculated from the association and dissociation sensorgrams, respectively, using a simple bimolecular association model (94) and the apparent dissociation constant, K_d, calculated from the ratio of the rate constants (i.e., k_{off}/k_{on}). For the binding of full-length syntrophin to full length Grb2 (Figure 3.7), K_d = 563 ±15 nM. For the binding of full-length syntrophin to the two separate SH3 domains of Grb2, K_d = 351 ± 4 nM and 438 ± 4 nM for Grb2-N-SH3 and Grb2-C-SH3, respectively (data not shown).

To confirm the binding affinity of syntrophin for Grb2, $[His]_6$-Syn or -Syn A was

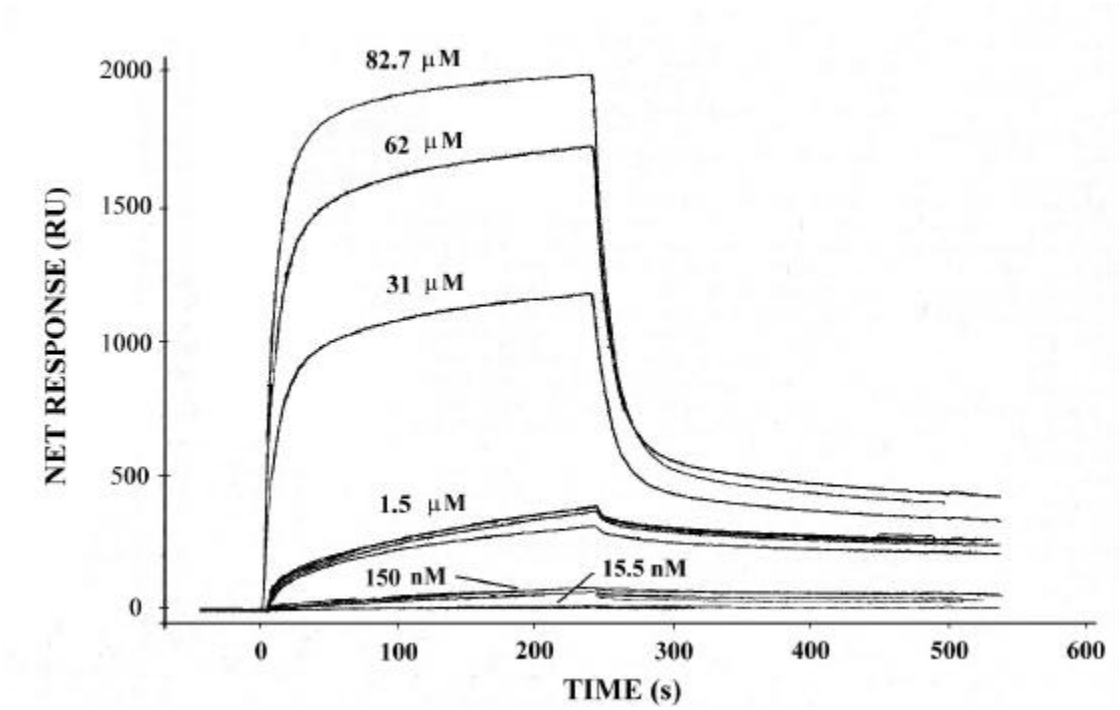

Figure 3.7 Surface plasmon resonance profiles of the binding of soluble Syn to Grb2 immobilized to the sensor chip.

Individual curves from bottom to top were obtained with Syn concentrations ranging from 15.5 nM to 82.7 μM. Association and dissociation phases were started at 0 s and at 240 s, respectively.

used to coat the wells of a microtiter plate, and the binding of GST-Grb2 was assessed. The results in Figure 3.8 demonstrate an interesting phenomenon – that Syn A binds Grb2 with considerably higher affinity than does the full-length Syn. For Syn, the affinity was 355 ± 25 nM in reasonably good agreement with the value (563 nM) measured in the surface plasmon resonance experiment (Figure 3.7). However, Syn A bound with an apparent affinity of 35 ± 10 nM, an order of magnitude higher affinity (both are the average ± standard deviation for three separate determinations). Syn A was also mixed with Syn B to reconstitute the complete sequence in two parts and this mixture was assayed for binding to Grb2. The affinity was not significantly different from that observed for Syn A alone (data not shown).

To determine if Grb2 was binding preferentially to either Syn H or Syn I, [GST] – Grb2 or GST alone was used to coat the wells of a microtiter plate, and overlaid with MBP-Syn H or MBP-Syn I. The binding was detected with anti-MBP antibody. The results in Figure 3.9 demonstrate that Syn H and Syn I bind Grb2 with a Kd of 182 nM and 171 nM, respectively. The issue of whether the Grb2-C-SH3 or Grb2-N-SH3 domains bound preferentially to either Syn H or Syn I was addressed in a similar experiment (data not shown). The result was that Grb2-C-SH3 is bound to higher levels by both Syn H and SynI but both Grb2 SH3 domains bind to both regions of syntrophin and the affinities are quite similar. Thus, both syntrophin sequences show some preference for the Grb2-C-SH3, but the differences are not large. A peptide containing polyproline sequences in Syn H -EPGAAPPQLPEALLLQ (63-78) was synthesized and used in an ELISA experiment. It did not inhibit the interaction between Syn A and Grb2 (data not shown), supporting the results observed in Figure 3.9 that the polyproline sites

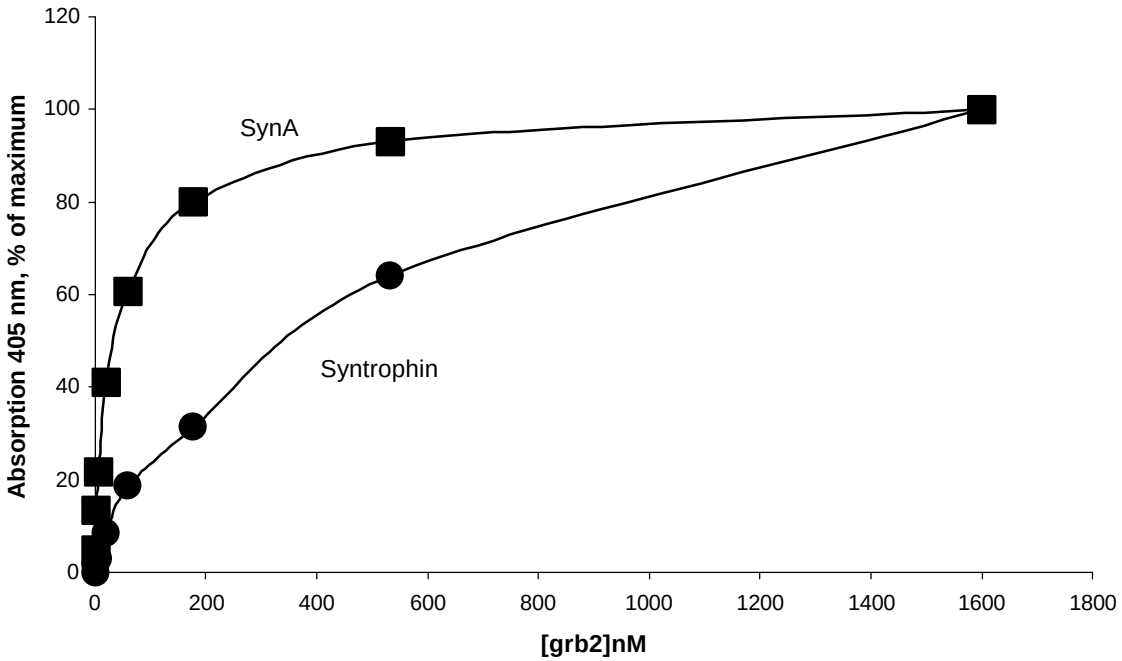

Figure 3.8 Grb2 binds to Syn A with higher affinity than to full-length syntrophin. Solid phase immunoassay was performed on Syn or Syn A coated mocrititer plates as described in experimental procedures. Binding of GST-Grb2 was detected by using anti-GST antibody. Absorption 405 nm measures the amount of GST-Grb2 bound by syntrophin (circles) and Syn A (squares). The data were scaled by subtracting blank values (obtained using GST coated plate wells) and defining the maximum signal for each data set as 100%.

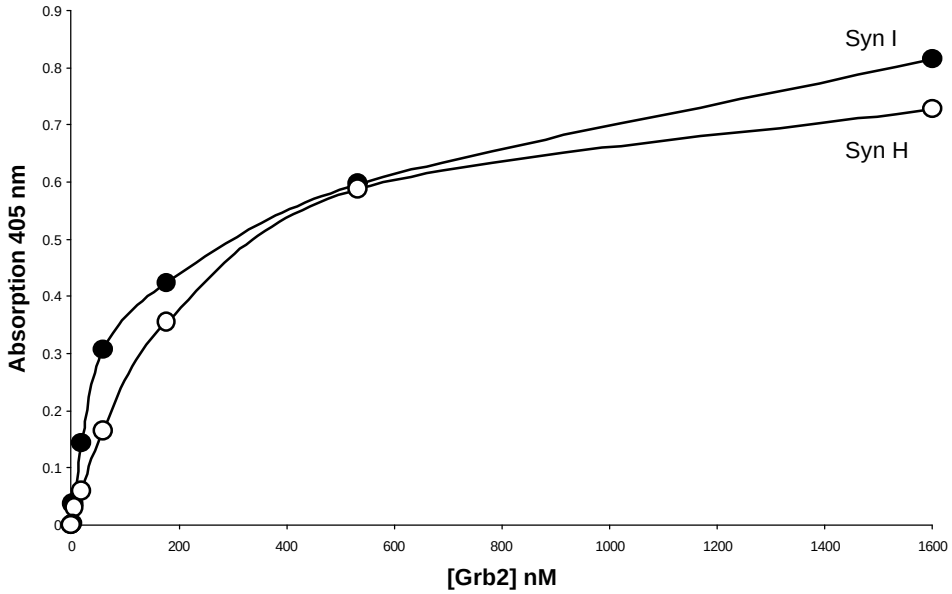

Figure 3.9 Grb2 binds to Syn H and Syn I with similar affinities.

Solid phase immunoassay was performed on GST-Grb2 coated microtiter plates as described in experimental procedures. Binding of MBP-Syn H (open circles) or MBP–Syn I (closed circles) was detected by using anti-MBP antibody. Absorption 405 nm measures the amount of MBP-Syn H, MBP-Syn I bound by Grb2. The data were scaled by subtracting blank values (obtained using GST coated plate wells).

present in both Syn H and Syn I are required for the high affinity Grb2 binding.

To further localize the Grb2-syntrophin interaction, $[His]_6$-Syn A was used to coat the wells of a microtiter plate, and the binding of GST-Grb2, GST-Grb2-C-SH3, and GST-Grb2-N-SH3 was assessed in the presence of 1 mM EGTA. Binding was detected using the anti-GST antibody. A typical experiment is presented in Figure 3.10. Averaging the data from three different experiments gave half maximal binding at 35 ± 10 nM Grb2, 80 ± 10 nM for Grb2-N-SH3, and 60 ± 10 nM for Grb2-C-SH3. This assay was also used to confirm that other fusion proteins, including Syn I and Syn H, bound Grb2. Furthermore, experiments in Ca^{2+} or EGTA gave similar binding affinities showing that this interaction is independent of Ca^{2+} (data not shown).

Syntrophin has been shown to bind dystrophin but this binding has no effect on the syntrophin-Grb2 interaction, since we find that the DysS9 fusion protein, containing the C-terminus of dystrophin that binds syntrophin (98), does not interfere with Grb2 binding (data not shown). The N-terminal of the PH1 domain and the N-terminal of the PDZ domain have been reported (54) to also bind calmodulin. Binding of calmodulin to syntrophin in the presence or absence of Ca^{2+} also does not influence the Grb2 interactions (data not shown). Phosphatidylinositol-4,5 bisphosphate binds syntrophin's PH1 domain (52) but it does not influence the syntrophin-Grb2 interaction (data not shown). Binding this lipid probably serves the role of localizing syntrophin to the membrane surface.

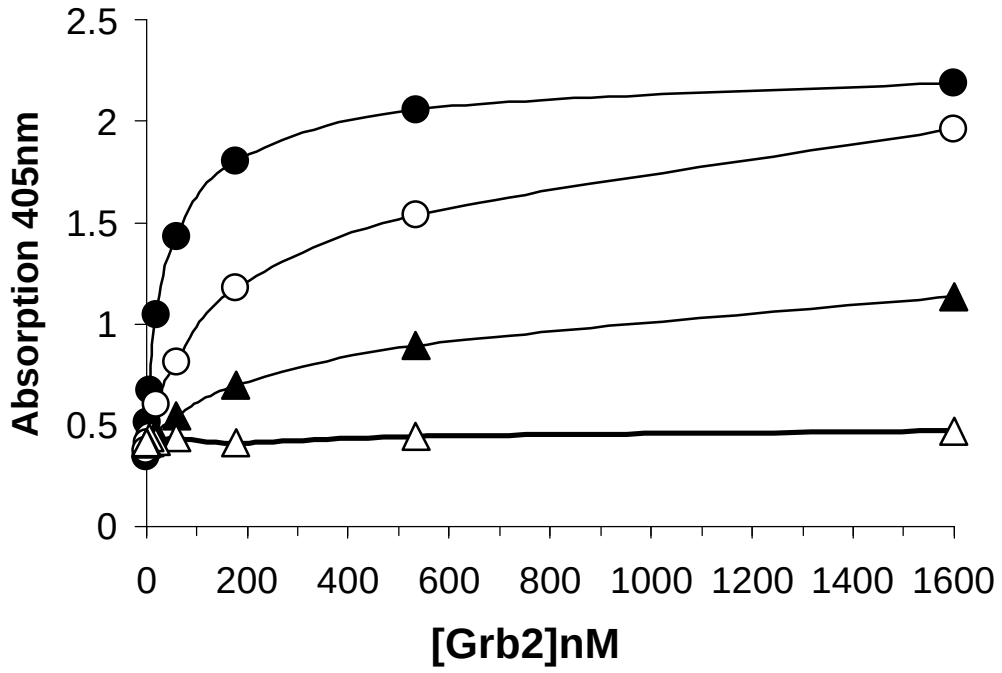

Figure 3.10 Syn A binds best to Grb2's C-terminal SH3 domain.

Solid phase immunoassay was performed as described in experimental procedures using $[His]_6$-Syn A coated microtiter plates. Binding of GST-Grb2 fusion proteins was detected by using anti-GST antibody. Absorption 405 nm measures the amount of GST-Grb2 (closed circles), GST-Grb2-C-SH3 (open circles), GST-Grb2-N-SH3 (closed triangles) or GST (open triangles) bound.

Discussion

Syntrophins have been suggested to function as adapters, linking cellular proteins to the DGC (76). It is now clear that this adapter protein binds another adapter, the SH2/SH3 domain protein Grb2. (96). Syntrophin contains polyproline sequences that bind Grb2. This binding is Ca^{2+}-independent (Figure 3.5, 3.9, and 3.10). This Ca^{2+}-independence is significant since Ca^{2+}-binding by syntrophin results in large syntrophin oligomers and oligomerization occurs utilizing PH1 sequences (91). Ca^{2+}-binding or oligomerization could block Grb2 binding but this is apparently not the case.

Binding does not occur with fusion proteins lacking the polyproline sequences (Figure 3.5 and 3.6). The Grb2-C-SH3 and Grb2-N-SH3 domains bind with similar affinity (Figure 3.10) and both bind to both of syntrophins polyproline regions (in Syn H and I, data not shown). The affinities measured here are quite high for SH3 interactions which typically occur in the 1-10 μM range (99) while here we observed affinities ranging from 35 nM (for Syn A, Figure 3.10) to 563 nM (for full-length Syn, Figure 3.7). Thus, syntrophin binding to Grb2 represents one of the highest affinity interactions known for either protein, which argues strongly for its physiological relevance. Both the proline-rich sequences at syntrophin 44-75 (present in Syn H) and the one at 181-229 (present in Syn I) bind Grb2 (Figure 3.6 and Figure 3.9). The Kd of Syn H and Syn I are 182 nM and 171 nM, respectively, which are intermediate between that of Syn (563 nM) and Syn A (35 nM), suggesting that binding to both sequences are required for highest affinity Grb2 binding. Since Grb2 has two SH3 domains that bind to syntrophin with similar affinity (Figure 3.10) presumably the two domains of Grb2 bind the two sequence

regions of syntrophin. In their study to design peptides which bound with high affinity to the SH2/SH3 adapter protein Crk, Posern, et al.(99) found that affinities as high as 96 nM (for Crk-N-SH3) or 11 μM (for Grb2-N-SH3) could be achieved with peptides only 11 amino acids long. Sparks, et al.(97) have used 16-long combinatorial libraries to characterize the PXXP SH3-binding motifs. Thus, 10-16 amino acids should be sufficient to define the binding sites on syntrophin. There are four PXXP motifs in Syn A, which fall into two groups: group 1 containing one PXXP motif

EPGAAPPQLPEALLLQ (63-78)

present in Syn H and group 2 containing three PXXP motifs:

VGWASPPASPLQRQPS (179-194)

SPLQRQPSSPGPQPRN (187-202)

VSRRCTPTDPEPRYLE (216-231)

present in Syn I.

Both groups bind Grb2 (Figure 3.6 and Figure 3.9). Some Grb2 interactions, such as the Grb2-dynamin or Grb2-SOS interaction, are essentially mediated by the single N-terminal SH3 domain of Grb2 (100,101), however, our data strongly suggest that both SH3 domains of Grb2 bind syntrophin well and both PXXP-regions of syntrophin are bound by both SH3 domains of Grb2. The interaction is specific for Grb2; muscle Grb2 binds, while muscle Crk-L is not bound. SH3 domains are thus necessary but not sufficient for this specific interaction. (97,102). As can be seen from Figure 3.9, Grb2 does not bind preferentially to either one of the PXXP regions. The difference in the binding affinities for the Syn-Grb2 interaction and that of the Syn A-Grb2 interaction is interesting. The binding affinities for the Syn-Grb2 interaction (563 nM) and that of the

Syn A-Grb2 interaction (35 nM) differ by an order of magnitude (Figure 3.8) but either one is still a quite high affinity. This is possible if the polyproline sites that are involved in Grb2 interaction are less accessible in the full-length syntrophin and by removing the C-terminal part of syntrophin (Syn B), these sites are made more accessible in Syn A. When the PXXP motifs are separated and are more accessible in Syn H and Syn I, the apparent dissociation constants are 182 nM and 171 nM, respectively, which are intermediate between that of Syn (563 nM) and Syn A (35 nM). Both Grb2 SH3 domains bind to both regions of syntrophin (data not shown) and the affinities are quite similar. Our model to account for the affinities is that the two motif groups are less accessible in Syn and become more so in Syn A. The two SH3 domains of Grb2 can bind to each motif group, resulting in many possible ways to bind the multiple sites and high affinity binding. When the motifs are separated in Syn I and Syn H, binding is restricted to simple, single interaction of lower apparent affinity.

Simply mixing the Syn A and Syn B sequences did not reconstitute the lower affinity suggesting that the intact, covalent structure is required. The binding affinity for Syn-Grb2 interaction would probably be of more significance to the *in vivo* situation.

Syntrophins are PH/PDZ domain adapter proteins that bind Na^+-channels (60), NO synthetase (57,58), dystrophin, α- and γ- sarcolglycans (46), SAPK3 (59) and to themselves (91). This self-association could bring together cellular signaling components and ion channels. That syntrophin binds the SH2/SH3 adapter protein, Grb2, brings together a large number of motifs important to cellular signaling in one place within the cell. SH2/SH3 adapters are necessary for MAP kinase pathway activation and tyrosine kinase recruitment in many different cell processes. Grb2 has

also been shown to recruit focal adhesion kinase, FAK^{125}, to the DGC (72,73). Phosphorylated tyrosines on FAK^{125} act as docking sites for molecules such as Grb2 that participate in multiple signal transduction pathways (103). The Grb2-SOS complex also binds to small G proteins such as Ras or Rac1 leading to activation of signaling pathways to initiate cell growth and differentiation. Thus, the association of Grb2 with syntrophin (this report) and β–dystroglycan (45) could have important roles in muscle regulation and growth.

Syntrophin also binds calmodulin (48,53,54) and while Ca^{2+}-calmodulin inhibits the syntrophin-dystrophin interaction (48) it does not affect syntrophin/Grb2 binding. Syntrophins are also found associated near the acetylcholine receptor at the neuromuscular junction (97) and Grb2 is also bound by the tyrosine phosphorylated acetylcholine receptor δ-subunit (104). Grb2 additionally binds the C-terminus of β-dystroglycan (45), through its N-terminal SH3 domain. Grb2 has been reported to be present in DGC preparations from bovine brain synaptosomes (72). The presence of Grb2 and syntrophin in the dystrophin glycoprotein complex preparation (72) and our ability to trap Grb2 (but not Crk) directly from muscle extracts with syntrophin-Sepharose strongly supports the hypothesis that the interaction between them observed *in vitro* also occurs *in vivo* (72,73). Indeed, the numerous signal transduction proteins now known to have association with the DGC makes it almost certain that this complex is involved somehow in cell signaling as we originally suggested in 1992 (53). Within this complex, the dystroglycan proteins bind the muscle laminin, merosin (105). This may be the receptor function of the complex, much as the binding of fibronectin and other RGD sequence proteins initiate integrin signaling. In fact, there is great similarity

between what is known of the signal transduction proteins associated with the DGC and what is known of integrin signaling, as has been pointed out by Yoshida, et al. (73). It may be that signaling cellular attachment to laminin is the long sought function of this complex.

Chapter 4. Skeletal Muscle Signaling Pathway Through The Dystrophin Glycoprotein Complex And Rac 1

Introduction

In skeletal muscles, dystrophin and syntrophins are found in a complex with other proteins and glycoproteins, the dystrophin glycoprotein complex (DGC^{1}) (6,20) whose defects cause Duchenne, Becker, various limb girdle, and other inheritable muscular dystrophies. The integrity of the complex is essential for muscle cell viability (63,106-110). The DGC provides a link between laminin in the extracellular matrix and the cytoskeleton (16,37).

Madhavan and Jarrett originally proposed in 1992 that the DGC was a signal transduction complex (53). Indeed, the numerous signal transduction proteins now known to have association with the DGC makes it almost certain that this complex is involved somehow in cell signaling. β-dystroglycan has been shown to bind to Grb2, suggesting that it may have a role in signal transduction mechanisms. Grb2 has also been shown to recruit focal adhesion kinase, FAK^{125}, to the DGC (72,73). Phosphorylated tyrosines on FAK^{125} act as docking sites for molecules such as Grb2 that participate in multiple signal transduction pathways.

Syntrophin has been shown to bind neuronal nitric oxide synthetase (56,111) muscle and nerve voltage gated Na^{+} channels (60), and the MAP kinase, SAPK3 (59). Syntrophins also bind calmodulin (53). A domain unique to syntrophins, the SU domain, has been shown to bind Ca^{2+}-calmodulin (48) and the SU domain in addition to other sequences in the C-terminal of the protein binds to dystrophin. Ca^{2+}-calmodulin binding

inhibits the syntrophin-dystrophin interaction (48). The N-terminal of the PH1 domain and the N-terminal of the PDZ domain have been reported to bind calmodulin (54) in a Ca^{2+}-independent manner (48,91). This domain has also been shown to be involved in the oligomerization of syntrophin *in vitro* in a Ca^{2+}-dependent manner. Calmodulin inhibits oligomerization in a Ca^{2+}-independent manner (91). Recently, syntrophin has been shown to bind Grb2, an SH2/SH3 adapter protein (112). Thus, syntrophins act as adapters between the dystrophin complex of proteins and components of the cell signaling apparatus.

Cell signaling often involves small G proteins. Adapter proteins such as Grb2 often recruit other proteins, which activate small G proteins. Rho family GTPases, such as Rac1, Cdc42, and Rho-A, regulate a wide spectrum of cellular functions, ranging from cell growth and cytoskeletal organization to secretion (113-116). They are critical for skeletal muscle differentiation and regulate the expression of MyoD and myogenin (117,118). Ras proteins are central to the control of cell growth and differentiation.

Within the DGC complex, the dystroglycans bind to muscle laminin2, merosin, the striated muscle isoform of laminin (119,120). We originally proposed that signaling cellular attachment to laminin might be the long sought function of this complex (112). We present here for the first time data suggesting that dystrophin glycoprotein complex is indeed a laminin receptor and through dystroglycans, dystrophin and syntrophin cause signaling which would promote muscle growth.

Experimental procedures

Materials

GDP, GTP, and GTP-γ-S were purchased from Sigma. Antibodies against H-Ras, phosphorylated JNK, Rho-A, and Sos were from Santa Cruz Biotechnology. Antibody against Rac1 was from Upstate Biotechnology. Antibody against Cdc42 was from Transduction Laboratories. Antibodies against β–dystroglycan and dystrophin were from Novocastra. Antibody against recombinant mouse α-syntrophin was produced in rabbit and purified by affinity chromatography on syntrophin A-Sepharose. Antibody against α and β–dystroglycan was a generous gift from Dr. Tamara C. Petrucci (Laboratorio di Biologia Cellulare, Instituto Superiore di Sanita, V. le Regina Elena, Roma, Italy). Goat anti-mouse IgG (H+L)- horseradish peroxidase conjugate and goat anti-rabbit IgG (H+L)-horseradish peroxidase conjugate were from BioRad. Ni^{2+}-NTA-agarose was from Qiagen. Cyanogen bromide pre-activated Sepharose and heparin-Sepharose were from Sigma. Mouse laminin was obtained from Collaborative Biomedical products. All other chemicals were of the highest purity available commercially.

Fusion proteins

The syntrophin fusion protein $[His]_6$-Syn was prepared and purified as described previously (48). GST-Rac1 (wild type), GST-Rac1 (V12), GST-Rac1 (N17) and GST-PAK1 were kindly provided by Dr. Yi Zheng (Department of Molecular Sciences, University of Tennessee, Memphis). GST-Rac1, GST-Rac1 (V12), GST-Rac1 (N17) and

GST-PAK1 were expressed in *E.coli* BL21 strain and purified by affinity chromatography on glutathione-agarose beads (Amersham Pharmacia Biotech) as described elsewhere (92,93). The purity of the proteins was determined by 12% SDS-polyacrylamide gel electrophoresis using the method of Laemmli (78). The major bands of the fusion proteins were of expected size and relatively high purity (data not shown). The Bradford assay (79) was used to determine the protein concentrations using bovine serum albumin as the standard.

Skeletal muscle membrane preparation

*3 g of f*rozen rabbit skeletal muscle (back muscle, predominantly fast twitch fibers) was homogenized in 7 volumes of pyrophosphate buffer (20 mM sodium pyrophosphate, 20 mM sodium phosphate, 1 mM $MgCl_2$, 0.303 M sucrose, and 0.5 mM EDTA, pH 7.0) in the presence of a protease inhibitor cocktail (1 μg/ml pepstatin A, 10 μg/ml leupeptin, 10 μg/ml aprotinin, 1 mM benzamidine, 0.1 mM phenylmethylsulfonyl fluoride) to minimize protein degradation (92). The homogenate was centrifuged 13,000 x g for 15 min at 4^0. The supernatant was then centrifuged for 30 min at 32,500 x g at 4^0 to pellet total muscle membrane. The precipitated total muscle membranes were suspended in 600 μl of 50 mM Tris, pH 7.5, 100 mM NaCl. 10 μl of muscle membrane preparation was saved and labeled as crude (Cr).

Preparation of PAK1-glutathione-agarose

A chimeric fusion of glutathione-S-transferase (GST) and the p21-binding domain of p21 activated kinase (PAK1) was expressed in *E. coli* BL21 strain. GST-PAK1 and

GST were then purified by affinity chromatography on glutathione-agarose beads as described earlier (92,93), the only difference being that after washing the beads thoroughly the protein was not eluted from the beads.

Solid phase binding assays

0.9 mg of $[His]_6$-Syn (0.9 mg/ml) was coupled to 1 g of cyanogen bromide-activated Sepharose (Sigma) using procedures recommended by the manufacturer (Pharmacia). The support was then washed with the coupling buffer (0.1 M $NaHCO_3$, pH 8.3, 0.5 M NaCl) and blocked for 2 hr with 0.1 M Tris-HCl, pH 8, 0.5 M NaCl. The amount of the protein coupled (0.120 mg Syn/ml 50% Sepharose slurry) was determined by the difference in the ultraviolet absorption of the added protein and that recovered from coupling in the wash fractions. For negative controls, CNBr-activated Sepharose was used to which no protein was coupled. Mouse laminin was coupled to cyanogen bromide-activated Sepharose by following a similar protocol (0.07 mg laminin/ml 50% Sepharose slurry).

Pull-down assay

100 μl of a 50% slurry of Syn-Sepharose (containing 12 μg Syn) was equilibrated with buffer K (20 mM Hepes, pH 7.5, 10 mM $MgCl_2$). Rabbit skeletal muscle membranes were incubated with control Sepharose (Ct), Syn-Sepharose (Syn), laminin-Sepharose (L), GST-PAK1-glutathione-agarose or GST-glutathione-agarose in buffer K containing 1 mM GTP-γ-S, 1 mM $CaCl_2$ for 1 hr at 4^0 with gentle mixing and then solubilized by addition of 2x Dig (50 mM Tris, pH 7.4, 0.5 M NaCl, 0.5 M sucrose, 2% digitonin).

Incubation was continued for another 1 hr at 4^0 with gentle mixing. The samples were centrifuged at room temperature for 5 min at 14000 rpm in a microfuge. The resin was washed three times with 1 ml of buffer K containing 1% digitonin. The bound protein was eluted using 60 μl of twice concentrated Laemmli sample buffer (78). Samples were heated for 5 min at 95^0 and centrifuged for 5 min at room temperature to remove the resin. The supernatants were applied to electrophoresis on a 12% SDS-PAGE gel (78), and electroblotted to nitrocellulose paper (80). The paper was blocked with 10 mg/ml BSA in TTBS. After washing three times with 1 mg/ml BSA/TTBS, the blot was incubated with affinity purified anti-Syn (1:3000 dilution), anti-Rac1 (Upstate Biotechnology, 1:1000 dilution), anti-RhoA (Santa Cruz Biotechnology, 1:50 dilution), anti H-Ras (Santa Cruz Biotechnology, 1:1000 dilution), anti-Cdc42 (Transduction Laboratories, 1:500 dilution), or anti-Sos (Santa Cruz Biotechnology, 1:1000 dilution). Goat anti-rabbit IgG (H+L)-horseradish peroxidase conjugate and goat anti-mouse IgG (H+L)-horseradish peroxidase conjugate (both 1:1000 dilution) were used for the rabbit and mouse primary antibodies, respectively. The blots were then developed using the enhanced chemiluminescence method (112).

For experiments where laminin was removed using heparin-Sepharose, the skeletal muscle membrane preparation was divided into two portions so that one portion was twice that of the other (200 and 400 μl each). The larger portion was incubated with heparin-Sepharose (200 μl of packed heparin-Sepharose) and the smaller portion was incubated with control-Sepharose (100 μl of packed Sepharose) for 1 hr at 4^0 with gentle mixing. The samples were then centrifuged in a microfuge at room temperature at 14000 rpm for 5 min. The supernatants were saved. The supernatant from heparin-

Sepharose was divided into two equal portions (200 μl each). To one part 2 μl of 1 mg/ml exogenous laminin was added. No laminin was added to the other portion. The rest of the experiment was performed as described above. Removal of laminin was confirmed by probing the supernatant from heparin-Sepharose with antibody against merosin (Novocastra, 1:100 dilution). The presence of dystrophin, and dystroglycans in the supernatant was confirmed by their respective antibodies (data not shown).

For the antibody blockade experiments, skeletal muscle membranes were divided into two equal portions. To one portion syntrophin antibody (α-Syn) while to the other portion anti maltose-binding protein antibody (α-MBP) was added as an unrelated antibody (both antibodies added to a final concentration of 1%) and incubated for 1 hr at 4^0 with gentle mixing. Then the muscle membrane preparation was incubated with 100 μl of control-Sepharose (Ct) or 100 μl of laminin-Sepharose (L) for 1 hr at 4^0 with gentle mixing in buffer K containing 1 mM GTP-γ-S, 1 mM $CaCl_2$ and then for another 1 hr with 1% digitonin. The rest of the experiment was performed as described above.

Phosphorylation of JNK

Laminin was removed from rabbit skeletal muscle microsomes using heparin-Sepharose as described above. To the laminin depleted portion of the microsomes either 3 μl of 1 mg/ml exogenous laminin, 1 μM RGDS, or 1 μM RGES peptide was added in buffer K containing 1 mM GTP-γ-S, 1 mM $CaCl_2$, and 1 mM ATP for 1 hr at 4^0 with gentle mixing. Microsomes were then solubilized by adding 1% Triton X-100, 0.5% IGEPAL and 0.5% sodium deoxycholate. Incubation was continued for another 1 hr at 4^0 with gentle mixing. Microsomes were then “pre-cleared” with Protein G Sepharose

(25 μl) by incubation for 30 min at 4^0 and then incubated with 5 μg of anti-βDG antibody. The immune complexes were then incubated with Protein G-Sepharose for 1 hr, precipitated and washed extensively with buffer K. The bound proteins were detected by anti-phosphorylated-JNK antibody (1:1000 dilution) and visualized by ECL.

Results

Two components of the DGC bind Grb2 and recruitment and activation of small G-proteins is usually a consequence of the action of Grb2. Since the DGC binds laminin we investigated if laminin binding to the DGC initiates signaling by activating small G-proteins. Laminin-Sepharose (L) or control –Sepharose (Ct) were incubated with rabbit skeletal muscle membranes. The gel blot of the bound protein was probed with antibodies against Rac1, Rho-A, Cdc42, and Ras, respectively. Laminin binding to Rac1 is shown in Figure 4.1. It can be seen from the figure that all the G-proteins tested are present in the rabbit skeletal muscle membrane preparation. Sepharose without any protein coupled to it was used as a negative control and did not show any binding of G-proteins. Cdc42 did not show any binding to the laminin receptor. Laminin-Sepharose showed strong binding of Rac1 and to a lesser extent of Rho-A and Ras.

Syntrophin binds Grb2 with high affinity (112) and Grb2 is often involved in pathways for activating small G proteins. Furthermore, syntrophin self-associates (91) and thus syntrophin-Sepharose can be used to bind complexes containing syntrophin. To investigate if syntrophin recruits any of the small G-proteins found in Figure 4.1, syntrophin-Sepharose (Syn) or control-Sepharose (Ct) were used in a pull-down assay. Briefly, syntrophin-Sepharose or control-Sepharose were incubated with detrgent

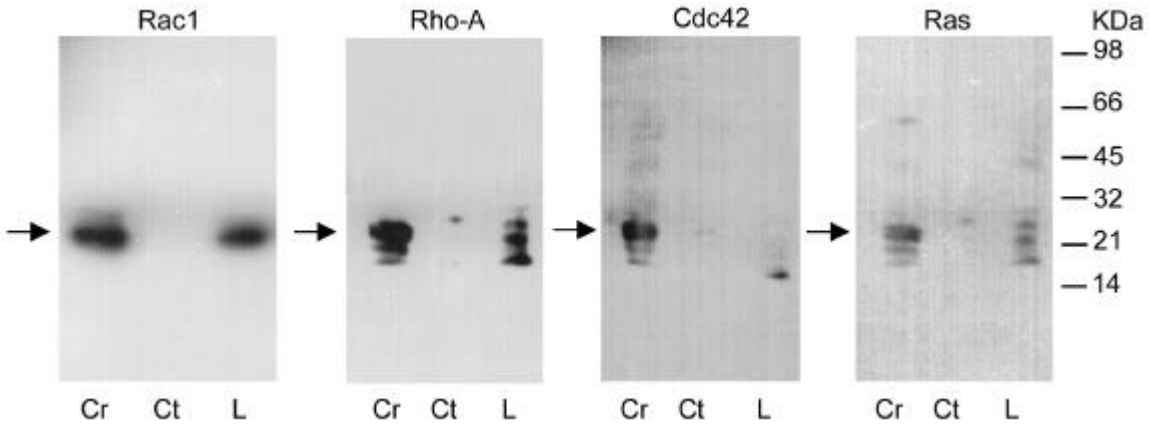

Figure 4.1 Rac1 from rabbit skeletal muscle membrane preparation precipitates with laminin.

Laminin-Sepharose (L) or control-Sepharose (Ct) was incubated with rabbit skeletal muscle membranes in buffer K containing 1 mM $CaCl_2$, 1 mM GTP-γ-S. After washing, bound proteins were eluted with SDS-PAGE sample buffer. Samples, after electrophoresis and electroblotting, were probed with antibodies against Rac1, Rho-A, Ras, and Cdc42. Cr represents crude extract, Ct represents control-Sepharose that was used as negative control, and L represents the laminin-Sepharose bound fraction. The arrows show the expected size of Rac1, Rho-A, Cdc42, and Ras, respectively. Molecular mass markers are shown to the right.

solubilized rabbit skeletal muscle membranes and the bound protein fraction was probed with antibodies against Rac1, Rho-A, Cdc42, and Ras, respectively. Figure 4.2 shows that syntrophin specifically binds to Rac1. None of the other G-proteins tested showed any appreciable binding, although all four G-proteins are present in the rabbit skeletal muscle membrane preparation. Control-Sepharose did not show any binding to any of the proteins tested.

α7β1 integrin is a laminin receptor on skeletal and cardiac muscles (121,122) and serves as a transmembrane link between basal lamina and muscle fibers. Laminin10/11 is more active than fibronectin in promoting cell migration and recruitment of Rac1, via the p130 ^{Cas}-Crk II –DOCK 180 complex (123). Therefore the observed recruitment of Rac1 could be through the laminin -integrin pathway. Heparin has been shown to inhibit the interaction of laminin with α–dystroglycan (124). Laminin binds heparin (125). Heparin-Sepharose has been used to purify laminin alpha 1 and alpha 4 chains (126). To prove our hypothesis that dystrophin glycoprotein complex is a laminin receptor and the recruitment of signaling proteins is in response to laminin binding to α–dystroglycan and not through the integrins, rabbit skeletal muscle membranes were incubated with heparin- Sepharose to remove any endogenous laminin. The supernatant, devoid of laminin (data not shown), was added to control-Sepharose (Ct) or Syn-Sepharose (Syn). To one set, exogenous laminin was also added. The gel blot of the bound protein was probed with the Rac1 antibody. It can be seen from Figure 4.3 that Rac1 (arrow on the right side) is recruited only when laminin is present in the muscle membrane preparation. When laminin was removed by using heparin-Sepharose, syntrophin did not recruit any detectable amount of Rac1. Rac1

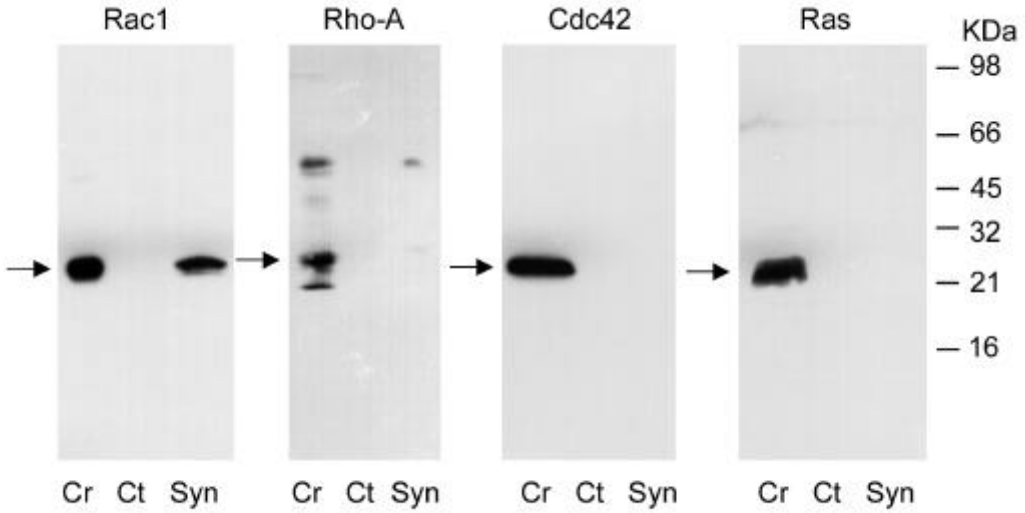

Figure 4.2 Syntrophin pulls down Rac1 specifically from rabbit skeletal muscle membranes.

Syntrophin-Sepharose (Syn) or control-Sepharose (Ct) was incubated with the rabbit skeletal muscle membranes in buffer K containing 1 mM $CaCl_2$, 1 mM GTP-γ-S. After extensive washing, bound proteins were eluted with SDS-PAGE sample buffer. Samples, after electrophoresis and electroblotting, were probed with antibodies against Rac1, Rho-A, Ras, and Cdc42. Cr represents crude extract, Ct represents control-Sepharose that was used as negative control, and Syn represents the Syn-Sepharose bound fraction. The arrows show the expected size of Rac1, Rho-A, Cdc42, and Ras, respectively. Molecular mass markers are shown to the right.

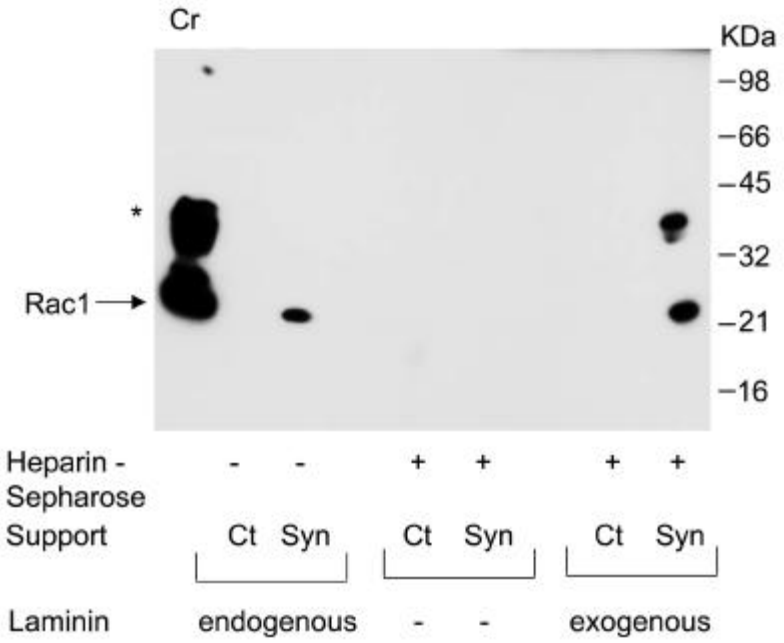

Figure 4.3 Rac1 is recruited only when DGC is attached to laminin.

Rabbit skeletal muscle membranes were incubated with heparin-Sepharose for 1 hr at 4^0. After centrifugation, the supernatant was incubated with Syn-Sepharose (Syn) or control-Sepharose (Ct) in buffer K containing 1 mM $CaCl_2$, 1 mM GTP-γ-S with or without addition of exogenous laminin. After extensive washing, bound proteins were eluted with SDS-PAGE sample buffer. Samples, after electrophoresis and electroblotting, were probed with antibody against Rac1. Cr represents crude extract, Ct represents control-Sepharose that was used as negative control, and Syn represents the syntrophin-Sepharose bound fraction. The arrows show the expected size of Rac1. Molecular mass markers are shown to the right.

was recruited by syntrophin when exogenous laminin was added. Muscle membranes with endogenous laminin were used as a positive control for recruitment of Rac1 by syntrophin. Rac1 has been shown to undergo oligomerization (127); the band shown with asterisk in the figure may be the dimeric form of Rac1. Laminin has been used to isolate DGC proteins (25) and therefore the DGC proteins could be removed by the heparin-Sepharose treatment. To show this was not the case, the presence of components of the DGC in the muscle membrane preparation was confirmed by probing the supernatant of heparin-Sepharose with antibodies against dystrophin, β-dystroglycan and α-dystroglycan (data not shown). Thus, heparin-Sepharose effectively removes laminin while leaving the DGC intact in muscle membranes.

To confirm that syntrophin is involved in the signaling through the DGC, skeletal muscle membranes were incubated for 1 hr with either syntrophin antibody (α-Syn) or maltose binding protein antibody (α-MBP, as a negative control) and then with either laminin-Sepharose (L) or control-Sepharose (Ct). The bound protein was detected with Rac1 antibody. It can be seen from Figure 4.4 that Rac1 is a part of the complex bound by laminin in the presence of anti-MBP, which serves as an unrelated antibody. In the presence of syntrophin antibody, laminin fails to pull-down Rac1 from skeletal muscle membranes. Thus, addition of syntrophin antibody blocks Rac1 recruitment, strongly suggesting that Rac1 is recruited to the DGC via syntrophin.

The serine/threonine protein kinases $p21^{Cdc42/Rac}$-activated kinases (PAKs) are activated upon binding to the GTP- bound form of Rac1 and Cdc42 (128,129). Since PAK1 is an effector of Rac1, a GST chimeric fusion with the p21-binding domain (PBD) of PAK1 on glutathione-agarose, and GST on glutathione-agarose (a negative control),

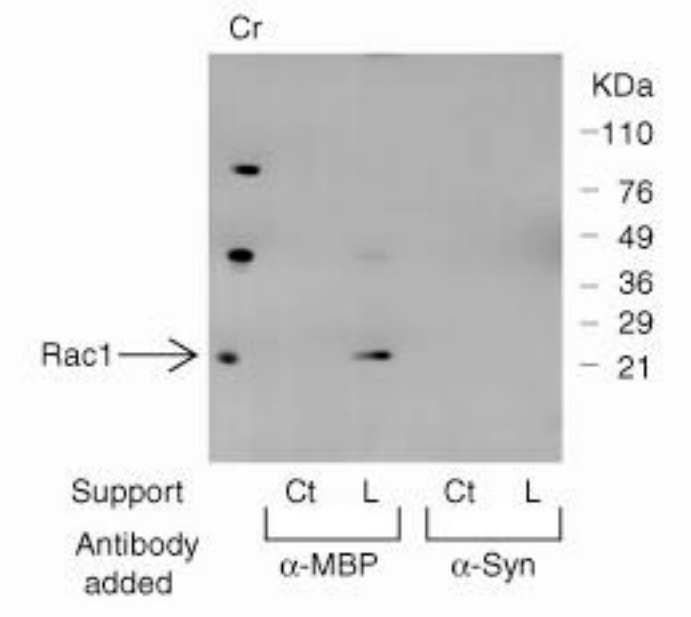

Figure 4.4 Rac1 is recruited to the DGC via syntrophin.

Rabbit skeletal muscle membranes were incubated with antibodies against maltose binding protein (α–MBP) or syntrophin (α-Syn) in buffer K containing 1 mM $CaCl_2$, 1 mM GTP--γ–S for 1 hr at 4^0 and then with control-Sepharose (Ct) or laminin-Sepharose (L) for 1 hr at 4^0. After extensive washing, bound proteins were eluted with SDS-PAGE sample buffer. Samples, after electrophoresis and electroblotting, were probed with antibody against Rac1. Cr represents crude extract, Ct represents control-Sepharose that was used as negative control, and L represents the laminin-Sepharose bound fraction. The arrow shows the expected size of Rac1. Molecular mass markers are shown to the right.

were incubated with skeletal muscle membranes. The gel blot of the bound protein was probed with antibodies against syntrophin, β–dystroglycan and Rac1. Figure 4.5 shows that PAK1 pulled down a complex containing syntrophin (top arrow), β–dystroglycan (middle arrow), and Rac1 (bottom arrow). The presence of β–dystroglycan and syntrophin shows that PAK1 is pulling down the DGC along with Rac 1.

Syntrophin, which itself is an adapter protein, has been recently shown to bind Grb2, an SH2/SH3 adapter protein (112). To identify the guanine nucleotide exchange factor involved, syntrophin-Sepharose (Syn) or control-Sepharose (Ct) were incubated with rabbit skeletal muscle membranes and the bound protein fraction was probed with antibody against son of sevenless, Sos. Figure 4.6 shows that Sos is present in the skeletal muscle membranes (Cr) and Sos shows strong binding to syntrophin (Syn) and to a lesser extent to control-Sepharose (Ct).

Sos catalyzes the exchange of GDP to GTP on Ras and Rac (130). In the activated GTP bound form Ras and Rac activate several downstream kinases such as JNK/SAPK (131-133). Figure 4.7 shows the effect of laminin binding to the DGC on JNK activation. The phosphorylation state of JNK in the presence or absence of laminin was detected using anti-phosphorylated-JNK antibody. JNK2 is activated only when laminin is present and bound to the DGC while JNK1 is activated when laminin is either absent (laminin depleted microsomes) or presumably not bound to the complex (in the presence of heparin). Activation of JNK2 seen by the addition of exogenous laminin to the microsomes confirms that the observed effect is due to laminin binding to the dystrophin glycoprotein complex. Heparin interrupts the interaction between laminin and α-dystroglycan and it can be seen from Figure 4.7 that heparin induces a laminin-

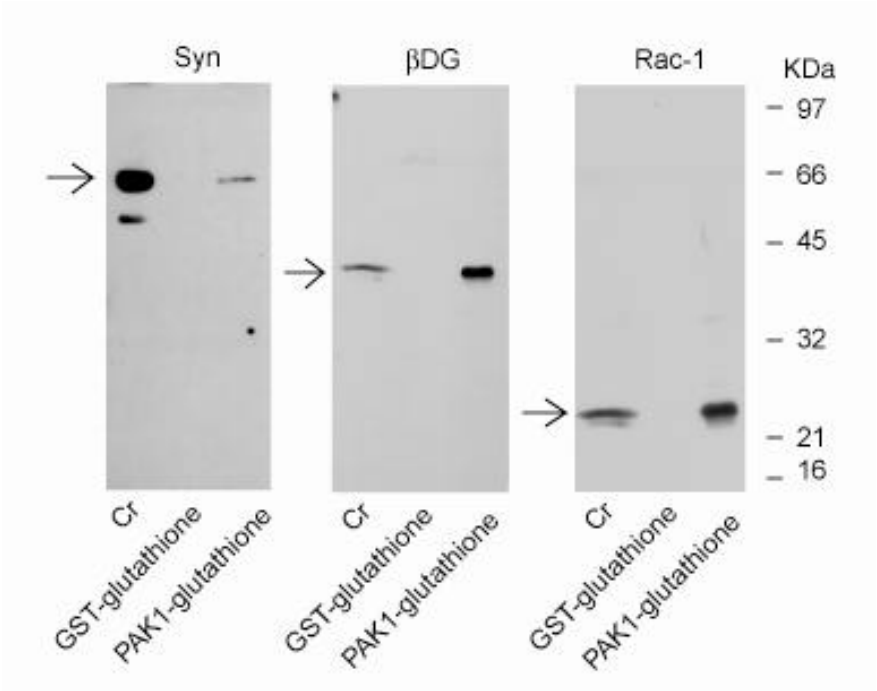

Figure 4.5 Syntrophin recruits p21-activated kinase.

Rabbit skeletal muscle membranes were incubated with GST or GST-PAK1 bound to glutathione-Sepharose in buffer K containing 1 mM $CaCl_2$, 1 mM GTP-γ-S for 1 hr at 4^0 and then digitonin was added to the muscle membranes and incubated for 1 hr at 4^0. After extensive washing, bound proteins were eluted with SDS-PAGE sample buffer. Samples, after electrophoresis and electroblotting, were probed with antibodies against syntrophin (αSyn), β-dystroglycan (βDG), and Rac1 (Rac1). Cr represents crude extract. The top arrow shows the expected size of syntrophin detected by its antibody (αSyn), the middle arrow shows the band detected by β -dystroglycan antibody (βDG), and the bottom arrow shows the band detected by the Rac1 antibody (Rac1). Molecular mass markers are shown to the right.

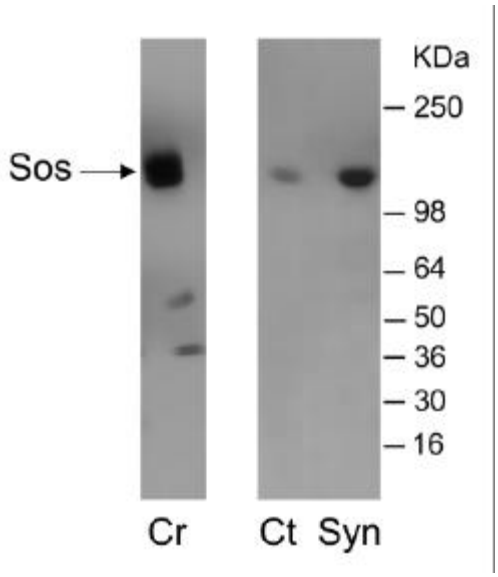

Figure 4.6 Son of sevenless (Sos) is recruited by syntrophin.

Rabbit skeletal muscle membranes were incubated syntrophin-Sepharose (Syn) or control-Sepharose (Ct) in buffer K containing 1 mM $CaCl_2$, 1 mM GTP-γ-S. After extensive washing, bound proteins were eluted with SDS-PAGE sample buffer. Samples, after electrophoresis and electroblotting, were probed with antibody against Sos. Cr represents crude extract, Ct represents control-Sepharose that was used as negative control, and Syn represents the syntrophin-Sepharose bound fraction. The arrow shows the expected size of Sos. Molecular mass markers are shown to the right.

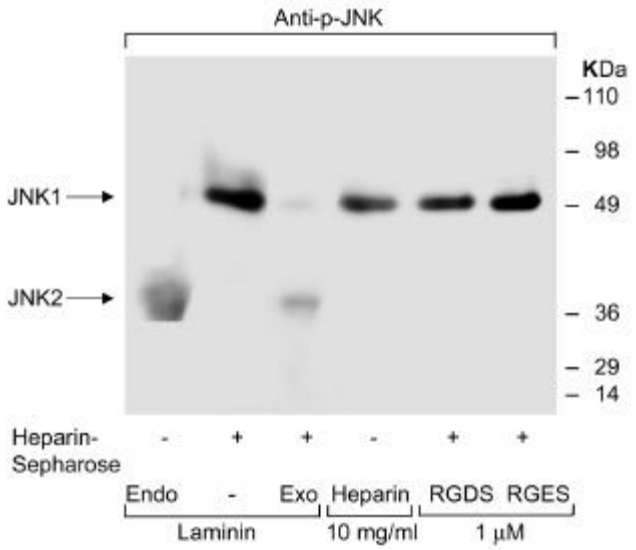

Figure 4.7 JNK2 is activated only when DGC is attached to laminin while JNK1 is activated when interaction of laminin with DGC is interrupted.

Rabbit skeletal muscle membranes were incubated with heparin-Sepharose for 1 hr at 4^0. After centrifugation, the supernatant was incubated in buffer K containing 1 mM $CaCl_2$, 1 mM GTP-γ-S, 1 mM ATP with or without addition of exogenous laminin. 1 μM RGDS or RGES peptide was added to the laminin depleted microsomes. This incubation was followed by another incubation with anti β-dystroglycan antibody for 1 hr at 4^0. The immune complex was precipitated using Protein G Sepharose. After extensive washing, bound proteins were eluted with SDS-PAGE sample buffer. Samples, after electrophoresis and electroblotting, were probed with antibody against phosphorylated JNK. The arrows show the band detected by phosphorylated JNK antibody. Molecular mass markers are shown to the right.

depleted state, showing activated JNK1 while JNK2 is not activated at a detectable level.

Laminin has also been shown to bind $\alpha 7\beta 1$ integrin and therefore to confirm that the observed activation of JNK is due to laminin binding to the DGC and not to the integrins, laminin was removed from the microsomes with heparin-Sepharose as described in the materials and method section. To the laminin depleted microsomes, 1 μM RGDS or 1 μM RGES peptide was added. It can be clearly seen from Figure 4.7 that the addition of either RGDS or RGES peptide has no effect on the phosphorylation state of JNK. Different experiments with peptide concentrations of 10 μM, 100 μM, 1 mM, and 2 mM were performed and gave similar results (data not shown). Thus, over a wide range of concentrations, RGDS, an integrin ligand can not mimic the laminin-induced signaling found here. Furthermore, the inactive RGES has the same effect as RGDS. Thus signaling is not by way of a laminin-integrin interaction but rather is DGC mediated.

To determine if syntrophin binds to Rac1 directly, an Elisa type experiment was performed where a microtiter plate was coated with syntrophin and overlaid with GST-Rac1 (WT), GST-Rac1 (V12) or GST-Rac1 (N17). None of the forms of Rac1 such as wild type, GDP-bound or GTP bound forms showed any direct association with syntrophin (data not shown).

Discussion

Cell signaling proteins are associated with the DGC. Syntrophin and Grb2, PH/PDZ and SH2/SH3 adapter proteins, respectively, are associated with the DGC

along with other signaling components (112). These adapter proteins bind to other proteins and frequently recruit different signal transduction components, which control cell growth and death. In muscular dystrophies, muscle cells die instead of growing, suggesting defects in these signaling pathways.

Just as integrins bind to fibronectin to initiate cell signaling, in the present study, we have shown that the DGC binds to laminin and initiates cell signaling; i.e., the DGC is a laminin receptor and this is a GTPase coupled receptor. A laminin receptor recruits Rac1, Ras, and Rho-A (Figure 4.1). The DGC laminin-receptor recruits Rac1 (Figure 4.4). Laminin has been shown to bind α-dystroglycan and integrins (121,122,124).

Recently, we have shown that syntrophin binds with very high affinity to Grb2, an SH2/SH3 adapter protein (112). Grb2 is often associated with son of sevenless, Sos. Sos has activity as a guanine nucleotide exchange factor (GEF) for Ras and Rac1. Sos is composed of multiple functional domains including a Dbl homology domain, PH domain, a Ras Guanine nucleotide exchange factor (GEF) domain, and a C-terminal proline rich region. This proline rich region is a binding site for the SH3 domain adapter proteins such as Grb2, Nck, and CrkII, etc. Syntrophin recruits Sos, presumably through Grb2 (Figure 4.6). The Dbl homology domain of Sos has been reported to also have a GEF activity for Rac and to stimulate its downstream kinases, JNK/SAPK (134). Syntrophin recruits Rac1 from skeletal muscle membranes through a Grb2-Sos complex but not other G proteins (Figure 4.2, Figure 4.3). Thus, at least one of the small G proteins, Rac1, is associated with the DGC. The interaction between α-dystroglycan and laminin is inhibited by heparin (124,135). So when laminin is removed from the skeletal muscle membranes using heparin-Sepharose, syntrophin can no longer

precipitate Rac1. On the other hand when exogenous laminin is added to the skeletal muscle membranes, syntrophin again precipitates a complex containing Rac1. Thus, DGC is associated with Rac1 only when DGC is attached to laminin (Figure 4.3). Inhibition of recruitment of Rac1 by the syntrophin antibody strongly suggests that Rac1 is being recruited to the complex via syntrophin (Figure 4.4). p21-activated kinase (PAK1) is found to be activated upon binding to the GTP-bound forms of Rac1 and Cdc42 (136,137). PAK1 is implicated in mediating signaling from Rac1 and Cdc42 to the c-Jun N terminal kinase (138,139), and in certain cases, to the actin cytoskeleton (140). PAK1 being recruited by syntrophin has been shown in the reverse pull-down experiment where PAK1-glutathione-agarose was used to pull-down syntrophin along with β-dystroglycan (Figure 4.5). In addition, PAK1 is being recruited by syntrophin via Rac1 (Figure 4.5) but not Cdc42 (Figure 4.2).

The role of Rho family proteins (including Rho A, Rac1, and Cdc42) in the activation of SAPK/JNK has been demonstrated independently by Coso et al. (132) and Minden et al. (133). Activation of the Rho family G proteins often leads to activation of Jun N terminal kinases that leads to phosphorylation of c-jun. The stress activated protein kinases (SAPK) are directly involved in phosphorylation of c-jun. Though often these Jun N terminal kinases are SAPK1 and SAPK2, this function is also shared by SAPK3 (141). SAPK3 is associated with syntrophin (59). JNK2 is phosphorylated only when laminin is attached to the DGC while JNK1 is phosphorylated when the interaction of laminin with the DGC is interrupted (Figure 4.7). Addition of 1 μM-2 mM RGDS or RGES peptide shows no effect on the phosphorylation state of JNK1 or JNK2 in the absence of laminin (Figure 4.7 and data not shown), thus confirming our hypothesis that

the observed signaling is due to laminin binding to α-dystroglycan and not because of laminin binding to integrins. Kolodziejczyk et al. (142) have shown that murine models of DMD display a muscle-specific activation of JNK1. They also reported that independent activation of JNK1 resulted in defects in myotube viability and integrity *in vitro*, similar to a dystrophic phenotype. In addition, direct muscle injection of an adenoviral construct containing the JNK1 inhibitory protein, JIP1, dramatically attenuated the progression of dystrophic myofiber destruction. Taken together, these results suggest that a JNK1-mediated signal cascade could contribute to the progression of the disease pathogenesis.

We show that the dystrophin glycoprotein complex is a laminin receptor which signals and propose the effect of signaling is to cause the cell to grow normally whenever it is attached to merosin (muscle laminin). This signaling pathway is depicted in Figure 4.8. Merosin (muscle laminin) binds to α-dystroglycan (61), which then signals through β−dystroglycan, dystrophin and syntrophin. Syntrophin in turn binds to Grb2, an SH2/SH3 adapter protein. Syntrophin thus bridges the dystrophin glycoprotein complex, a laminin receptor, to the other proteins namely Grb2 and Sos, which activates the small G protein Rac1. The GTP-bound form of Rac1 in turn activates p21-activated kinase. PAK1 then probably leads to subsequent activation of currently unidentified component of a MAP kinase pathway. The phosphorylation and activation of Jun N-terminal kinase2 may lead to subsequent phosphorylation of c-jun and as a result would regulate AP1 mediated transcription. Phosphorylation of c-jun prevents apoptosis and premature cell senescence (143). Thus, we propose that the dystrophin glycoprotein complex, by acting as a laminin receptor, signals the normal muscle cell to grow.

Figure 4.8 Diagrammatic representation of the signaling pathway.

Laminin by binding to α–dystroglycan (α-DG) through dystrophin glycoprotein complex recruits Rac1 through Grb2-Sos complex and may signal the normal muscle cell to grow. The components of the DGC are shown in light gray color, the interactions that are shown to occur in this report are shown in dark gray color while the proposed but currently unidentified interactions are shown in white color. The abbreviations for the DGC proteins are given in the paranthesis. Dystrophin (Dys), α-sarcoglycan (α-SG), β-dystroglycan (β-DG), and γ-dystroglycan (γ-SG), β-Sarcoglycan (β-SG), δ-sarcoglycan (δ-SG) and sarcospan (SP), syntrophin (Syn).

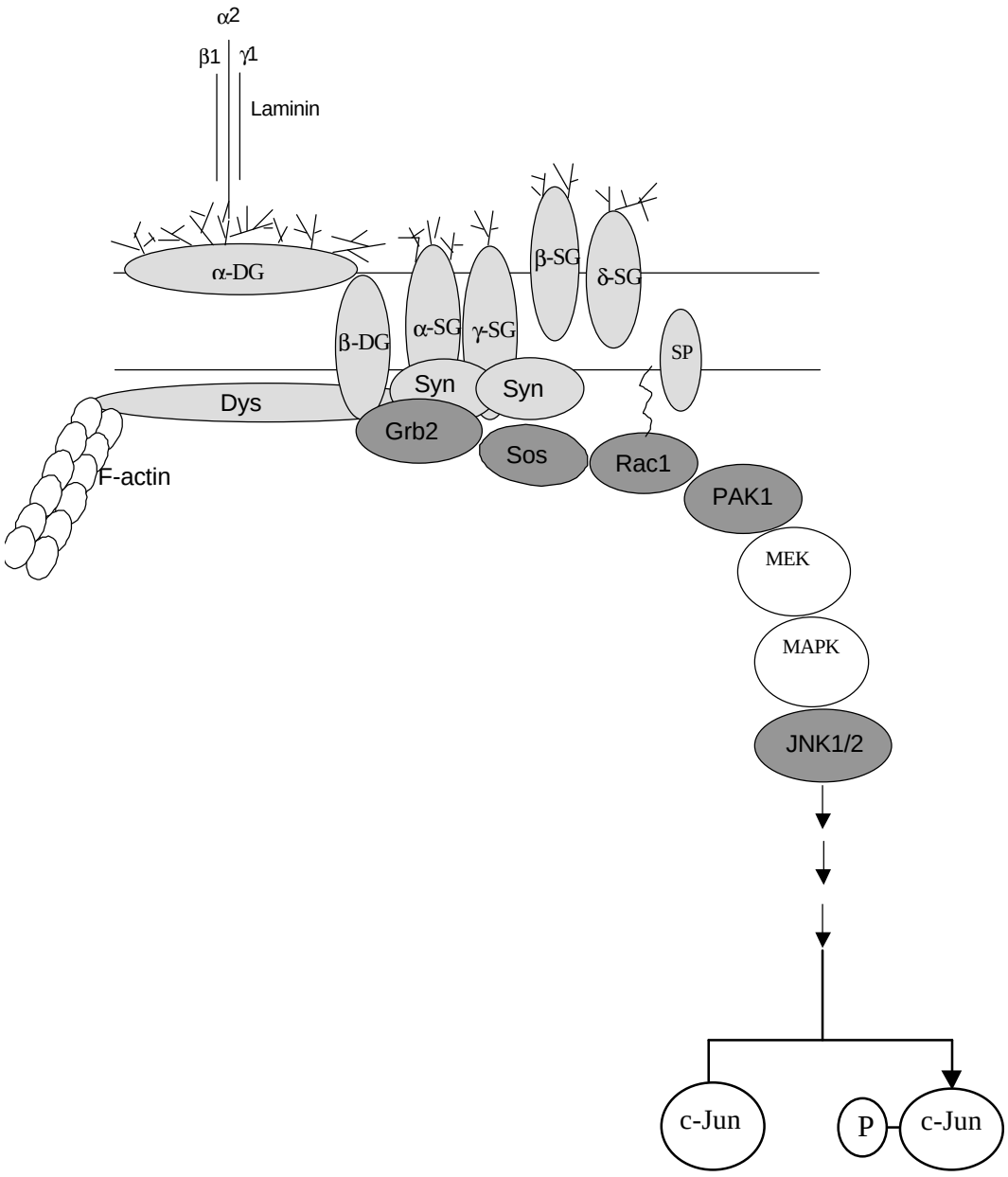
α2
β1
γ1
Laminin
α-DG
β-DG
α-SG
γ-SG
β-SG
δ-SG
SP
Syn
Syn
Dys
Grb2
Sos
Rac1
PAK1
MEK
MAPK
JNK1/2
F-actin
c-Jun
P
c-Jun

It has also been reported that agrin, a major component of the basal lamina of the neuromuscular junction leads to muscle-specific activation of Rac and Cdc42 in differentiated myotubes and this activation is essential for AchR clustering at synaptic sites (144). In our lab, we have found that after tenotomy the muscle is no longer subjected to normal stretching and the DGC receptor down-regulates. In addition to the down-regulation of the DGC, there is a large effect on G protein signaling through Ras, Rho-A, and Cdc42 while having very little or no effect on Rac1 signaling (145). Since atrophied muscle has the potential to rapidly recover from atrophy, it must maintain all of the components necessary for the recovery. These results also support the importance of Rac1 signaling.

We have proposed earlier that the DGC may function as a stretch receptor (145). The signal transduction mechanism for this stretch receptor is not known. However, stretch signaling of an elastin-laminin receptor involves Grb2 and small GTPase in smooth muscles (146). In bladder smooth muscles, SAPK2 and JNK are activated as a result of stretch (147), a frequent consequence of Grb2 and small GTPase signaling. Thus, our model that the DGC-laminin receptor promotes muscle growth and its putative function as a stretch receptor regulating atrophy/hypertrophy are similar concepts. In such a stretch receptor paradigm, laminin would remain attached to its DGC receptor but would be stressed by stretching.

Chapter 5. Conclusions

Duchenne and Becker muscular dystrophies are tragic diseases that leave the victim without much hope for cure. Understanding the molecular basis of these diseases in order to develop effective treatments for afflicted individuals has been of highest priority to both scientists and clinicians. A major breakthrough was made about 15 years ago when the genetic locus causing these myopathies was identified (8).

When we began our studies on syntrophin, nearly 4 years ago, syntrophin was shown to bind calmodulin (53), PtdIns4,5P2 (52), nNOS (56), Ca^{2+} (48), SAPK3 (59), voltage gated sodium channels (60), etc. While the function of syntrophin, and the DGC, in muscle is unknown, DGC was proposed to play a role as a signal transduction complex (53), and syntrophin was proposed to function as a modular adapter in recruiting signaling proteins to the DGC and the membrane (44).

Work in our laboratory has focussed on syntrophin interactions with the cell signaling proteins and the role of DGC in skeletal muscle. We have shown in this study that syntrophin undergoes oligomerization in a Ca^{2+}-dependent manner and calmodulin inhibits it. Ca^{2+} chelators such as EGTA inhibit oligomerization. Calmodulin is present in many tissues as high as micromolar and is probably in sufficient concentration to inhibit or limit the oligomerization of syntrophin.

The presence of a high concentration of solute ions frequently alters the solubility of proteins and other macromolecules: (i) it causes aggregation or structural collapse of proteins because of enhancement of hydrophobic interactions; (ii) it interferes with essential electrostatic interactions within or between molecules because of charge

shielding. However, syntrophin oligomerization is caused by Ca^{2+} and not because of bulk ionic strength. In the case of syntrophin, 1 μM free Ca^{2+} was added to the buffer containing 50 mM Tris, pH 7.5, 100 mM NaCl. Addition of 1 μM free Ca^{2+} would not change the ionic strength of the buffer significantly. In addition, syntrophin did not show any precipitation in absence of Ca^{2+} (at virtually the same ionic strength).

Aggregates form as a result of the nonspecific interaction between partially folded intermediates or denatured protein. Aggregation occurs in a continuum and aggregates of virtually any size can occur. The hydrophobic nature of the partially folded intermediates is believed to be responsible for self-association and thus the formation of aggregates. While oligomerization is a more structured process caused by the association of properly folded proteins, in specific stiochiometry and specific domains.

The observed effect was due to oligomerization and not aggregation because i) specific sequences in and adjacent to the PH1 domain were involved ii) this oligomerization was inhibited by a specific Ca^{2+} binding protein, calmodulin. iii) In addition, in the size exclusion chromatography experiment, several distinct peaks were observed indicating oligomeric species occur in certain stoichiometries more abundantly than others. If the observed phenomenon was aggregation then we would have observed a continuum in one peak instead of several distinct peaks. The syntrophin oligomerization is also similar to that of actin (84) and tubulin (85) in that Ca^{2+} is a regulator and oligomer stoichiometry is affected by regulatory proteins.

In the resting muscle, Ca^{2+} would be submicromolar in concentration and this would also limit oligomerization. The calmodulin bound would be the Ca^{2+}-free, apocalmodulin conformer (55) and our results suggest that each syntrophin would retain

a calmodulin, increasing the local calmodulin concentration even further. As intracellular Ca^{2+} increases, preceding and during muscle contraction, this Ca^{2+} could bind to syntrophin and favor syntrophin self-association. Additionally, as Ca^{2+} binds calmodulin, calmodulin would be able to bind to other more numerous cell proteins, which bind only the Ca^{2+}-calmodulin conformer. Thus, Ca^{2+}-calmodulin could be bound elsewhere, allowing syntrophin's oligomerization. Thus, one can envision syntrophin as monomeric or simple oligomer (e.g. dimer, etc) in the resting cell and oligomeric in the contracting muscle. In support of this view, syntrophin is present in 2:1 molar ratio to dystrophin and other DGC components when isolated in the absence of Ca^{2+} (19). The oligomeric state of syntrophin may be important to maintaining the clusters of ion channels at the neuromuscular junction during contraction (60) and the distribution of calmodulin within the myofibril (55). Alternatively, syntrophins may respond to Ca^{2+} during contraction in a way that makes the protein complexes which contain it more tightly (or loosely) associated.

Syntrophins are PH/PDZ domain adapter proteins that bind Na^{+}-channels (60), NO synthetase (56), dystrophin, α- and γ- sarcolglycans (46), SAPK3 (59) and to themselves (91 and chapter 2). This self-association could bring together cellular signaling components and ion channels. It is now clear that this adapter protein binds another adapter, the SH2/SH3 domain protein Grb2 (112 and chapter 3). Syntrophin contains polyproline sequences that bind Grb2. This binding is Ca^{2+}-independent. This Ca^{2+}-independence is significant since Ca^{2+}-binding by syntrophin results in large syntrophin oligomers and oligomerization occurs utilizing PH1 sequences (91). Syntrophin binds the SH2/SH3 adapter protein, Grb2, and may bring together a large

number of motifs important to cellular signaling in one place within the cell. SH2/SH3 adapters are necessary for MAP kinase pathway activation and tyrosine kinase recruitment in many different cell processes. The Grb2-SOS complex also binds to small G proteins such as Ras and Rac1 leading to activation of signaling pathways which could potentially initiate cell growth and differentiation.

Just as integrins bind to fibronectin to initiate cell signaling, in this study, we have shown that the DGC binds to laminin and initiates cell signaling; i.e., the DGC is a laminin receptor and this is a GTPase coupled receptor. A laminin receptor recruits Rac1, Ras, and Rho-A. The DGC laminin-receptor recruits Rac1. Rac1 is recruited to the complex via syntrophin. Activation of the Rho family G proteins often leads to activation of Jun N terminal kinases (JNK) that leads to phosphorylation of c-Jun. JNK2 is phosphorylated only when laminin is attached to the DGC while JNK1 is phosphorylated when the interaction of laminin with the DGC is interrupted.

We have shown that the dystrophin glycoprotein complex is a laminin receptor which signals and propose the effect of signaling is to cause the cell to grow normally whenever it is attached to merosin (muscle laminin).

Biochemical characterization of DGC proteins is important not only for a molecular understanding of the cellular protein complex, but also for developing potential therapeutic and diagnostic techniques. Cox et al. (148) have shown that the dystrophin gene when expressed in dystrophic tissue can reverse myopathic symptoms. Kolodziejczyk et al. (142) have shown that murine models of DMD display a muscle-specific activation of JNK1. They also reported that independent activation of JNK1 resulted in defects in myotube viability and integrity *in vitro*, similar to a dystrophic

phenotype. In addition, direct muscle injection of an adenoviral construct containing the JNK1 inhibitory protein, JIP1, dramatically attenuated the progression of dystrophic myofiber destruction. Taken together, these results suggest that a JNK1-mediated signal cascade could contribute to the progression of the disease pathogenesis. These studies describe the syntrophin at the sarcolemma and its interactions with other proteins and help us understand the role played by this complex. Signaling pathways such as the one we have helped elucidate provide numerous targets for pharmacological intervention, which may lead to ways to attenuate or alleviate the destructive course of muscular dystrophies.

A cure for DMD and BMD will have to await a more complete understanding of all the functions of the DGC proteins and the complex as a whole. Our studies describe certain important functions of syntrophin, signaling through the DGC, and along with the pioneering work of several other investigators, attempt to characterize the function and role of this complex in muscle. The role of the DGC is emerging from these studies and understanding is tantalizingly close but still elusive.

List Of References

1. Fernandez-Valle, C., Gwynn, L., Wood, P. M., Carbonetto, S., and Bunge, M. B. (1994) *J Neurobiol* 25(10), 1207-26
2. Wewer, U. M., and Engvall, E. (1996) *Neuromuscul Disord* 6(6), 409-18
3. Engel, A. G., Yamamoto, M., and Fischbeck, K. M. (1994) in *Dystrophinopathies* Vol. 2, 2 nd edition Ed., pp. 1133-87, McGraw-Hill, Inc, New York
4. Bertorini, T. E. (2001) in *Neuromuscular Diseases: expert clinician's views* (Pourmans, R., ed), pp. 227-94, Butterworth-Heinemann, Boston
5. Hoffman, E. P., and Kunkel, L. M. (1989) *Neuron* 2(1), 1019-29
6. Yoshida, M., and Ozawa, E. (1990) *J Biochem* 108, 748-52
7. Ervasti, J. M., Kahl, S. D., and Campbell, K. P. (1991) *J Biol Chem* 266, 9161-65
8. Monaco, A. P., Neve, R. L., Colletti-Feener, C., Bertelson, C. J., Kurnit, D. M., and Kunkel, L. M. (1986) *Nature* 323(6089), 646-50
9. Koenig, M., Hoffman, E. P., Bertelson, C. J., Monaco, A. P., Feener, C., and Kunkel, L. M. (1987) *Cell* 50(3), 509-17
10. Hoffman, E. P., Brown, R. H., and Kunkel, L. M. (1987) *Cell* 51, 919-28
11. Emery, A. E. (1993) *Duchenne muscular dystrophy*, 2nd edition Ed. History, 24, Oxford; Oxford University Press, New York
12. Matsumura, K., Nonaka, I., Tome, F. M., Arahata, K., Collin, H., Leturcq, F., Recan, D., Kaplan, J. C., Fardeau, M., and Campbell, K. P. (1993) *Am J Hum Genet* 53(2), 409-16
13. Higuchi, I., Niiyama, T., Fukunaga, H., Nakamura, K., Nakagawa, M., and Osame, M. (1994) *Intern Med* 33(6), 334-36

14. Watkins, S. C., Hoffman, E. P., Slayter, H. S., and Kunkel, L. M. (1988) *Nature* 333(6176), 863-66

15. Ervasti, J. M., and Campbell, K. P. (1993) *Curr Opin Cell Biol* 5(1), 82-87

16. Ohlendieck, K., and Campbell, K. P. (1991) *J Biol Chem* 115, 1685-94

17. Minetti, C., Chang, H. W., Medori, R., Prelle, A., Moggio, M., Johnsen, S. D., and Bonilla, E. (1991) *Neurology* 41(8), 1288-92

18. Masuda, T., Fujimaki, N., Ozawa, E., and Ishikawa, H. (1992) *J Cell Biol* 119(3), 543-48

19. Ervasti, J. M., Ohlendieck, K., Kahl, S. D., Gaver, M. G., and Campbell, K. P. (1990) *Nature* 345, 315-19

20. Ervasti, J. M., and Campbell, K. P. (1991) *Cell* 66, 1121-31

21. Ibraghimov-Beskrovnaya, O., Milatovich, A., Ozcelik, T., Yang, B., Koepnick, K., Francke, U., and Campbell, K. P. (1993) *Hum Mol Genet* 2(10), 1651-57

22. Yoshida, M., Suzuki, A., Yamamoto, H., Noguchi, S., Mizuno, Y., and Ozawa, E. (1994) *Eur J Biochem* 222(3), 1055-61

23. Mizuno, Y., Yoshida, M., Yamamoto, H., Hirai, S., and Ozawa, E. (1993) *J Biochem (Tokyo)* 114(6), 936-41

24. Yamamoto, H., Mizuno, Y., Hayashi, K., Nonaka, I., Yoshida, M., and Ozawa, E. (1994) *J Biochem (Tokyo)* 115(1), 162-67

25. Ervasti, J. M., and Campbell, K. P. (1993) *J Cell Biol* 122(4), 809-23

26. Henry, M. D., Williamson, R. A., and Campbell, K. P. (1998) *Ann N Y Acad Sci* 857, 256-59

27. Colognato, H., Winkelmann, D. A., and Yurchenco, P. D. (1999) *J Cell Biol*

145(3), 619-31

28. Henry, M. D., and Campbell, K. P. (1996) *Curr Opin Cell Biol* 8(5), 625-31

29. Williamson, R. A., Henry, M. D., Daniels, K. J., Hrstka, R. F., Lee, J. C., Sunada, Y., Ibraghimov-Beskrovnaya, O., and Campbell, K. P. (1997) *Hum Mol Genet* 6, 831-41

30. Straub, V., and Campbell, K. P. (1997) *Curr Opin Neurol* 10, 168-75

31. Xu, H., Christmas, P., Wu, X. R., Wewer, U. M., and Engvall, E. (1994) *Proc Natl Acad Sci U S A* 91(12), 5572-76

32. Mayer, U., Saher, G., Fassler, R., Bornemann, A., Echtermeyer, F., von der Mark, H., Miosge, N., Poschl, E., and von der Mark, K. (1997) *Nat Genet* 17(3), 318-23

33. Tome, F. M., Evangelista, T., Leclerc, A., Sunada, Y., Manole, E., Estournet, B., Barois, A., Campbell, K. P., and Fardeau, M. (1994) *C R Acad Sci III* 317(4), 351-57

34. Chan, Y. M., Bonnemann, C. G., Lidov, H. G., and Kunkel, L. M. (1998) *J Cell Biol* 143(7), 2033-44

35. Crosbie, R. H., Heighway, J., Venzke, D. P., Lee, J. C., and Campbell, K. P. (1997) *J Biol Chem* 272(50), 31221-24

36. Ben Hamida, M., Fardeau, M., and Attia, N. (1983) *Muscle Nerve* 6(7), 469-80

37. Matsumura, K., Tome, F. M., Collin, H., Azibi, K., Chaouch, M., Kaplan, J. C., Fardeau, M., and Campbell, K. P. (1992) *Nature* 359(6393), 320-22

38. Passos-Bueno, M. R., Oliveira, J. R., Bakker, E., Anderson, R. D., Marie, S. K., Vainzof, M., Roberds, S., Campbell, K. P., and Zatz, M. (1993) *Hum Mol Genet*

2(11), 1945-57

39. Yamanouchi, Y., Mizuno, Y., Yamamoto, H., Takemitsu, M., Yoshida, M., Nonaka, I., and Ozawa, E. (1994) *Neuromuscul Disord* 4(1), 49-4

40. Crosbie, R. H., Lebakken, C. S., Holt, K. H., Venzke, D. P., Straub, V., Lee, J. C., Grady, R. M., Chamberlain, J. S., Sanes, J. R., and Campbell, K. P. (1999) *J Cell Biol* 145(1), 153-65

41. Froehner, S. C., Murnane, A. A., Tobler, M., Peng, H. B., and Sealock, R. (1987) *J Cell Biol* 104(6), 1633-46

42. Yamamoto, H., Hagiwara, Y., Mizuno, Y., Yoshida, M., and Ozawa, E. (1993) *J Biochem (Tokyo)* 114(1), 132-39

43. Ahn, A. H., Freener, C. A., Gussoni, E., Yoshida, M., Ozawa, E., and Kunkel, L. M. (1996) *J Biol Chem* 271, 2724-30

44. Peters, M. F., Adams, M. E., and Froehner, S. C. (1997) *J Cell Biol* 138(1), 81-93

45. Yang, B., Jung, D., Rafael, J. A., Chamberlain, J. S., and Campbell, K. P. (1995) *J Biol Chem* 270(10), 4975-78

46. Madhavan, R., and Jarrett, H. W. (1995) *Biochemistry* 34(38), 12204-09

47. Suzuki, A., Yoshida, M., Hayashi, K., Mizuno, Y., Hagiwara, Y., and Ozawa, E. (1994) *Eur J Biochem* 220(2), 283-92

48. Newbell, B. J., Anderson, J. T., and Jarrett, H. W. (1997) *Biochemistry* 36, 1295-05

49. Koch, W. J., Inglese, J., Stone, W. C., and Lefkowitz, R. J. (1993) *J Biol Chem* 268, 8256-60

50. Harlan, J. E., Yoon, H. S., Hajduk, P. J., and Fesik, S. W. (1995) *Biochemistry*

34, 9859-64

51. Harlan, J. E., Hajduk, P. J., Yoon, H. S., and Fesik, S. W. (1994) *Nature* 371, 168-70

52. Chockalingam, P. S., Gee, S. H., and Jarrett, H. W. (1999) *Biochemistry* 38, 5596-02

53. Madhavan, R., Massom, L. R., and Jarrett, H. W. (1992) *Biochem Biophys Res Commun* 185, 753-59

54. Iwata, Y., Pan, Y., Yoshida, T., Hanada, H., and Shigekawa, M. (1998) *FEBS Lett* 423, 173-77

55. Jurado, L. A., Chockalingam, P. S., and Jarrett, H. W. (1999) *Physiol Reviews* 79, 661-82

56. Brenman, J. E., Chao, D. S., Gee, S. H., McGee, A. W., Craven, S. E., Santillano, D. R., Wu, Z., Huang, F., Xia, H., Peters, M. F., Froehner, S. C., and Bredt, D. S. (1996) *Cell* 84(5), 757-67

57. Gibson, T. J., Hyvonen, M., Birney, E., Musacchio, A., and Saraste, M. (1994) *Trends Biochem Sci* 19, 349-53

58. Adams, M. E., Dwyer, T. M., Dowler, L. L., White, R. A., and Froehner, S. C. (1995) *J Biol Chem* 270, 25859-65

59. Hasegawa, M., Cuenda, A., Spillantini, M. G., Thomas, G. M., Buee-Scherrer, V., Cohen, P., and Goedert, M. (1999) *J Biol Chem* 274, 12626-31

60. Gee, S. H., Madhavan, R., Levinson, S. R., Caldwell, J. H., Sealock, R., and Froehner, S. C. (1998) *J Neuroscience* 18, 128-37

61. Ibraghimov-Beskrovnaya, O., Ervasti, J. M., Leveille, C. J., Slaughter, C. A., Sernett, S. W., and Campbell, K. P. (1992) *Nature* 355, 696-02

62. Hammonds, R. G., Jr. (1987) *Cell* 51(1), 1

63. Campbell, K. P. (1995) *Cell* 80(5), 675-79

64. Cheung, W. Y. (1980) *Science* 207(4426), 19-27

65. Turner, P. R., Westwood, T., Regen, C. M., and Steinhardt, R. A. (1988) *Nature* 335, 735-38

66. Hunter, T. (1995) *Cell* 80(2), 225-36

67. Madhavan, R., and Jarrett, H. W. (1994) *Biochemistry* 33, 5797-04

68. Milner, R. E., Busaan, J. L., Holmes, C. F. B., Wang, J. H., and Michalak, M. (1993) *J Biol Chem* 268, 21901-05

69. Wagner, K. R., and Huganir, R. L. (1994) *J Neurochem* 62(5), 1947-52

70. Luise, M., Presotto, C., Senter, L., Betto, R., Ceoldo, S., Furlan, S., Salvatori, S., Sabbadini, R. A., and Salviati, G. (1993) *Biochem J* 293, 243-47

71. Walsh, M. P., Busaan, J. L., Fraser, E., Fu, S. Y., Pato, M. D., and Michalak, M. (1995) *Biochemistry* 34, 5561-68

72. Cavaldesi, M., Macchia, G., Barca, S., Defilippi, P., Tarone, G., and Petrucci, T. C. (1999) *J Neurochem* 72(4), 1648-55

73. Yoshida, T., Pan, Y., Hanada, H., Iwata, Y., and Shigekawa, M. (1998) *J Biol Chem* 273(3), 1583-90

74. Froehner, S. C. (1984) *J Biol Chem* 99, 88-96

75. Campbell, K. P., and Kahl, S. D. (1989) *Nature* 338(6212), 259-62

76. Froehner, S. C., Adams, M. E., Peters, M. F., and Gee, S. H. (1997) in

Cytoskeletal Regulation of Membrane Function (Froehner, S. C., and Bennett, V., eds), pp. 197-07, The Rockefeller University Press, New York

77. Jarrett, H. W., and Foster, J. L. (1995) *J Biol Chem* 270(10), 5578-86

78. Laemmli, U. K. (1970) *Nature* 227, 680-85

79. Bradford, M. M. (1976) *Anal Biochem* 72, 248-54

80. Towbin, H., Staehelin, T., and Gordon, J. (1979) *Proc Natl Acad Sci U S A* 76(9), 4350-54

81. Jarrett, H. W., and Taylor, W. L. (1998) *J Chromatogr A* 803, 131-39

82. Hom, L. G., and Volkman, L. E. (1998) *BioTechniques* 25(1), 20-22

83. Mahadevan, D., Thanki, N., Singh, J., McPhie, P., Zangrilli, D., Wang, L.-M., Guerrero, C., LeVine, H. I., Humblet, C., Saldanha, J., Gutkind, J. S., and Najmabadi-Haske, T. (1995) *Biochemistry* 34, 9111-17

84. Wang, L. L., and Spudich, J. A. (1984) *J Cell Biol* 99(3), 844-51

85. Soto, C., Rodriguez, P. H., and Monasterio, O. (1996) *Biochemistry* 35(20), 6337-44

86. Klein, D. E., Lee, A., Frank, D. W., Marks, M. S., and Lemmon, M. A. (1998) *J Biol Chem* 273(42), 27725-33

87. Kramarcy, N. R., Vidal, A., Froehner, S. C., and Sealock, R. (1994) *J Biol Chem* 269(4), 2870-76

88. Adams, M. E., Butler, M. H., Dwyer, T. M., Peters, M. F., Murnane, A. A., and Froehner, S. C. (1993) *Neuron* 11(3), 531-40

89. Ahn, A. H., Yoshida, M., Anderson, M. S., Feener, C. A., Selig, S., Hagiwara, Y., Ozawa, E., and Kunkel, L. M. (1994) *Proc Natl Acad Sci U S A* 91(10), 4446-50

90. Yang, B., Ibraghimov-Beskrovnaya, O., Moomaw, C. R., Slaughter, C. A., and Campbell, K. P. (1994) *J Biol Chem* 269(8), 6040-44

91. Oak, S. A., and Jarrett, H. W. (2000) *Biochemistry* 39(30), 8870-77

92. Rosa, G., Ceccarini, M., Cavaldesi, M., Zini, M., and Petrucci, T. C. (1996) *Biochem Biophys Res Commun* 223(2), 272-77

93. Pelicci, G., Lanfrancone, L., Salcini, A. E., Romano, A., Mele, S., Grazia Borrello, M., Segatto, O., Di Fiore, P. P., and Pelicci, P. G. (1995) *Oncogene* 11(5), 899-07

94. Herzog, A., Szegedi, C., Jona, I., Herberg, F. W., and Varsanyi, M. (2000) *FEBS Lett* 472, 73-77

95. Yang, B., Jung, D., Motto, D., Meyer, J., Koretzky, G., and Campbell, K. P. (1995) *J Biol Chem* 270(20), 11711-14

96. Roberds, S. L., Anderson, R. D., Ibraghimov-Beskrovnaya, O., and Campbell, K. P. (1993) *J Biol Chem* 268(32), 23739-42

97. Sparks, A. B., Rider, J. E., Hoffman, N. G., Fowlkes, D. M., Quillam, L. A., and Kay, B. K. (1996) *Proc Natl Acad Sci U S A* 93, 1540-44

98. Anderson, J. T., Rogers, R. P., and Jarrett, H. W. (1996) *J Biol Chem* 271(12), 6605-10

99. Posern, G., Zheng, J., Knudsen, B. S., Kardinal, C., Muller, K. B., Voss, J., Shishido, T., Cowburn, D., Cheng, G., Wang, B., Kruh, G. D., Burrell, S. K., Jacobson, C. A., Lenz, D. M., Zamborelli, T. J., Adermann, K., Hanafusa, H., and Feller, S. M. (1998) *Oncogene* 16, 1903-12

100. Vidal, M., Goudreau, N., Cornille, F., Cussac, D., Gincel, E., and Garbay, C.

(1999) *J Mol Biol* 290(3), 717-30

101. Simon, J. A., and Schreiber, S. L. (1995) *Chem Biol* 2(1), 53-60

102. Margolis, B. (1994) *Prog Biophys Mol Biol* 62, 223-44

103. Ilic, D., Damsky, C. H., and Yamamoto, T. (1997) *J Cell Sci* 110, 401-07

104. Peters, M. F., Kramarcy, N. R., Sealock, R., and Froehner, S. C. (1994) *Neuroreport* 5(13), 1577-80

105. Colledge, M., and Froehner, S. C. (1997) *J Neurosci* 17, 5038-45

106. Roberds, S. L., Leturcq, F., Allamand, V., Piccolo, F., Jeanpierre M, Anderson, R. D., Lim, L. E., Lee, J. C., Tome, F. M., Romero, N. B. (1994) *Cell* 78, 625-33

107. Tinsley, J. M., Blake, D. J., Zuellig, R. A., and Davies, K. E. (1994) *Proc Natl Acad Sci U S A* 91(18), 8307-13

108. Lim, L. E., Duclos, F., Broux, O., Bourg, N., Sunada, Y., Allamand, V., Meyer, J., Richard, I., Moomaw, C., Slaughter, C. (1995) *Nat Genet* 11(3), 257-65

109. Noguchi, S., McNally, E. M., Ben Othmane, K., Hagiwara, Y., Mizuno, Y., Yoshida, M., Yamamoto, H., Bonnemann, C. G., Gussoni, E., Denton, P. H., (1995) *Science* 270(5237), 819-22

110. Nigro, V., de Sa Moreira, E., Piluso, G., Vainzof, M., Belsito, A., Politano, L., Puca, A. A., Passos-Bueno, M. R., and Zatz, M. (1996) *Nat Genet* 14(2), 195-58

111. Brenman, J. E., Chao, D. S., Xia, H., Aldape, K., and Bredt, D. S. (1995) *Cell* 82, 743-52

112. Oak, S. A., Russo, K., Petrucci, T. C., and Jarrett, H. W. (2001) *Biochemistry* 40(37), 11270-78

113. Hall, A. (1998) *Science* 279, 509-14

114. Bar-Sagi, D., and Hall, A. (2000) *Cell* 103(2), 227-38

115. Kaibuchi, K., Kuroda, S., and Amano, M. (1999) *Annu Rev Biochem* 68, 459-86

116. Sander, E. E., and Collard, J. G. (1999) *Eur J Cancer* 35(9), 1302-08

117. Carnac, G., Primig, M., Kitzmann, M., Chafey, P., Tuil, D., Lamb, N., and Fernandez, A. (1998) *Mol Biol Cell* 9(7), 1891-02

118. Takano, H., Komuro, I., Oka, T., Shiojima, I., Hiroi, Y., Mizuno, T., and Yazaki, Y. (1998) *Mol Cell Biol* 18(3), 1580-89

119. Colledge, M., and Froehner, S. C. (1997) *J Neurosci* 17(13), 5038-45

120. Sunada, Y., Bernier, S. M., Kozak, C. A., Yamada, Y., and Campbell, K. P. (1994) *J Biol Chem* 269(19), 13729-32

121. von der Mark, H., Durr, J., Sonnenberg, A., von der Mark, K., Deutzmann, R., and Goodman, S. L. (1991) *J Biol Chem* 266(35), 23593-01

122. Song, W. K., Wang, W., Foster, R. F., Bielser, D. A., and Kaufman, S. J. (1992) *J Cell Biol* 117(3), 643-57

123. Gu, J., Sumida, Y., Sanzen, N., and Sekiguchi, K. (2001) *J Biol Chem* 276(29), 27090-97

124. Pall, E. A., Bolton, K. M., and Ervasti, J. M. (1996) *J Biol Chem* 271(7), 3817-21

125. Skubitz, A. P., McCarthy, J. B., Charonis, A. S., and Furcht, L. T. (1988) *J Biol Chem* 263(10), 4861-68

126. Yamaguchi, H., Yamashita, H., Mori, H., Okazaki, I., Nomizu, M., Beck, K., and Kitagawa, Y. (2000) *J Biol Chem* 275(38), 29458-65

127. Zhang, B., Gao, Y., Moon, S. Y., Zhang, Y., and Zheng, Y. (2001) *J Biol Chem* 276(12), 8958-67

128. Bishop, A. L., and Hall, A. (2000) *Biochem J* 348(2), 241-55

129. Bagrodia, S., and Cerione, R. A. (1999) *Trends Cell Biol* 9(9), 350-55

130. Nimnual, A. S., Yatsula, B. A., and Bar-Sagi, D. (1998) *Science* 279(5350), 560-63

131. Crews, C. M., and Erikson, R. L. (1993) *Cell* 74(2), 215-17

132. Coso, O. A., Chiariello, M., Yu, J. C., Teramoto, H., Crespo, P., Xu, N., Miki, T., and Gutkind, J. S. (1995) *Cell* 81(7), 1137-46

133. Minden, A., Lin, A., Claret, F. X., Abo, A., and Karin, M. (1995) *Cell* 81(7), 1147-57

134. Akamatsu, M., Aota, S., Suwa, A., Ueda, K., Amachi, T., Yamada, K. M., Akiyama, S. K., and Kioka, N. (1999) *J Biol Chem* 274(50), 35933-37

135. Underwood, P. A., Bennett , F. A., Kirkpatrick, A., Bean, P. A., and Moss, B. A. (1995) *Biochem J* 309(3), 765-61

136. Manser, E., Leung, T., Salihuddin, H., Zhao, Z. S., and Lim, L. (1994) *Nature* 367(6458), 40-6

137. Martin, G. A., Bollag, G., McCormick, F., and Abo, A. (1995) *Embo J* 14(9), 1970-78

138. Bagrodia, S., Derijard, B., Davis, R. J., and Cerione, R. A. (1995) *J Biol Chem* 270(47), 27995-98

139. Zhang, S., Han, J., Sells, M. A., Chernoff, J., Knaus, U. G., Ulevitch, R. J., and Bokoch, G. M. (1995) *J Biol Chem* 270(41), 23934-36

140. Sells, M. A., Knaus, U. G., Bagrodia, S., Ambrose, D. M., Bokoch, G. M., and Chernoff, J. (1997) *Curr Biol* 7(3), 202-10

141. Cuenda, A., Cohen, P., Buee-Scherrer, V., and Goedert, M. (1997) *EMBO J* 16, 295-05

142. Kolodziejczyk, S. M., Walsh, G. S., Balazsi, K., Seale, P., Sandoz, J., Hierlihy, A. M., Rudnicki, M. A., Chamberlain, J. S., Miller, F. D., and Megeney, L. A. (2001) *Curr Biol* 11(16), 1278-82

143. Behrens, A., Sibilia, M., and Wagner, E. F. (1999) *Nat Genet* 21(3), 326-29

144. Weston, C., Yee, B., Hod, E., and Prives, J. (2000) *J Cell Biol* 150(1), 205-12

145. Chockalingam, P. S., Cholera, R., Oak, S. A., Zheng, Y., Jarrett, H. W., Cheadle, C., Becker, K., and Thomason, D. B. (2001) *Am J Physiol Cell Physiol in press*

146. Spofford, C. M., and Chilian, W. M. (2001) *Am J Physiol Heart Circ Physiol* 280(3), H1354-60

147. Nguyen, H. T., Adam, R. M., Bride, S. H., Park, J. M., Peters, C. A., and Freeman, M. R. (2000) *Am J Physiol Cell Physiol* 279(4), C1155-67

148. Cox, G. A., Cole, N. M., Matsumura, K., Phelps, S. F., Hauschka, S. D., Campbell, K. P., Faulkner, J. A., and Chamberlain, J. S. (1993) *Nature* 364(6439), 725-29

Vita

Shilpa Oak was born on the 10th of February, 1974. She received a Master's degree from the Department of Environmental Sciences, university of Pune, India, in the july of 1996. She joined the department of biochemistry at the University of Tennessee, Memphis, in August of 1998.